CONTRIBUTION OF THE T CELL REPERTOIRE TO RESISTANCE IN MAREK'S DISEASE

Ву

Cari Jacqueline Hearn

A DISSERTATION

Submitted to
Michigan State University
in partial fulfillment of the requirements
for the degree of

Comparative Medicine and Integrative Biology—Doctor of Philosophy

2019

ABSTRACT

CONTRIBUTION OF THE T CELL REPERTOIRE TO RESISTANCE IN MAREK'S DISEASE

By

Cari Jacqueline Hearn

Marek's disease (MD) is an alpha-herpesvirus-induced lymphoproliferative disease of chickens which results in CD4+ T cell lymphomas in multiple organ systems, as well as peripheral and central nervous system disorders. Genetic studies of MD-resistant and susceptible chicken lines have identified the major histocompatibility complex (MHC) locus as the most important disease resistance locus in chickens; however, the contribution of the T cell receptor (TCR) repertoire to MD resistance mediated by the peptide-MHC-TCR synapse has not yet been characterized, in contrast to the extensive TCR repertoire studies that have been performed in human herpesviral infections. In this study, we identified differences in the TCR Vbeta repertoire of MD-resistant and susceptible chicken lines, and sought to determine the genetic basis of these differences. Additionally, we studied the contribution of thymic tolerance to MD neuropathogenicity in a non-oncogenic MD model, identifying a potential role of adaptive immune dysregulation in the acute disease.

Model pairs of genetically MD-resistant and susceptible chickens that are either MHC-matched or MHC congenic were studied in order to characterize the T cell response, particularly the TCR Vbeta repertoire, during Marek's disease virus (MDV) infection. In contrast to previous models of T cell-mediated genetic resistance which suggested that resistant birds might have less-easily activated CD4+ T cells and thus be resistant to transformation, we were unable to find differences in *in vitro* mitogen response within the CD4+ T cell populations of MHC-

matched MD-resistant and susceptible chickens. However, TCR Vbeta repertoire in vivo differed between MD-resistant and susceptible birds, and shifts towards higher TCR Vbeta-1 usage in response to MDV-infection could be identified within the CD8+ T cell populations, most notably within MD-resistant birds, consistent with CTL-mediated resistance. Chickens resistant to MD showed higher usage of Vbeta-1 TCRs, in both the CD8 and CD4 subsets in the MHC-matched model, and in the CD8 subset only in the MHC-congenic model. Using Illumina sequencing and PacBio long-read sequencing, we characterized the TCR beta locus of the MHCmatched lines, and found that the MD-resistant line expressed a greater number of Vbeta-1 TCRs and an increased number of Vbeta-1 CDR1 loops with a Trp-45 residue. TCR Vbeta-1 CDR1 usage in MHC-matched F1 birds was studied with Illumina RNA-seq, and usage of a susceptible line CDR1 variant was disproportionately high, suggesting that selection for resistance in the MHC-matched model has optimized the TCR repertoire away from dominant recognition of one of the MHC molecules. We also studied TCR down-regulation by MDV infection, and found that in vitro down-regulation could be mediated by viral reactivation independently of TCR activation or apoptosis, suggesting a TCR-targeting immune evasion strategy by MDV.

Lastly, we studied a potentially immune-mediated phenotype associated with MD, acute transient paralysis, using an MDV virus which lacks the Meq oncogene. We describe a fatal neuropathy of chicks induced by injection of Meq-deleted MDV in ovo during the thymic tolerizing window (prior to 15 days of embryogenesis), which induces severe bursa and thymic atrophy as well as mild lymphocytic peripheral nerve lesions. This establishes that oncogenicity is not absolutely required for the acute neuropathic syndrome, and suggests that vaccine strains may be capable of inducing neuropathic disease in T-cell-immunity-disregulated birds.

ACKNOWLEDGMENTS

I must, first and foremost, thank Hans Cheng for the years of patient mentorship he has put into my training. Hans allowed me to take some notable risks by giving me the freedom to explore several relatively challenging projects quite early in my graduate career, and when my interests in immunology led me to develop this project, he was supportive even when the work expanded outside the usual genomics focus of his laboratory. I have always found his careful and insightful approach to doing science to be of great benefit to both my education and my projects, and am grateful for everything I have learned from him about running a successful research program. I very much look forward to continuing our fruitful research discussions as fellow ARS scientists.

My committee members, Jerry Dodgson, Gisela Hussey, and Vilma Yuzbasiyan-Gurkan, deserve great appreciation for setting the bar high but always offering constructive criticism, and for their flexibility when my project plans went in unexpected directions.

I would be remiss if I failed to acknowledge the excellent assistance I received from the technicians at ADOL. It would not be exaggerating to say that Lonnie Milam taught me most of what I know about molecular biology and cell culture, and whenever something in the lab didn't work the first time, he was always willing to help me troubleshoot or process a problem sample. Laurie Molitor's expert help was also invaluable—I have her to thank for many plates of RNA extractions and spectratyping assays processed, and for joining me in necropsy and willingly learning new tissue collection protocols, then rapidly becoming more efficient at them than I could ever hope to be!

My several undergraduate, DVM and visiting graduate students also deserve a word of appreciation. Craig Willette, Kayla Niel, Chelsey Von Lau, Emmillie Ray and Özge Şahin all contributed time and effort to working on the projects I had going at the time they worked under me, and teaching them gave me opportunities to grow as an educator and mentor. I wish all of them great success in their own endeavors.

I must acknowledge the loving support of my family and friends during this long journey... my parents, JC and Carolyn, have always made it clear that they believed I could do whatever I set my mind to, and I thank them for that confidence. (I also thank my mother for helping me format my reference lists—and catching my mistakes!) My sister Carli (the "other half of my brain") has been a rock of support in uncountable ways, and I'm lucky to have her as my oldest and dearest friend. My musical compatriots, Amber Mohr and Sonya Rousseau, have provided listening ears as I pulled the threads of this project together (you girls are the birds in my birdhouse!) And finally, my labmates, Evin Hildebrandt, Sudeep Parambakkum, Steve Conrad, Alec Steep, and others, have made our lab at ADOL a fun, sometimes incredibly silly, place to work; and I'm so glad I can continue to be a part of such a vibrant group of scientists and friends.

TABLE OF CONTENTS

LIST OF TABLES	viii
LIST OF FIGURES	ix
KEY TO ABBREVIATIONS	xi
CHAPTER 1	1
Introduction	1
Abstract	1
Section 1: Immunopathogenicity of Marek's Disease and Disease Resistance	2
Section 2: TCR repertoire in human herpesviral infections: EBV and CMV	6
Section 2a: Peptide specificity in human herpesviral infections	7
Section 2b. Effects of MHC on TCR diversity in human herpesviral	
infections	11
Section 2c. TCR repertoire-intrinsic effects in herpesvirus infections	12
Section 2d. Conclusion	14
Section 3: Chicken TCR repertoire	15
Section 4: Conclusion	17
REFERENCES	19
CHAPTER 2	28
Contribution of the TCR Repertoire to MD Resistance in the Chicken	28
Abstract	28
Introduction	29
Materials and Methods	33
Animals and Viruses	33
Flow Cytometry	33
Reactivation Assay	34
Reactivation-Inhibition Assay	34
Proliferation Assay	35
Cell Cycle Analysis Assay	35
Spectratyping Assay	36
DNA Sequence Analysis	36
CDR3 Identification in RNA Sequence Data	37
Vbeta-1 CDR1 Haplotyping of RNA Sequence Data	37
Protein Sequence Analysis	38
PacBio Long Read DNA Sequencing	38
Statistics	39
Results	39

In vitro splenic 1 cell proliferation in response to mitogens are similar	
between Lines 6 and 7	
Lines 6 and 7 differentially express TCR $\alpha\beta$ Vb1 and TCR $\alpha\beta$ Vb2	40
TCR spectratype analysis demonstrates early clonal responses to MDV	
infection in both resistant and susceptible birds	47
Lines B.21 and B.19 differentially express TCR $lpha eta$ Vb1 and TCR $lpha eta$ Vb2 in the	
CD8+, but not CD4+ splenocyte populations	47
TCR usage in Line 6C.7 congenic lines is tightly controlled and TCR $lphaeta$ V1+	
lymphocyte fraction correlates with MD resistance	50
Lines 6 and 7 encode differing TCR variable beta-1 genes	51
MDV downregulates TCR surface expression differentially in Lines 6 and 7	64
TCR expression is reduced in an MDV-reactivated cell line	64
Discussion	68
APPENDICES	76
APPENDIX A Supplemental Figures	77
APPENDIX B tcr_analysis: a simple script for analysis of TCRs in chicken	
transcriptomics data	82
REFERENCES	88
CHAPTER 3	
Neurovirulence of a Meq-deleted MDV in Early In Ovo Challenge	94
Abstract	94
Introduction	94
Materials and Methods	100
Animals	100
Viruses	100
Tolerization Experiments	100
Immunohistochemistry	102
DNA extraction	102
Quantitative PCR	103
Statistics	104
Results	104
Experiment 1	104
Experiment 2	113
Discussion	118
APPENDIX	121
REFERENCES	
CHAPTER 4	128
Conclusions and Further Work	
REFERENCES	

LIST OF TABLES

Table 3.1. Quantitative PCR primers and probes	103
Table 3.2. MD lesions from Experiment 1	106
Table 3.3. Additional necropsy findings from Experiment 1	112

LIST OF FIGURES

Figure 2.1. Splenic T cell proliferation.	41
Figure 2.2. S-phase fraction	42
Figure 2.3. TCR usage in MHC-matched lines.	44
Figure 2.4. TCR spectratyping of splenocytes from MHC-matched lines	48
Figure 2.5. TCR usage in MHC congenics	52
Figure 2.6. TCR usage in RCS lines.	54
Figure 2.7. Swiss-Model predicted structures of line 6 and 7 TCR Vbeta-1 alleles	57
Figure 2.8. TCR Vbeta-1 CDR1 haplotypes in line 6x7 F1 RNA-seq data	58
Figure 2.9. 3' TCR Vbeta-1 sequences in Illumina data.	60
Figure 2.10. Vbeta-1 CDR1 alignments from long-read Pacbio DNA-seq	62
Figure 2.11. TCR beta locus model.	63
Figure 2.12. TCR Vbeta expression on CD3+ splenocytes	65
Figure 2.13. UAO4 cell reactivation assays	66
Figure 2.S1. Swiss-Model predicted ribbon models of TCR Vbeta-1 alleles	77
Figure 2.S2. De novo assembly of line 6 and line 6 Pacbio DNA-seq in Canu	78
Figure 2.S3. 3' TCR Vbeta-2 sequences identified in Illumina DNA-seq	80
Figure 2.S4. Swiss-Model predicted structure of line 6 3' deletion variant	81
Figure 3.1. Experiment 1 survival and clinical scores.	107
Figure 3.2. Variable results from <i>in ovo</i> injection of MDV-delta-Meq at EID 14	109
Figure 3.3. Gross nathology	110

Figure 3.4. Viremia in Experiment 1	. 114
Figure 3.5. Nerve Histopathology in Experiment 1	. 114
Figure 3.6. Viremia in Experiment 2	. 116
Figure 3.7. Viral replication in peripheral nerve tissue, Experiment 2	. 117
Figure 3.S1. Variable necropsy results from <i>in ovo</i> injection at EID 14	. 122
Figure 3.S2. Viremia in individual birds, Experiment 2	123

KEY TO ABBREVIATIONS

15.B19: An ADOL Line 15 congenic strain expressing the B19 MHC haplotype

15.B21: An ADOL Line 15 congenic strain expressing the B21 MHC haplotype

ABI: Applied Biosystems, Inc.

ADOL: USDA-ARS Avian Disease and Oncology Lab, East Lansing, Michigan.

ANOVA: analysis of variance

APC: antigen presenting cell

B2: a chicken MHC haplotype

B19: a chicken MHC haplotype

B21: a chicken MHC haplotype

BAC: bacterial artificial chromosome

B-ALL: B cell acute lymphoblastic leukemia

BCR: B cell receptor

BG-1: blood group 1 (an MHC-linked blood group marker in chickens)

BLAT: BLAST-like Alignment Tool

BMLF1: an immediate-early protein of EBV

BrdU: 5-bromo-2'-deoxyuridine

BWA: Burrows-Wheeler Aligner

bZIP: basic leucine zipper protein

CD3: cluster of differentiation 3 (a pan-T cell marker, part of the TCR complex)

CD4: cluster of differentiation 4 (a co-stimulatory T cell marker)

CD8: cluster of differentiation 8 (a co-stimulatory T cell marker)

CD8a: The CD8 alpha chain

CD8aa: A CD8 heterodimer composed of two alpha chains

CD8ab: A CD8 heterodimer composed of an alpha and a beta chain

CD8b: the CD8 beta chain

cDNA: complementary DNA

CDR1: complementarity-determining region 1 (a variable gene-encoded TCR motif)

CDR2: complementarity-determining region 2 (a variable gene-encoded TCR motif)

CDR3: complementarity-determining region 3 (a TCR motif generated by VDJ recombination)

CMV: cytomegalovirus

CNS: central nervous system

ConA: concanavalin A, a lectin mitogen

CRISPR/Cas9: Clustered Regularly Interspaced Short Palindromic Repeats/CRISPR-associated

protein 9, a prokaryote-derived genome editing system

CTL: cytotoxic T lymphocyte

Dbeta: diversity gene in the TCR beta locus

DEF: duck embryo fibroblast

DNA: deoxyribonucleic acid

DNA-seq: DNA sequencing

dph: days post hatch

EAN: experimental allergic neuritis

EBV: Epstein-Barr virus

EDTA: Ethylenediaminetetraacetic acid

EdU: 5-Ethynyl-2´-deoxyuridine

EID: embryo incubation day

F1: first generation hybrid

FBS: fetal bovine serum

FLRGRAYGL: an immunodominant epitope of EBV

GAPDH: Glyceraldehyde 3-phosphate dehydrogenase

gB: MDV glycoprotein B

GLC: an immunodominant epitope of EBV

GLC-A2: a pMHC composed of the GLC epitope presented by HLA-A2

HB unit: Horsfall-Bauer unit

HBV: hepatitis B virus

HHV-6: human herpesvirus-6

HIV: human immunodeficiency virus

HLA: human leukocyte antigen (the human MHC)

HLA-A: a human MHC class I gene

HLA-A2: a serotype of HLA-A

HLA-B: a human MHC class I gene

HLA-B07: a serotype of HLA-B

HLA-B07*02: an allele of HLA-B07

HLA-B8: a serotype of HLA-B

HLA-B8-FLRGRAYGL: a pMHC composed of HLA-B8 presenting the FLRGRAYGL epitope

HLA-B14: a serotype of HLA-B

HLA-B35: a serotype of HLA-B

HLA-B35*01: an allele of HLA-B35

HLA-B35*08: an allele of HLA-B35

HLA-B44: a serotype of HLA-B

HLA-B55: a serotype of HLA-B

HPVG: an immundominant epitope of EBV

HVS: Herpesvirus saimiri

HVT: herpesvirus of turkeys (Gallid herpesvirus-3)

IACUC: Institutional Animal Care and Use Committee

IFN-y: Interferon gamma

IGV: Integrative Genome Viewer

IMDM: Iscove's Modified Dulbecco's Medium

IPS: an immunodominant epitope of CMV

Jbeta: joining gene in the TCR beta locus

Jbeta-1-4: a joining gene in the human TCR beta locus

LM: Lebowitz-McCoy's 5A media

M1: a matrix protein of influenza A

MCMV: murine cytomegalovirus

MD: Marek's disease

Md5: a very virulent strain of MDV

MDV: Marek's disease virus (Gallid herpesvirus-2)

Meq: MDV-EcoQ-protein (a viral oncogene)

MHC: major histocompatibility complex

mRNA: messenger RNA

NLV: an immunodominant epitope of CMV

NLV-A2: a pMHC composed of HLA-A2 presenting the NLV epitope

NK cell: natural-killer cell

PBLs: peripheral blood leukocytes

PBMCs: peripheral blood mononuclear cells

PBS: phosphate-buffered saline

PCR: polymerase chain reaction

PE: phycoerythrin

PE-Cy5: phycoerythrin/cyanine-5 tandem conjugate

PHA: phytohaemagglutinin, a lectin mitogen

PKC: protein kinase-C

PMA: phorbol 12-myristate 13-acetate, a PKC activator

pMHC: peptide-MHC complex

pfu: plaque-forming units

pp14: MDV phosphoprotein 14

pp38: MDV phosphoprotein 38

qPCR: quantitative PCR

QTL: quantitative trait locus

RCS: recombinant congenic strain

RNA: ribonucleic acid

RNase A: ribonuclease A

RPH: an immunodominant epitope of CMV

RPMI-1640: Roswell Park Memorial Institute medium formulation 1640

RSS: recombination signal sequence

SB-1: a strain of MDV serotype 2

SDS: sodium dodecyl sulfate

SNP: single-nucleotide polymorphism

SPF: specific pathogen-free

SPRD: Spectral Red®, a formulation of PE-Cy5

TCR: T cell receptor

TCR-2: a chicken TCRalpha/beta heterodimer using Vbeta-1

TCR-3: a chicken TCRalpha/beta heterodimer using Vbeta-2

TCRalpha: the alpha chain of the TCRalpha/beta heterodimer

TCRalpha/beta: the classical TCR heterodimer

TCRαβVb1: TCRalpha/beta heterodimer using Vbeta-1 (i.e. TCR-2)

TCR $\alpha\beta$ Vb2: TCRalpha/beta heterodimer using Vbeta-2 (i.e. TCR-3)

TCRgamma/delta: a non-classical TCR heterodimer

TCRbeta: the beta chain of the TCRalpha/beta heterodimer

TE: Tris/EDTA buffer

TH1: T-helper-1 response paradigm

TH2: T-helper-2 response paradigm

TLR: Toll-like receptor

Tris: tris(hydroxymethyl)aminomethane

UAO4: an MD-transformed chicken T cell line

USDA-ARS: United States Department of Agriculture-Agricultural Research Service

Valpha: variable gene in the TCR alpha locus

Valpha-20: a variable gene in the human TCR alpha locus

Valpha-29: a variable gene in the human TCR alpha locus

Vbeta: variable gene in the TCR beta locus

Vbeta-1: a variable gene family in the chicken TCR beta locus

Vbeta-2: a variable gene family in the chicken TCR beta locus

Vbeta-4-3: a variable gene in the human TCR beta locus

Vbeta-9: a variable gene in the human TCR beta locus

Vbeta-9*02: an allele of Vbeta-9

Vbeta-28: a variable gene in the human TCR beta locus

VDJ: variable-diversity-joining (gene recombination method used in lymphocyte receptors)

Z-VAD-FMK: N-Benzyloxycarbonyl-Val-Ala-Asp(O-Me) fluoromethyl ketone, a non-selective caspase inhibitor

CHAPTER 1

Introduction

Abstract

This chapter provides introductory materials on Marek's disease (MD), a herpesvirus-induced lymphoma of chickens; the kinetics and relevance of T cell receptor (TCR) repertoires in human immunomodulatory and oncogenic herpesvirus infections; and the TCR repertoire of the chicken, as it may pertain to infectious disease, including MD. MD is an alpha-herpesvirusinduced lymphoproliferative disease of chickens which leads to lymphomas in multiple organ systems, as well as peripheral and central nervous system disorders. The life cycle of Marek's disease virus (MDV), the causative pathogen, involves multiple immune cell types, but T cell infection is of particular relevance, as CD4+ T cells are the transformed cell population in this disease. Control of MD also likely relies on T cells, in particular the CD8+ cytotoxic T lymphocyte (CTL) population, as CTL markers have been associated with genetic resistance to MDV. Human CTL TCR repertoires have been extensively studied in a gamma-herpesvirus infection (CMV) and a beta-herpesvirus infection (EBV), and the relevance of three primary determinants of the TCR repertoire (peptide immunodominance, Human Leukocyte Antigen (HLA) haplotype, and TCR-intrinsic factors, such as genotype, age and antigenic experience) are considered in these infectious contexts. TCR repertoires integrate all of these factors to produce variously focused or diverse repertoires in response to specific viral antigens. Finally, the streamlined chicken TCR system is described; while the chicken TCR loci provide comparatively few germline elements, functional diversity is provided through similar VDJ

recombination mechanisms to those seen in mammals. Limited research has been performed on the relevance of chicken TCR repertoire to infection, including MDV, but it is suggested that one Vbeta family may be more important in the response to both *Eimeria coccidiosis* and MDV.

Section 1: Immunopathogenicity of Marek's Disease and Disease Resistance

Marek's disease (MD) is a lymphoproliferative disorder of chickens caused by the alphaherpesvirus Marek's disease virus (MDV), also known as Gallid herpesvirus-2 or MDV serotype 1, and closely related to nonpathogenic strains MDV serotype 2 (Gallid herpesvirus-1) and herpesvirus of turkeys (HVT; Gallid herpesvirus-3) (Davison 2002, Davison 2010). Uniquely to MDV serotype 1, the T cell tropism of this infection is oncogenic and leads to the development of CD4+ T cell lymphomas which can occur in most organ systems of the body, but are often pronounced in viscera, skin and peripheral nerves (Payne 1967). Additionally, MDV causes peripheral nerve lesions that may or may not be related to T cell transformation, and involve lymphocytic inflammatory infiltrates throughout major peripheral nerves, demyelination injury, and paralysis/paresis (Payne 1967). Probable diagnosis of MD is made on the basis of gross nerve enlargement; cases are typically recognized on the basis of paralytic signs in older birds, but early mortality, transient paralysis due to CNS involvement, and tumors alone can occur in some flocks. As there are multiple viral lymphomas of chickens, a laboratory diagnosis of MD can be made from tumor tissues by viral copy PCR (reviewed in Witter 1998).

The present model of viral infection in MD involves multiple organ systems in the acute, latent, and transformation phases (reviewed in Boodhoo 2016). As the only source of fully enveloped, infectious viral particles is feather or skin dander, it is believed that infection

probably occurs via the respiratory route (Calnek 1970); once in the respiratory tract, lung epithelium and macrophages and/or other professional antigen presenting cells (APCs) are thought to be the initially infected cell types, although it has proven difficult to conclusively demonstrate relevant levels of infection in macrophages (Barrow 2003). Once macrophages are infected, they are thought to infect B cells, as B cell infection can be demonstrated within the first week of infection (Shek 1983). Lymphoid atrophy also occurs in the primary B cellproducing organ, the bursa of Fabricious (reviewed in Gimeno 2018). Infection of T cells becomes predominant within the second week of infection, likely through interaction with either B cells or macrophages, and is likely most efficient in activated T cells (Shek 1983, Calnek 1984). Similarly to the bursa, thymic atrophy can be pronounced, and immunosuppression is a sequela (Gimeno 2018). Viral integration into the telomeres of both T and B cells can be seen as soon as 1 day after infection (Robinson 2014). An initial phase of lytic infection in the first week results in high viral copy numbers within the spleen, and shedding of infectious virus from the skin, particularly in the feather follicle epithelium (Calnek 1970), presumably after trafficking of virus to these sites by infected lymphocytes. Subsequent to the initial lytic phase of infection and shedding, around 7-10 days post infection, the immune response reduces viral titers, and the infection becomes primarily latent, a hallmark of herpesviruses; although a second lytic phase often occurs around the third week of infection in susceptible birds (reviewed in MacPherson 2016).

During latency, viral copy number decreases; however, the number of infected cells remains high, as transformation occurs during this phase, and transformed CD4+ T cells begin to proliferate. The viral oncogene Meq is necessary for transformation to occur, as Meq

deletion mutants do not cause transformation (Lupiani 2004); Meq is a bZIP transcription factor, and is only weakly oncogenic alone in fibroblasts (Levy 2005), suggesting it interacts with cellular factors (e.g. transcription factors and regulated gene pathways) to induce transformation. Recently, our lab has identified the lymphocyte developmental regulator, IKAROS, as a secondary cellular driver of oncogenesis in MDV tumors (Steep et al, in preparation); this gene is involved in lymphoid oncogenesis in other models such as human B-ALL (mechanisms reviewed in Hu 2017). Variation between virus strains occurs, with some virus strains inducing lymphoma at very high rates; these strains also tended to have the highest mortality in unvaccinated birds, although vaccination reduces the correlation between these variables (Witter 1997). Maternal antibodies can prolong the course of disease (reviewed in Boodhoo 2016), allowing the development of large tumors. The frequent incidence of gross tumors with some strains makes MD a useful model for studying virally-induced T cell lymphoma.

MD is of continued interest to the poultry industry because MDV is ubiquitous in poultry flocks, causes devastating losses in unvaccinated birds, and has repeatedly broken through vaccine protection since the introduction of effective vaccines in the 1970's (Witter 1997, Witter 1998). Vaccination against the disease does not prevent infection with pathogenic strains, nor does it prevent the induction of viral latency (Churchill 1969, Okazaki 1970); therefore, even vaccinated birds may be a source of viral shedding (especially during periods of stress or immunosuppression), and it has been theorized that the use of non-sterilizing vaccines in high-capacity poultry rearing systems with rapid flock turnover is applying strong selection pressure to increase viral replication and transmission, and as a side-effect, probably virulence

(Read 2015). Thus, strategies to increase or augment vaccine protection are of great interest, and artificial selection of highly MD-resistant chicken lines has been a strategy pursued both by researchers and commercial poultry companies (Cole 1968, Stone 1975, Chang 2014). The MHC locus was identified as a major resistance locus (Briles 1977, Longenecker 1977, reviewed in Miller 2016), and additionally plays a role in responsiveness to vaccination against MDV (Bacon 1992, Bacon 1993). However, the successful selection of genetically resistant and susceptible chicken lines sharing the same MHC locus indicates that sources of variation outside of the MHC also contribute to MD resistance, and multiple studies have focused on identifying these factors, such as immune functional studies, QTL studies, and integrated genomics studies (Lee 1983, Fredericksen 1983, Vallejo 1998, Yonash 1999, Liu 2001, Luo 2013, Luo 2012a,b, Tian 2013, MacEachern 2012; Perumbakkam 2013, Cheng 2015). To date, a number of QTL have been identified which contribute to genetic resistance (Vallejo 1998, Yonash 1999), and a handful of individual genes have been identified, such as chicken growth hormone (Liu 2001) and the BG-1 blood group within the MHC locus (Goto 2009), although mechanisms have not been thoroughly explored for these genes. The largest source of non-MHC variation appears to be located in transcriptional regulatory elements, based on allele-specific expression studies of (advanced intercrosses) between MHC-matched genetically resistant and susceptible bird lines; allele-specific expression explained as much as 83 percent of the variation in disease incidence of tested progeny in this study (Cheng 2015).

Common themes across studies of genetic resistance to MD include cell survival and apoptotic pathways (as expected in an oncogenic disease), but also multiple immune pathways, indicating that there are roles for both innate and adaptive immunity in the control of either

viral infection or tumor cell proliferation which affect resistance to MD (reviewed in Hag 2010). For example, CD8 and the TCR beta locus have both been identified as loci associated with MD resistance (Yu 2011, Sarson 2008), although it is unclear whether mechanisms involved are due to direct regulation of these genes, or to the increased presence of CD8+ TCR beta+ cells contributing to an effective adaptive immune response in sampled tissues. In this study, I focused on the role of the T cell-mediated adaptive immune response, and in particular the role of the T cell receptor beta repertoire in contributing to immune control of MD in the MHCmatched genetically resistant Line 6 and susceptible Line 7 chicken model (Chapter 2). Secondly, I describe a mechanism by which non-oncogenic infection may contribute to fatal MD neuropathogenicity (Chapter 3) through a potentially immune-mediated mechanism, thus demonstrating the importance of fully elucidating the contribution of adaptive immunity to mechanisms of both resistance and disease in the MD model. In the remaining sections of this introductory chapter, I outline what is currently known about the contribution of the TCR repertoire to the control of other herpesvirus infections, particularly the medically important EBV and CMV viruses (section 2); and what is currently understood about the chicken TCR system and its interaction with MDV (section 3).

Section 2: TCR repertoire in human herpesviral infections: EBV and CMV

In recent decades, a great deal of effort has been expended on clarifying the roles of antigen immunodominance and the TCR repertoire in controlling important herpesviral infections in humans, particularly those associated with severe illness in immunocompromised patients (e.g., cytomegalovirus) or the development of certain cancers (Epstein Barr Virus). Epstein Barr Virus

(EBV) is a lymphotrophic gamma-herpesvirus which primarily infects tonsillar epithelium and B cells, and causes acute reactive T cell lymphadenopathy (mononucleosis) in its lytic phase, as well as an increased risk of cancers such as Hodkin's lymphoma during latency (reviewed in Balfour 2015). In contrast, human cytomegalovirus (CMV) is a beta-herpesvirus, has a broad cell tropism in vivo, and is primarily of interest for its ability to reactivate and cause acute disease in immunocompromised patients (such as in late-stage HIV infection or organ and tissue transplant recipients undergoing immunosuppressive therapy) (reviewed in Steininger 2007). Initial studies on CTL responses in these infections resulted in the identification of immunodominant responses against two viral proteins in CMV infection (Glusman 2001) and three viral proteins in EBV infection (Rickinson 1997), with potential overlapping explanations including increased peptide presentation from highly-expressed or efficiently processed proteins; epitope restriction by common HLA alleles; or stochastic effects of TCR repertoire generation on epitope recognition.

Section 2a: Peptide specificity in human herpesviral infections

Interactions between peptide, restricting MHC molecule, and potentially reactive TCRs have been explored in numerous *in vitro* studies using immunodominant peptides (and substituted peptides) and clonally expanded CTLs from herpesvirus-infected individuals (human or murine models). Primary effects of peptide sequence on MHC binding or TCR selection has been studied by alanine scanning, solved binding structures, and comparisons to sequence-similar peptides from other pathogens. Importantly, in vitro methods using synthetic peptides can separate the complex interactions between peptide availability and peptide-MHC-TCR binding

affinity; early studies recognized that peptide availability due to protein expression and processing plays an important role in TCR repertoire selection (de Campos-Lima 1997, Wynn 2008), but does not fully explain peptide immunodominance.

Several studies of CMV and EBV immudominant peptides have focused on the effects of peptide length on peptide-MHC (pMHC) surface structure, finding that long peptides that form "bulged" pMHC surfaces can affect docking modes between pMHC and TCR complexes, leading to biased TCR repertoire selection (Wynn 2008, Liu 2013). Interestingly, however, even pMHC structures which support noncanonical TCR docking modes may also be recognized by TCRs that dock in more traditional conformations, indicating the breadth of potential solutions to pMHC recognition present within the TCR repertoire (Liu 2013). Each pMHC complex presents a unique structural problem to be solved, and the TCR repertoire integrates pMHC affinity (binding kinetics) and avidity (pMHC availability for binding) with an enormous TCR recombinatorial diversity to solve it; thus it is surprising that biases in TCR repertoire response to even noncanonical pMHCs may be as narrow as a single responding Vbeta family, as in the case of one CMV peptide (Wynn 2008).

Studies have also focused on sequence-specific effects of immunodominant peptides in both CMV and EBV. Gras et al. (2009a) found that the NLV-A2 pMHC (HLA-A2 presenting the NLV dominant epitope of CMV) selected strongly for a set of TCR binding motifs that recognized an unusually high proportion of the peptide sequence and skewed the TCR repertoire towards V and J elements and public (common across individuals) CDR3 sequences that provided these motifs; in contrast, other pMHC complexes may present minimal peptide sequence to the TCR clones that recognize them, as in the EBV pMHC GLC-A2, which only contacts a TCR through 3

amino acid residues and therefore largely determines its repertoire through MHC-TCR interactions (Miles 2010). Interestingly, public TCRs which recognized GLC-A2 included minimal novel CDR3 sequence (i.e., N-added bases during VDJ recombination), indicating that the responding TCR germline elements encoded the relevant motifs for recognizing this peptide. As noted by the authors in Miles et al., this suggests that the human MHC-TCR system may have co-evolved with EBV to present this dominant epitope efficiently, potentially to the benefit of both host and virus through the long-term survival of EBV-infected hosts (Miles 2010).

Two relevant studies shed light on the complexity of interactions between peptide immunodominance and TCR diversity. Koning, et al. (2013) performed a broad study of the CTL TCR beta diversity against multiple immunodominant peptides from both CMV and EBV in 54 healthy individuals of varying HLA haplotypes, finding that the diversity of the repertoire generated was highly specific to each pMHC, and failed to correlate with HLA-A or HLA-B usage; virus; or even peptide immunodominance, as immunodominant peptides could generate either a broad response or a narrow response within the responding CTL population (Koning 2013). This study complemented earlier findings that this phenomenon also occurs in the CD4+ memory response to CMV, and individuals of varying HLA haplotype may recognize different immunodominant peptides, or the same peptides with very different patterns of TCR clonality (Bitmansour 2001).

An additional potentially important characteristic of the immunodominant peptide repertoire of herpesvirus infection is the presence of cross-reactivity with other antigens, such as the cross-reactivity that occurs between the HLA-B8-restricted EBV peptide FLRGRAYGL and the HLA-B44, B14, B35 and B55 alleles presenting self-antigen (Burrows 1995, Burrows 1997,

D'Orsogna 2009). Such cross-reactivity has the potential to bias the TCR repertoire away from self-reactive anti-EBV responses that would otherwise be dominant, and in fact presence of the HLA-B44 allele was found to diversify the TCR repertoire against this peptide, suggesting that some TCR repertoire narrowing is due to competition between responding T cell clones (Burrows 1995). Surprisingly, in that study, public clones still composed a significant portion of the repertoire, indicating that repertoire selection away from a self-reactive binding strategy did not completely diversify the optimal pMHC-TCR binding mode (Burrows 1995). Equally interesting was this group's later finding that the cross-reactivity seen against HLA-B8-FLRGRAYGL relied on as few as 3 peptide residues, suggesting that peptides that present minimal epitopes might have a greater risk of triggering self-reactivity, and that cross-reactivity to HLA-B35 was only seen with one target cell type (PHA-induced lymphoblasts), raising the possibility that in some cases cross-reactive TCRs might escape deletion depending on the kinetics of self-antigen expression (Burrows 1997).

In contrast to the cross-reactivity that occurs between certain HLA alleles, TCR cross-reactivity between sequence-related immunodominant peptides of different viruses presented by the same MHC is controversial. Clute et al. (2010) demonstrated cross-reactive *in vitro*-expanded CTL populations that responded to both the EBV immunodominant HLA-A2-presented GLC peptide of the BMLF1 protein and a sequence-related influenza A epitope from the M1 matrix protein, also presented on HLA-A2; two cross-reactive populations could be demonstrated, of which a population which primarily bound BMLF1+ tetramers but responded in vitro to the M1 peptide differed in TCR beta repertoire from the non-cross-reactive anti-BMLF1 repertoire, while dual-staining cross-reactive CTLs shared a repertoire with a subset of

non-cross-reactive populations (Clute 2010). In contrast, a more recent study was unable to demonstrate any cross-reactivity between these two peptides using both ex vivo analysis and limited in vitro culture (Grant 2016), and structural analysis indicated that these epitopes presented significantly different pMHC surface landscapes despite sharing 58% sequence similarity (Grant 2016). Thus, a complete understanding of the interactions between a pMHC and its potential TCR binding partners is necessary to understand the effects of any given epitope on TCR repertoire.

Section 2b. Effects of MHC on TCR diversity in human herpesviral infections

As eluded to above, cross-reactivity between different self- and non-self-pMHCs may modulate the diversity in the TCR repertoire to a viral infection by deleting certain TCRs during T cell maturation. Similarly, the presence of differing HLA alleles plays an important role in determining what epitopes are available to shape the TCR repertoire, given the general requirements for HLA-allele-specific binding motifs in immunogenic peptides (reviewed in Biddison 2001). HLA-specific responses in human herpesviral infections can be demonstrated as biases toward the use of specific TCR elements, such as the frequent use of Vbeta-9 in the HLA-B35 restricted TCR response to the HPVG epitope of EBV, which pairs with either Valpha-20 or Valpha-29 depending on whether the HLA-B35*01 or HLA-B35*08 allele is present (Miles 2006). Similarly, HLA-B35*01 donors uniformly responded to the CMV IPS epitope with a 13-amino acid TCRbeta CDR3 region with a strong consensus motif, composed of Vbeta-28/Jbeta-1-4 elements and paired with a similarly restricted TCRalpha chain; only 1 out of five donors expressed this public TCR at less than 10% of responding CTLs (Brennan 2007). Structural and

kinetic analysis of such pMHC-TCR pairings can provide detail about the binding specificities involved, all the way down to peptide-MHC-TCR interactions resulting from the single amino acid substitution between HLA-B35*01 and HLA-B35*08, or in the stabilizing peptide (Liu 2014).

Section 2c. TCR repertoire-intrinsic effects in herpesvirus infections

TCR element deletions and polymorphisms can affect repertoire diversity and potentially epitope immundominance. For example, the deletion of TCR Vbeta-4-3, which occurs in 40% of humans, results in the abrogation of a dominant public TCR clone against the HLA-B07*02presented RPH epitope of CMV, which uses that element; in individuals without the deletion, from 2% to nearly 100% of antigen-specific CTLs used the public clone. In contrast, RPH-specific TCR repertoires in Vbeta-4-3-deleted individuals were composed of a broad range of diverse Vbeta elements. However, overall numbers of RPH-specific CTLs were not clearly differentiated between Vbeta-4-3+ and Vbeta-4-3-deleted groups, and were variable enough between individuals that no clear effect on immunodominance of the RPH epitope could be determined (Brennan 2012). Similarly, even small polymorphisms in TCR elements can strongly affect pMHC binding and thus repertoire selection. Mutation of a single residue in Vbeta-9 found in the Vbeta-9*02 allele prevents selection of this element in the otherwise Vbeta-9-dominant anti-HPVG response (Gras 2010), again potentially diversifying the TCR response, although this is yet to be confirmed.

Age effects can also play a role in shaping the virus-specific TCR repertoire. In mice, it was recently shown that neonatal TCR repertoires are composed to a much larger degree by germline-encoded sequences lacking N-addition, likely due to a developmental delay in the

expression of terminal deoxynucleotidyl transferase needed to include N-added nucleotides during VDJ arrangement; and that these germline TCRs persist and contribute to the anti-MCMV response in immune-privileged CNS tissue, despite the gradual diversification of the overall TCR repertoire with age (Venturi 2016). Additionally, a number of studies have examined the effect of age on human anti-herpesviral TCR repertoires; such effects are of particular interest due to the life-long infection status that occurs with herpesviruses, and the concern for potential disease reactivation in elderly patients. Interestingly, long-term latent infection appears to drive the development of focused oligoclonal CTL repertoires in human CMV, in contrast to the repertoire broadening occurs with age in infected mice (Khan 2002, Smithey 2018); while latent EBV infection in older healthy adults is associated with maintenance of overall TCR usage but shifts in TCR element selection in the anti-EBV CTL response with age, combined with an increase in TH1-like cytokine responses which may be protective or pro-inflammatory (Cardenas 2014). On the other hand, EBV-specific TCR clones of varying affinity/activity are often maintained throughout the course of infection, and initial repertoire selection establishing the memory repertoire may be more important than long term selection effects (Levitsky 1998).

The development of allogeneic bone marrow transplant/reconstitution techniques has allowed the examination of TCR repertoire reconstitution in vivo, and the effects of herpesviral infection status on these repertoires very directly, as bone marrow ablation before BMT, and immunosuppressive treatment of graft-versus-host disease after, frequently reactivate latent herpesviruses such as CMV and EBV. Importantly, immune reconstitution in the presence of CMV reactivation results in massive clonal expansions of CMV-specific CD8+ effector memory

CTLs, and contraction of naïve and new thymic-emigrating CTLs, with the result that the reconstituted TCR Vbeta repertoire contains "holes" in the normal TCR element distribution (Suessmith 2015), potentially resulting in a disturbed TCR repertoire to other pathogens. A similar study demonstrated that the TCR Valpha repertoire was similarly perturbed, with CMV-infected BMT recipients developing CMV peptide-specific TCR Valpha repertoires that in some cases were composed entirely of a single clone, and made up 30% of the patients' total CTL repertoire (Link 2016). In contrast, reconstitution with autologous PBMCs did not result in similar repertoire skewing within the EBV-reactive CTL subset; TCR repertoires remained similar to pre-ablation, although increased effector differentiation occurred (lancu 2013). These findings suggest that the presence of highly immunogenic viral antigens during initial constitution of CTL populations may be more selective for the final TCR repertoire than reactivating disease.

Section 2d. Conclusion

In human chronic herpesvirus infections, TCR repertoire is shaped by at least three major factors, including the presence of immunodominant viral peptides, the repertoire of MHC molecules available to present these viral peptides, and TCR repertoire-intrinsic effects, including the presence of TCR mutations, and the effects of early and late immunological events that shape the overall repertoire over time. While TCR repertoires in specific HLA contexts against dominant CMV and EBV epitopes have been established, fully integrating these findings will require very high-throughput analysis of many patients and very deep repertoire sequencing, given the complexity of human antigen receptor systems and their potential viral

ligands. One study has attempted to perform such an analysis, demonstrating that it was possible to identify a CMV-associated TCR repertoire signature without a priori knowledge of dominant peptides, HLA molecules, or TCRs (Emerson 2017). Understanding the relevance of TCR repertoire diversity to human herpesviral infection and clinical disease may ultimately help guide the development of immune-specific therapies.

Section 3: Chicken TCR repertoire

The chicken TCR system has been progressively defined since the late 1980's (Chen 1988, Chen 1989, Char 1990, Vainio 1990, Tjoelker 1990, Lahti 1991, Gobel 1994, Six 1996, Shigeta 2004, Parra and Miller 2012, Parra 2012). Similarly to mammals, chickens express both TCRalpha/beta heterodimers and TCRgamma/delta heterodimers, although the TCRgamma/delta population constitutes a larger proportion of T cells in the chicken than in mammals (Sowder 1988, Chen 1988). This overview will focus on the classical TCRalpha/beta repertoire, although TCRgamma/delta cells are thought to play an important role in avian immunity as well, particularly in gut epithelial immune surveillance (Sowder 1988, Bucy 1990, Lillehoj 1993). The chicken TCRalpha/beta population has been traditionally subdivided into monoclonal antibody-identified TCR-2 and TCR-3 populations (Chen 1989, Char 1990), which were found to distinguish the usage of 2 different TCR Vbeta gene families (Tjoelker 1990, Lahti 1991); functional differences between these TCR Vbeta families may be relevant in CTL responses to specific pathogens, including MDV and *Eimeria* coccidiosis (Omar 1997, Ren 2014; see below).

The chicken TCR alpha and beta loci have been approximately characterized based on cDNA probe analysis (Gobel 1994, Kubota 1999, Cooper 1991, Lahti 1991, Shigeta 2004). As with Vbeta, there are also two Valpha families in the chicken; however, in contrast to Vbeta families, which contains approximately six and three members respectively (Cooper 1991), the Valpha families contain approximately 15 and 25 genes each (Kubota 1999). The TCR alpha locus contains approximately 25 J elements, and surrounds the delta locus, as in other species; in contrast, the TCR beta locus contains only 4 J elements (Kubota 1999, Shigeta 2004). Despite the comparatively limited diversity provided by the elements in the TCR alpha and beta loci, recombinational diversity is preserved through the N- and P-addition and deletion of nucleotides in VDJ recombination, as in mammals (McCormack 1991), although the apparent use of a single Dbeta element does bias the chicken TCR beta repertoire toward incorporation of a conserved D-encoded glycine (McCormack 1991).

CTL TCR beta repertoire diversity in the chicken was recently studied in the context of *Eimeria* infection (Ren 2014). Although sample size from each bird was very limited (only 40 sequences were profiled each), two public Vbeta/CDR3 sequences were identified across multiple birds, although J segment usage was not conserved across these public motifs. The most prevalent TCR sequences used one of two Vbeta-1 genes, suggesting a potentially immunodominant response to this coccidial infection. The authors hypothesized that the lack of conservation in J segments in the context of either the public CDR3 motifs or the dominant Vbeta segments suggests that there is no J element biasing in this infection (Ren 2014), and therefore the 4 Jbeta elements may be functionally equivalent, at least against the immunodominant epitope(s) in *Eimeria*.

Functional differences between the two TCR Vbeta families have also been considered in the context MDV infection. The effectiveness of TCR Vbeta-1 and TCR Vbeta-2 expressing CTLs in lysing target cells infected with the non-oncogenic SB-1 strain of MDV serotype 2 was examined, and Vbeta-1, but not Vbeta-2 TCRs were required to efficiently lyse these cells (Omar 1997). This has been taken as an indication that Vbeta-1 TCRs are likely to be more important to a vaccinal response against oncogenic MDV, at least where MDV serotype 2 is used as a vaccine. Additionally, TCR Vbeta-1 is more frequently expressed on MDV lymphomas (Mwangi 2011), which could reflect a bias in infectivity or transformation capacity, although this may also simply be a result of the increased usage of Vbeta-1 TCRs in general (Ewald 1996).

Section 4: Conclusion

In this chapter I have described the pathobiology of MDV infection, emphasizing the role of adaptive immunity and particularly T cell-mediated immunity in both the disease process and disease resistance, providing context for studies of the T cell receptor repertoire and neuro-immunopathology in MDV infection. Secondly, I have outlined what is currently understood about the dynamics and relevancies of CTL T cell receptor repertoires in two clinically relevant human herpesviral infections, CMV and EBV. Finally, I have overviewed the current status of knowledge about the chicken TCR system, and several recent insights into its relevance to diseases of poultry. In contrast to the higher complexity of mammalian (e.g. human) TCR repertoires, the chicken TCR repertoire provides a more streamlined system in which to examine the effects of germline and recombinatorial diversity on response to pathogens; while comparatively little work has been done in this field to date, the study of chicken TCR

repertoire diversity and response to an oncogenic herpesvirus infection (MDV) may yield additional insights that complement the research that has been done on human herpesviral pathogens.

REFERENCES

REFERENCES

Bacon, L. D. & Witter, R. L. Influence of turkey herpesvirus vaccination on the B-haplotype effect on Marek's disease resistance in 15.B-congenic chickens. Avian Dis. 36, 378–385 (1992).

Bacon, L. D. & Witter, R. L. Influence of B-haplotype on the relative efficacy of Marek's disease vaccines of different serotypes. Avian Dis. 37, 53–59 (1993).

Balfour, H. H., Dunmire, S. K. & Hogquist, K. A. Infectious mononucleosis. Clin. Transl. Immunology 4, e33 (2015).

Barrow, A. D. Infection of macrophages by a lymphotropic herpesvirus: a new tropism for Marek's disease virus. J. Gen. Virol. 84, 2635–2645 (2003).

Biddison, W. E. & Martin, R. Peptide binding motifs for MHC class I and II molecules. in Current Protocols in Immunology (eds. Coligan, J. E., Bierer, B. E., Margulies, D. H., Shevach, E. M. & Strober, W.) (John Wiley & Sons, Inc., 2001). doi:10.1002/0471142735.ima01is36

Bitmansour, A. D. et al. Clonotypic structure of the human CD4+ memory T cell response to cytomegalovirus. J. Immunol. 167, 1151–1163 (2001).

Boodhoo, N., Gurung, A., Sharif, S. & Behboudi, S. Marek's disease in chickens: a review with focus on immunology. Vet. Res. 47, 119-137 (2016).

Brennan, R. M. et al. Predictable T-cell receptor selection toward an HLA-B*3501-restricted human cytomegalovirus epitope. J. Virol. 81, 7269–7273 (2007).

Brennan, R. M. et al. The Impact of a large and frequent deletion in the human TCR locus on antiviral immunity. J. Immunol. 188, 2742–2748 (2012).

Briles, W. E., Stone, H. A. & Cole, R. K. Marek's disease: effects of B histocompatibility alloalleles in resistant and susceptible chicken lines. Science 195, 193–195 (1977).

Bucy, R. P., Chen, C. H. & Cooper, M. D. Ontogeny of T cell receptors in the chicken thymus. J. Immunol. 144, 1161–1168 (1990).

Burrows, S. R. T cell receptor repertoire for a viral epitope in humans is diversified by tolerance to a background major histocompatibility complex antigen. J. Exp. Med. 182, 1703–1715 (1995).

Burrows, S. R. et al. Cross-reactive memory T cells for Epstein-Barr virus augment the alloresponse to common human leukocyte antigens: degenerate recognition of major histocompatibility complex-bound peptide by T cells and its role in alloreactivity. Eur. J. Immunol. 27, 1726–1736 (1997).

Calnek, B. W., Adldinger, H. K. & Kahn, D. E. Feather follicle epithelium: a source of enveloped and infectious cell-free herpesvirus from Marek's disease. Avian Dis. 14, 219–233 (1970).

Calnek, B. W., Schat, K. A., Ross, L. J., Shek, W. R. & Chen, C. L. Further characterization of Marek's disease virus-infected lymphocytes. I. In vivo infection. Int. J. Cancer 33, 389–398 (1984).

Campos-Lima, P.-O. de, Levitsky, V., Imreh, M. P., Gavioli, R. & Masucci, M. G. Epitope-dependent election of highly restricted or diverse T cell receptor repertoires in response to persistent infection by Epstein-Barr virus. J. Exp. Med. 186, 83–89 (1997).

Cárdenas, S. D., Vélez Colmenares, G., Orfao de Matos, A., Fiorentino Gómez, S. & Quijano Gómez, S. M. Age-associated Epstein-Barr virus-specific T cell responses in seropositive healthy adults: Immune response to EBV in healthy individuals. Clin. Exp. Immunol. 177, 320–332 (2014).

Chang, S. et al. Host genetic resistance to Marek's disease sustains protective efficacy of herpesvirus of turkey in both experimental and commercial lines of chickens. Vaccine 32, 1820–1827 (2014).

Char, D., Sanchez, P., Chen, C. L., Bucy, R. P. & Cooper, M. D. A third sublineage of avian T cells can be identified with a T cell receptor-3-specific antibody. J. Immunol. 145, 3547–3555 (1990).

Chen, C. H. et al. TCR3: a third T-cell receptor in the chicken. Proc. Natl. Acad. Sci. U.S.A. 86, 2351–2355 (1989).

Chen, C. L. Identification of a T3/T cell receptor complex in chickens. J. Exp. Med. 164, 375–380 (1986).

Cheng, H. H. et al. Fine mapping of QTL and genomic prediction using allele-specific expression SNPs demonstrates that the complex trait of genetic resistance to Marek's disease is predominantly determined by transcriptional regulation. BMC Genomics 16, 816-824 (2015).

Churchill, A. E., Payne, L. N. & Chubb, R. C. Immunization against Marek's disease using a live attenuated virus. Nature 221, 744–747 (1969).

Clute, S. C. et al. Broad cross-reactive TCR repertoires recognizing dissimilar Epstein-Barr and influenza A virus epitopes. J. Immunol. 185, 6753–6764 (2010).

Cole, R. K. Studies on genetic resistance to Marek's disease. Avian Dis. 12, 9-28 (1968).

Cooper, M. D., Chen, C. L., Bucy, R. P. & Thompson, C. B. Avian T cell ontogeny. Adv. Immunol. 50, 87–117 (1991).

D'Orsogna, L. J. et al. New tools to monitor the impact of viral infection on the alloreactive T-cell repertoire. Tissue Antigens 74, 290–297 (2009).

Davison, A. J. Evolution of the herpesviruses. Vet. Microbiol. 86, 69-88 (2002).

Davison, A. J. Herpesvirus systematics. Vet. Microbiol. 143, 52–69 (2010).

Emerson, R. O. et al. Immunosequencing identifies signatures of cytomegalovirus exposure history and HLA-mediated effects on the T cell repertoire. Nat. Genet. 49, 659–665 (2017).

Ewald, S. J., Yi-Yang Lien, Lanqing Li & L. Warren Johnson. B-haplotype control of CD4/CD8 subsets and TCR V beta usage in chicken T lymphocytes. Vet. Immunol. Immunopathol. 53, 285–301 (1996).

Fredericksen, T. L. & Gilmour, D. G. Ontogeny of ConA and PHA responses of chicken blood cells in MHC-compatible lines 6(3) and 7(2). J. Immunol. 130, 2528–2533 (1983).

Gimeno, I. M. & Schat, K. A. Virus-induced immunosuppression in chickens. Avian Dis. 62, 272–285 (2018).

Glusman, G. et al. Comparative genomics of the human and mouse T cell receptor loci. Immunity 15, 337–349 (2001).

Gobel, T. W. F. et al. Identification of T-cell receptor alpha-chain genes in the chicken. Proc. Natl. Acad. Sci. U.S.A. 91, 1094–1098 (1994).

Goto, R. M. et al. BG1 has a major role in MHC-linked resistance to malignant lymphoma in the chicken. Proc. Natl. Acad. Sci. U.S.A. 106, 16740–16745 (2009).

Grant, E. J. et al. Lack of heterologous cross-reactivity toward HLA-A*02:01 restricted viral epitopes Is underpinned by distinct $\alpha\beta T$ cell receptor signatures. J. Biol. Chem. 291, 24335–24351 (2016).

Gras, S. et al. Structural bases for the affinity-driven selection of a public TCR against a dominant human cytomegalovirus epitope. J. Immunol. 183, 430–437 (2009).

Gras, S. et al. Allelic polymorphism in the T cell receptor and its impact on immune responses. J. Exp. Med. 207, 1555–1567 (2010).

Haq, K., Brisbin, J. T., Thanthrige-Don, N., Heidari, M. & Sharif, S. Transcriptome and proteome profiling of host responses to Marek's disease virus in chickens. Vet. Immunol. Immunopathol. 138, 292–302 (2010).

Hu, Y., Yoshida, T. & Georgopoulos, K. Transcriptional circuits in B cell transformation. Curr. Opin. Hematol. 24, 345–352 (2017).

lancu, E. M. et al. Persistence of EBV antigen-specific CD8 T cell clonotypes during homeostatic immune reconstitution in cancer patients. PLoS One 8, e78686 (2013).

Khan, N. et al. Cytomegalovirus seropositivity drives the CD8 T cell repertoire toward greater clonality in healthy elderly individuals. J. Immunol. 169, 1984–1992 (2002).

Koning, D. et al. CD8+ TCR repertoire formation Is guided primarily by the peptide component of the antigenic complex. J. Immunol. 190, 931–939 (2013).

Kubota, T. et al. Characterization of an avian (Gallus gallus domesticus) TCR alpha delta gene locus. J. Immunol. 163, 3858–3866 (1999).

Lahti, J. M., Thompson, C. B. & Cooper, M. D. Two distinct alpha-beta T-cell lineages can be distinguished by the differential usage of T-cell receptor V beta gene segments. Proc. Natl. Acad. Sci. U.S.A. 88, 10956–10960 (1991).

Lee, L. F. & Bacon, L. D. Ontogeny and line differences in the mitogenic response of chicken lymphocytes. Poult. Sci. 62, 579–584 (1983).

Levitsky, V., de Campos-Lima, P.-O., Frisan, T. & Masucci, M. G. The clonal composition of a peptide-specific oligoclonal CTL repertoire selected in response to persistent EBV infection is stable over time. J. Immunol. 161, 594–601 (1998).

Levy, A. M. et al. Marek's disease virus Meq transforms chicken cells via the v-Jun transcriptional cascade: A converging transforming pathway for avian oncoviruses. Proc. Natl. Acad. Sci. U.S.A., 14831–14836 (2005).

Lillehoj, H. S. Avian gut-associated immune system: implication in coccidial vaccine development. Poult. Sci. 72, 1306–1311 (1993).

Link, C. S. et al. Abundant cytomegalovirus (CMV) reactive clonotypes in the CD8 + T cell receptor alpha repertoire following allogeneic transplantation: $TCR-\alpha$ repertoire allogeneic transplantation. Clin. Exp. Immunol. 184, 389–402 (2016).

Liu, H.-C., Cheng, H. H., Tirunagaru, V., Sofer, L. & Burnside, J. A strategy to identify positional candidate genes conferring Marek's disease resistance by integrating DNA microarrays and genetic mapping. Anim. Genet. 32, 351–359 (2001).

Liu, Y. C. et al. A molecular basis for the interplay between T cells, viral mutants, and human leukocyte antigen micropolymorphism. J. Biol. Chem. 289, 16688–16698 (2014).

Liu, Y. C. et al. Highly divergent T-cell receptor binding modes underlie specific recognition of a bulged viral peptide bound to a human leukocyte antigen class I molecule. J. Biol. Chem. 288, 15442–15454 (2013).

Longenecker, B. M. et al. Role of the major histocompatibility complex in resistance to Marek's disease: restriction of the growth of JMV-MD tumor cells in genetically resistant birds. Adv. Exp. Med. Biol. 88, 287–298 (1977).

Luo, J. et al. Histone methylation analysis and pathway predictions in chickens after MDV Infection. PLoS One 7, e41849 (2012).

Luo, J. et al. DNA methylation fluctuation Induced by virus infection differs between MD-resistant and -susceptible chickens. Front. Genet. 3, doi:10.3389/fgene.2012.00020 (2012).

Luo, J. et al. Genome-wide copy number variant analysis in inbred chickens lines with different susceptibility to Marek's disease. G3-Genes Genom. Genet. 3, 217–223 (2013).

Lupiani, B. et al. Marek's disease virus-encoded Meq gene is involved in transformation of lymphocytes but is dispensable for replication. Proc. Natl. Acad. Sci. U.S.A. 101, 11815–11820 (2004).

MacEachern, S., Muir, W. M., Crosby, S. D. & Cheng, H. H. Genome-wide identification and quantification of cis- and trans-regulated genes responding to Marek's disease virus infection via analysis of allele-specific expression. Front. Genet. 2, 10.3389/fgene.2011.00113 (2012).

McCormack, W. T., Tjoelker, L. W., Stella, G., Postema, C. E. & Thompson, C. B. Chicken T-cell receptor beta-chain diversity: an evolutionarily conserved D beta-encoded glycine turn within the hypervariable CDR3 domain. Proc. Natl. Acad. Sci. U.S.A. 88, 7699–7703 (1991).

McPherson, M. C. & Delany, M. E. Virus and host genomic, molecular, and cellular interactions during Marek's disease pathogenesis and oncogenesis. Poult. Sci. 95, 412–429 (2016).

Miles, J. J. et al. TCR genes direct MHC restriction in the potent human T cell response to a class I-bound viral epitope. J. Immunol. 177, 6804–6814 (2006).

Miles, J. J. et al. Genetic and structural basis for selection of a ubiquitous T cell receptor deployed in Epstein-Barr virus infection. PLoS Pathog. 6, e1001198 (2010).

Miller, M. M. & Taylor, R. L. Brief review of the chicken Major Histocompatibility Complex: the genes, their distribution on chromosome 16, and their contributions to disease resistance. Poultry Sci. 95, 375–392 (2016).

Mwangi, W. N. et al. Clonal structure of rapid-onset MDV-driven CD4+ lymphomas and responding CD8+ T cells. PLoS Pathog. 7, e1001337 (2011).

Okazaki, W., Purchase, H. G. & Burmester, B. R. Protection against Marek's disease by vaccination with a herpesvirus of turkeys. Avian Dis. 14, 413 (1970).

Omar, A. R. & Schat, K. A. Characterization of Marek's disease herpesvirus-specific cytotoxic T lymphocytes in chickens inoculated with a non-oncogenic vaccine strain of MDV. Immunology 90, 579–585 (1997).

Parra, Z. E., Mitchell, K., Dalloul, R. A. & Miller, R. D. A second TCR locus in Galliformes uses antibody-like V domains: insight into the evolution of TCR and TCR genes in tetrapods. J. Immunol. 188, 3912–3919 (2012).

Parra, Z. E. & Miller, R. D. Comparative analysis of the chicken $TCR\alpha/\delta$ locus. Immunogenetics 64, 641–645 (2012).

Payne, L. N. & Biggs, P. M. Studies on Marek's disease. II. Pathogenesis. J. Natl. Cancer Inst. 39, 281–302 (1967).

Read, A. F. et al. Imperfect vaccination can enhance the transmission of highly virulent pathogens. PLoS Biol. 13, e1002198 (2015).

Ren, C. et al. CDR3 analysis of TCR V β repertoire of CD8+ T cells from chickens infected with Eimeria maxima. Exp. Parasitol. 143, 1–4 (2014).

Rickinson, A. B. & Moss, D. J. Human cytotoxic T lymphocyte responses to Epstein-Barr virus infection. Annu. Rev. Immunol. 15, 405–431 (1997).

Robinson, C. M., Cheng, H. H. & Delany, M. E. Temporal kinetics of Marek's disease herpesvirus: integration occurs early after infection in both B and T cells. Cytogenet. Genome Res. 144, 142–154 (2014).

Sarson, A. J., Parvizi, P., Lepp, D., Quinton, M. & Sharif, S. Transcriptional analysis of host responses to Marek's disease virus infection in genetically resistant and susceptible chickens: Transcriptional analysis of host response to MDV. Anim. Genet. 39, 232–240 (2008).

Shek, W. R., Calnek, B. W., Schat, K. A. & Chen, C. H. Characterization of Marek's disease virus-infected lymphocytes: discrimination between cytolytically and latently infected cells. J. Natl. Cancer Inst. 70, 485–491 (1983).

Shigeta, A. et al. Genomic organization of the chicken T-cell receptor β Chain D-J-C region. J. Vet. Med. Sci. 66, 1509–1515 (2004).

Six, A. et al. Characterization of avian T-cell receptor genes. Proc. Natl. Acad. Sci. U.S.A. 93, 15329–15334 (1996).

Smithey, M. J. et al. Lifelong CMV infection improves immune defense in old mice by broadening the mobilized TCR repertoire against third-party infection. Proc. Natl. Acad. Sci. U.S.A. 115, E6817–E6825 (2018).

Sowder, J. T. A large subpopulation of avian T cells express a homologue of the mammalian T gamma/delta receptor. J. Exp. Med. 167, 315–322 (1988).

Steininger, C. Clinical relevance of cytomegalovirus infection in patients with disorders of the immune system. Clin. Microbiol. Infect. 13, 953–963 (2007).

Stone, H. A. USDA Tech. Bull. No. 1514, United States Department of Agriculture, Boca Raton. (1975).

Suessmuth, Y. et al. CMV reactivation drives posttransplant T-cell reconstitution and results in defects in the underlying TCR β repertoire. Blood 125, 3835–3850 (2015).

Tian, F. et al. DNMT gene expression and methylome in Marek's disease resistant and susceptible chickens prior to and following infection by MDV. Epigenetics 8, 431–444 (2013).

Tjoelker, L. W. et al. Evolutionary conservation of antigen recognition: The chicken T-cell receptor beta chain. Proc. Natl. Acad. Sci. U.S.A. 87, 7856–7860 (1990).

Vainio, O., Lassila, O., Cihak, J., Lösch, U., and Houssaint, E. Tissue distribution and appearance in ontogeny of alpha/beta T Cell Receptor (TCR2) in Chicken. Cell. Immunol. 1245, 254–260 (1990).

Vallejo, R. L. et al. Genetic mapping of quantitative trait loci affecting susceptibility to Marek's disease virus induced tumors in F2 Intercross Chickens. Genetics 148, 349–360 (1998).

Venturi, V. et al. The neonatal CD8 + T Cell repertoire rapidly diversifies during persistent viral infection. J. Immunol. 196, 1604–1616 (2016).

Witter, R. L. Increased virulence of Marek's disease virus field isolates. Avian Dis. 41, 149-163 (1997).

Witter, R. L. The changing landscape of Marek's disease. Avian Pathol. 27, S46–S53 (1998).

Wynn, K. K. et al. Impact of clonal competition for peptide-MHC complexes on the CD8+ T-cell repertoire selection in a persistent viral infection. Blood 111, 4283–4292 (2008).

Yonash, N., Bacon, L. D., Witter, R. L. & Cheng, H. H. High resolution mapping and identification of new quantitative trait loci (QTL) affecting susceptibility to Marek's disease. Anim. Genet. 30, 126–135 (1999).

Yu, Y. et al. Temporal transcriptome changes induced by MDV in Marek's disease-resistant and susceptible inbred chickens. BMC Genomics 12, (2011).

CHAPTER 2

Contribution of the TCR Repertoire to MD Resistance in the Chicken

Abstract

Marek's disease (MD) is a commonly diagnosed herpesviral-induced T cell lymphoproliferative disease of chickens, which has increased in virulence over time and prompted the search for continued improvements in control, both through improved vaccines and increased flock genetic resistance. Model pairs of genetically MD-resistant and susceptible chickens that are either B2 MHC-matched or B21 and B19 MHC-congenic has allowed the study of both non-MHC-linked and MHC-linked genetic resistance; here, we have applied these models to characterizing the T cell receptor (TCR) repertoires in MDV infection. Chickens resistant to MD showed higher usage of Vbeta-1 TCRs than susceptible chickens, in both the CD8 and CD4 subsets in the MHC-matched model, and in the CD8 subset only in the MHC-congenic model; and Vbeta-1+ CD8 cells expanded during MDV infection. The TCR locus was found to be divergent between MD-resistant and susceptible chickens in the MHC-matched model, with MD-resistant chickens expressing a greater number of Vbeta-1 TCRs and an increased representation of Vbeta-1 CDR1 loops with an aromatic residue at position 45. TCR Vbeta-1 CDR1 usage in resistant x susceptible F1 birds indicated that the most commonly used CDR1 variant was present only in the susceptible line, suggesting that selection for resistance in the MHC-matched model has optimized the TCR repertoire away from dominant recognition of one of the B2 MHC molecules. Finally, TCR downregulation during MDV infection in the MHCmatched model was observed most strongly in the MD-susceptible line, and TCR

downregulation due to viral reactivation in a tumor cell line could be demonstrated to be virusspecific and not due to apoptosis induction.

Introduction

Marek's disease (MD) is a commonly diagnosed T cell lymphoproliferative disease in chickens, first identified as an infectious polyneuritis by Joseph Marek in 1907 (Marek, 1907). The causative agent, Marek's disease virus (MDV) was later identified and characterized as an alphaherpesvirus (Churchill 1967). Since its identification, MDV has been found to cause a series of progressively more severe pathogenic syndromes associated with increasing virulence, likely in response to intensive poultry housing, selection for fast growing chickens, and widespread use of non-sterilizing vaccines (Witter 1997, Atkins 2013, Gimeno 2008, Nair 2005). These syndromes include the development of gross lymphoid tumors, neurologic involvement, and acute early mortality (Payne 1967). While vaccination strategies have proved largely protective within most flocks, virulence shifts occurring historically every 2 or 3 decades (Witter 1997) have prompted the continued search for better control strategies, such as improving genetic host resistance to viral infection and tumorigenesis.

The feasibility of increasing genetic resistance to MD with selection-based methods was demonstrated through the development of a series of highly inbred layer lines of differing MD resistance in at Cornell (Cole 1968) and at our laboratory (Stone 1975, Bacon 2000). Early research into genetic based MD resistance focused on the MHC (Briles 1977), as MHC haplotype was found to exert a major effect on resistance to the disease, with the B21 haplotype conferring particularly high resistance (Cole 1968, Briles 1977, Bacon 2000, reviewed in Miller

2016). Research into mechanisms of MHC-based resistance has identified differences in the frequency of peptide MHC class I binding motifs between several alleles (Koch 2007, Sherman 2008, Chappell 2015). However, differential genetic resistance to MD is still possible in the context of fixed MHC haplotype, as demonstrated by Line 6 and Line 7, which are inbred resistant and susceptible layer lines, respectively, with a shared B2 haplotype MHC. This indicates that there is additional contributing non-MHC genetic variation to MD resistance which, if characterized, could be used in rational breeding strategies to develop highly MD-resistant chicken lines. One caveat is that prior genetic screens of Line 6 and Line 7 have failed to identify any single locus beyond the MHC as a major contributing factor (Cheng 2015), so contributing mechanisms are likely to be polygenic and complex, prompting us to take a broader look at the integrated immune systems of these differentially susceptible lines rather than relying solely on linkage-based genetic screens.

Genomic screens of Lines 6 and 7 have been performed at the DNA, transcriptome, and epigenetic levels (Vallejo 1998, Yonash 1999, Liu 2001, Luo 2013, Luo 2012a,b, Tian 2013). Not surprisingly, immune genes and immune pathways are frequently identified as associated with differential response to infection in this model, and differentially expressed genes such as CD8a, IL8, CTLA-4, IL17A, and IL12Rb2 implicate T cell transcriptional pathways in MD resistance (Yu 2011). Recently, transcriptomics work in our laboratory has identified many candidate resistance genes and pathways that are differentially expressed (DE) or regulated (showing allele-specific expression, ASE) by MD infection in line 6 and 7 (MacEachern 2011, 2012; Perumbakkam 2013). Multiple immune pathways including innate (TLRs, apoptosis), NK cell and cytokine signaling (JAK-STAT) pathways have been identified using these techniques. In

addition, studies of local cytokine expression in the spleens of MDV-infected birds have indicated that susceptible Line 7 birds primarily upregulate genes in the T-regulatory and TH-2 response paradigms, while Line 6 birds have a more robust TH-1 component to their immune response (Kumar 2009).

Early studies on the functionality of T cells in MD-resistant and susceptible lines focused on bulk lymphocyte responses to nonspecific mitogens, such as lectins (Fredericksen 1983, Lee 1983, Calnek 1989). Differential T cell proliferation capacity was offered as a potential source of variability in either cellular immunity or oncogenic transformation. However, results have conflicted between studies, with whole blood proliferation assays suggesting a consistently higher ConA mitogen response in the susceptible Line 7 even when very different T cell counts are taken into consideration (Fredericksen 1983) while purified lymphocyte assays indicate that Line 6 and Line 7 do not differ in PHA mitogen response (Lee 1983). Functional assays of specific T cell subsets were not performed, as these studies occurred prior to the development of T cell marker-specific antibodies.

Increasing knowledge about the immunobiology of non-mammalian species, including avians, has allowed us to begin characterizing the T cell responses of these species to important pathogens. Functionally, the chicken T cell receptor system appears to overlap, at least broadly, with mammalian immunity, with homologous TCR complex components, including TCR heterodimers, CD3 chains, and CD4 and CD8 co-receptors (Chen 1988, Chen 1989, Vainio 1990, Berry 2014, Luhtala 1998). Importantly, the avian immune system is characterized by reductions in the size of antigen receptor multi-gene blocks, including MHC, TCR and immunoglobulin loci, possibly as an adaptation to flight (Kaufman 2000, Parham 1999); while

recombinatorial diversity is preserved in B and T cells through VDJ recombination, pre-existing diversity in MHC loci and the TCR and BCR genes available for recombination is reduced, which may allow larger selection effects to occur in the immune receptors of birds, and precipitate an "arms race" between avian pathogens and their hosts (Kaufman 2000). For example, the MHC locus only encodes two genes each of class I and class II (reviewed in Miller 2016), and these appear to be co-evolving with antigen processing machinery in order to maximize utility for response to specific pathogens (Kaufman 2000). Similarly, the chicken TCR beta locus includes approximately 10 variable genes (less than a one-third that of a mouse), and these can be categorized into only two families of closely related genes (Lahti 1991).

Here, we show that the TCR beta repertoire of MD resistant Line 6 chicken and susceptible Line 7 chicken are divergent, and that this divergence correlates with differences in CD8+ T cell responses, but not CD4+ T cell responses, in vivo. Additionally, we demonstrate that MHC haplotypes that show differential MD resistance also induce differences in the TCR beta repertoire of CD8+ T cells. Together, these findings suggest that the streamlined avian TCR system can be optimized either for, or against, resistance to pathogens such as MDV, and, due to its reduced size, may be more susceptible to changes induced by natural or artificial selection.

Materials and Methods

Animals and Viruses

Experiment 1:

Birds were housed and managed according to ADOL IACUC guidelines, and all experiments were performed in accordance with ADOL IACUC-approved animal use protocols. Chicks from ADOL Lines 6 and 7 (Stone 1975) were housed in Horsfall-Bauer isolators at 1 day post hatch and given food and water ad libitim. Moribund birds were removed and humanely euthanized within 24 hours. For experiment 1, replicates 1 and 2, chicks were inoculated at 1 day post hatch with 500 pfu of Md5 strain MDV by intraperitoneal injection. Birds were humanely euthanized at the specified collection days and spleens were collected for flow cytometry. Experiment 2:

A single replicate was conducted as in Experiment 1; however, chicks from ADOL MHC congenic lines 15.B19 and 15.B21 were used for this experiment (Bacon 2000).

Flow Cytometry

Spleens were homogenized to single-cell suspension in LM media (50% Lebowitz, 50% McCoy's 5A) and counted. For each sample, ~1 million cells were immunolabelled with the following antibody panel: CD3-Alexa Fluor 700 (clone CT-3, Southern Biotech); CD8 α -FITC (clone 11-39, Bio-Rad); CD8 β -APC (clone EP42, Novus); TCR $\alpha\beta$ Vb1-PE (clone TCR2, Southern Biotech); TCR $\alpha\beta$ Vb2-SPRD (clone TCR3, Southern Biotech). Samples were washed three times in PBS with 1% FBS (FACS buffer) and resuspended in FACS buffer for analysis. Flow cytometry was

performed on BD Influx or BD FacsCalibur machines. Data were analyzed in Flowjo versions 9 and 10 (Treestar, Inc.).

Reactivation Assay

Lymphocyte cell lines were routinely cultured in RPMI-1640 (ATCC) with 20% FBS, penicillin (100 IU/mL, streptomycin (100 ug/mL), and 1 x Gluta-Max (Invitrogen). For reactivation assays, cells were cultured at $1e^6$ cells/mL in the same media containing 10 ug/mL BrdU, or anti-CD3 (Southern Biotech) and anti-CD28 (Southern Biotech) antibodies at diluted equal concentrations ranging from 1:250 to 1:1000. Additional samples were cultured in wells which were pre-coated with anti-TCR α β Vb1 (clone TCR2; Southern Biotech) antibody at 1:100, 1:200 or 1:1000 dilution in PBS and rinsed with PBS prior to plating. At 48 hours, a 3/4ths-volume media replacement was performed for controls, BrdU, and anti-TCR α β Vb1 samples; anti-CD3/CD8 samples showed slowed growth and did not require media replacement. At 72 hours, samples were washed in PBS and labelled for flow cytometry with anti-TCR α β Vb1-PE (clone TCR2; Southern Biotech) or anti-MHC class II-PE (clone 2G11; Southern Biotech). Samples were analyzed by flow cytometry prior to and after immunolabelling.

Reactivation-Inhibition Assay

This assay was performed similarly to the reactivation assays except that cells were preincubated for 1 hour with 20 uM, 50 uM, or 100 uM of the caspase inhibitor compound Z-VAD-FMK (Santa Cruz Biotechnologies), or an equivalent volume of vehicle (2 uL/mL, 5 uL/mL, or 10 uL/mL DMSO) prior to addition of either 40 ug/mL BrdU, or anti-CD3/CD28 antibodies at 1:500 dilution. Z-VAD-FMK and BrdU were maintained in the media throughout the 72-hour culture, while additional anti-CD3/CD28 antibodies were not added during media replacement.

Proliferation Assay

Spleens from birds of 5 days old or less were pooled in groups of 4; samples from birds 7 days to 21 days were pooled in groups of two; and spleens from birds older than 21 days of age were assayed individually. Spleen lymphocytes were purified by gradient centrifugation over Histopaque-1077 (Sigma) and labelled with a fluorescent tracking dye (Cell Trace Far Red; Thermo-Fisher). 2e^6 cells/sample were cultured in 2 mL of IMDM (ATCC) with 8% FBS, 2% heat-inactivated chicken serum, plus penicillin/streptomycin. Additionally, concanavalin-A (ConA; 10 ug/mL; Sigma) or phytohaemagluttinin (PHA; 100 ug/mL; Sigma) were included in the media to stimulate proliferation, and samples were incubated at 41 °C in 5% CO₂ for 72 hours. Assays were prepared in triplicate when possible (depending on sample yields), and combined after incubation and prior to immunolabelling with anti-CD4-FITC (clone CT-4, Southern Biotech) and anti-CD8α-PE (clone CT-8, Southern Biotech). Immunolabelled samples were analyzed on a BD FacsCalibur machine.

Cell Cycle Analysis Assay

Spleens from 15-day old birds were pooled in groups of 2; spleens from 29-day old birds were processed individually. Spleen lymphocytes were purified by two rounds of gradient centrifugation over Histopaque-1077 (Sigma). Spleen lymphocytes were cultured for 48 hours with ConA or PHA as in the proliferation assays, then pulsed for 1 hour with 1 uL EdU/2mL

sample using the Far-Red Click-IT EdU Kit (Thermo Fisher) and click-labelled for EdU detection according to kit methods. Cells were immunolabelled with anti-CD4 and anti-CD8 antibodies subsequent to click-labelling and analyzed on a BD FacsCalibur machine.

Spectratyping Assay

CDNA was prepared from spleen samples preserved at -20 °C in RNAlater, using the Superscript II kit (Invitrogen) or High Capacity cDNA kit (Molecular Bio) and oligo-dT primers. Nested PCR was performed for TCR Vbeta-1 and TCR Vbeta-2 using the primers and methods as described in Hunt (2011). PCR products were diluted at 1:200 and fragment analysis was performed on an ABI (Applied Biosciences, Inc.) 3730xL machine.

DNA Sequence Analysis

Pooled blood cell samples from 7 birds of each line were previously extracted for DNA, from which Illumina libraries were prepared and sequenced by 100-bp Illumina sequencing.

Sequence data was aligned in BWA (Li., 2013) against the GalGal5 reference genome (Warren 2017) with default parameters, de-duplicated, and locally realigned. Vbeta-1 regions were identified within the reference sequence by BLAT search using published annotated chicken TCRbeta mRNAs. Mapped reads which overlapped these regions were realigned to a reference sequence for Vbeta-1 (Genbank ABU93628.1), and variants were called using Freebayes v. 1.2.0 (Garrison et al., 2012), using 3-bp and 10-bp haplotype windows. Long-window haplotypes

within the CDR1 region were identified manually in IGV (Robinson et al., 2011; Thorvaldsdóttir, 2013).

CDR3 Identification in RNA Sequence Data

Illumina RNA sequencing data from magnetic-column-sorted, MDV-infected Line 6x7 F1 CD4+ splenocytes was analyzed for the presence of CDR3 sequences via a custom script which searches for a set of conserved primer sequences (identified across Genbank submissions of chicken TCRbeta mRNAs) in proximity to the Vbeta and joining ends of the CDR3 region, using the fastq-grep tool (Jones, 2012). This custom script was developed for analysis of MD tumor clonality and is available online at GitHub (Appendix; Steep et al., in preparation).

Vbeta-1 CDR1 Haplotyping of RNA Sequence Data

Illumina RNA-seq data generated from a previously published study was analyzed for TCR Vbeta-1 usage. Briefly, Line 6x7 F1 hybrid chicks were infected at 2 weeks post hatch with 2,000 pfu of Md5 strain MDV or uninfected. At 4 days post-infection, spleen samples were collected, RNA extracted and 100 bp paired-end Illumina HiSeq RNA-seq was performed (Perumbakkam et al., 2013). RNA-seq data was quality-checked with FastQC v. 0.11.7 (Andrews, 2010), reads were trimmed to 90 bp with FastX-trimmer (Gordon, 2009), and aligned to the GalGal5 reference genome with BWA-MEM (Li., 2013). Alignment files were converted to BAM format, sorted and indexed, and reads mapping to chr1:78000000-78300000 (a region spanning the TCRbeta locus) were obtained using Samtools v. 1.9 (Li, 2009). The resulting truncated alignment files were converted to fastq sequences with Samtools, re-aligned in BWA

against a reference TCR Vbeta-1 sequence [Genbank ABU93628.1], and mapped reads from pair mates 1 and 2 were merged into a single alignment file using Samtools. TCR Vbeta-1-mapping alignments from 7 infected and 7 uninfected birds were analyzed together in Freebayes to identify CDR1 haplotypes, using the following commandline flags:

[--haplotype-length 40 -r <vb1_sequence>:190-240 -C 4 --pooled-continuous], which allows haplotype construction of up to 40 bp in length, limits the search to a 50-bp region spanning the CDR1 mutational hotspot, requires a minimum of 4 calls per haplotype, and treats the sample ploidy as unknown.

Protein Sequence Analysis

A Vbeta-1 protein structure was modeled for the chicken TCR beta reference sequence published in Genbank (ABU93628.1, submitted by Xia,C., Yang,T. and Zhang,T, 2007; contains Vbeta-1 and Jb4.2 segments; residues 17-257 were modelled), using default SWISS-MODEL parameters (Waterhouse et al, 2018; Bienert et al, 2017) with a crystallography-supported mouse TCR-pMHC structure as the template (PDB ID 3mbe.1.E; Yoshida et al., 2010). Substitutions were made in the Vbeta segment and re-modelled against the 3mbe.1.E template, followed by structural comparison between models in Raptor-X (Wang et al, 2013; Ma et al, 2013).

PacBio Long Read DNA Sequencing

Blood samples from one healthy adult male bird each of Lines 6 and 7 were extracted for DNA using a non-column method, which involved overnight lysis in SDS/TE buffer with proteinase K,

protein precipitation with Qiagen Precipitation Solution and ethanol precipitation of the soluble DNA phase to minimize shearing. DNA samples were resuspended in distilled water and submitted for PacBio Sequel sequencing by the USDA-ARS Genomics and Bioinformatics Unit (Stoneville, MS). Read correction, overlapping and de novo assembly was performed using Canu v. 1.8 (Koren et al, 2017), and assemblies were examined for contig continuity using Blast+ v. 2.7.1 (Zhang et al, 2000) and Bandage v. 0.8.1 (Wick et al, 2015). Alignment of TCR Vbeta sequences was performed with Clustal Omega (Sievers 2014).

Statistics

In vivo data was analyzed by three-way analysis of variance in JMP (SASS, Inc.) followed by post-hoc Tukey's tests for significance. In vitro data was analyzed by 2-way ANOVA with Bonferonni-corrected post-hoc Student's T testing in Excel (Microsoft, Inc.). TCR spectratyping data was analyzed for total divergence score (Memon, et al., 2012), using the following formula: Total Divergence Score = $\Sigma(|x_{peak fractional area} - \overline{x}_{c peak fractional area}|)$

Results

In vitro splenic T cell proliferation in response to mitogens are similar between Lines 6 and 7.

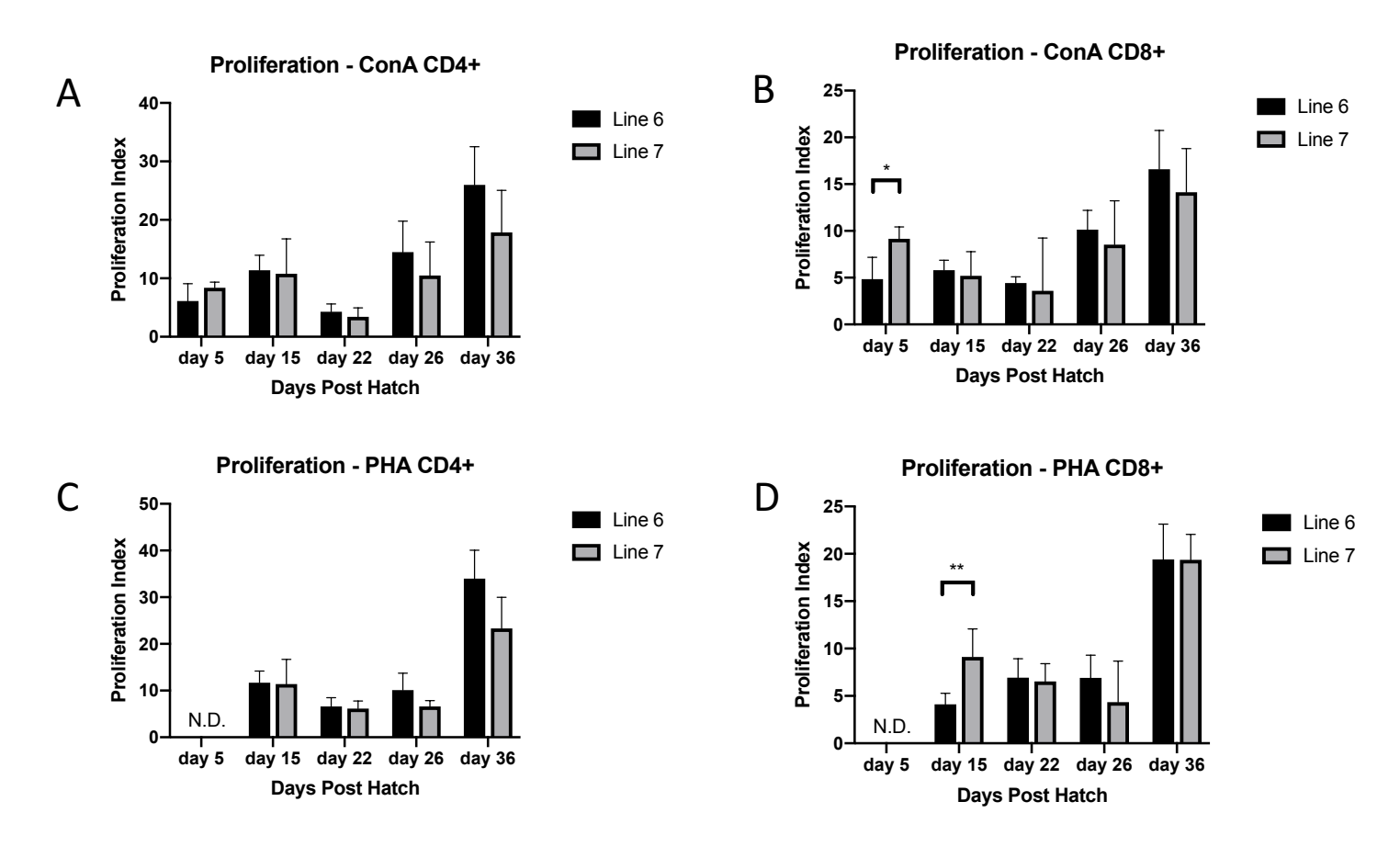
We compared the proliferative responses to lectin mitogens within the splenic CD4+ and CD8+

T cell subsets in MD-resistant (Line 6) and susceptible (Line 7) chickens. We separately analyzed the response of CD4+ and CD8+ populations to ConA and PHA stimulation using CellTrace cell labelling for proliferation, and confirmed that the proliferation indices of both cell types, as well as the samples in bulk, did not generally differ significantly between lines, except for CD8+ cells

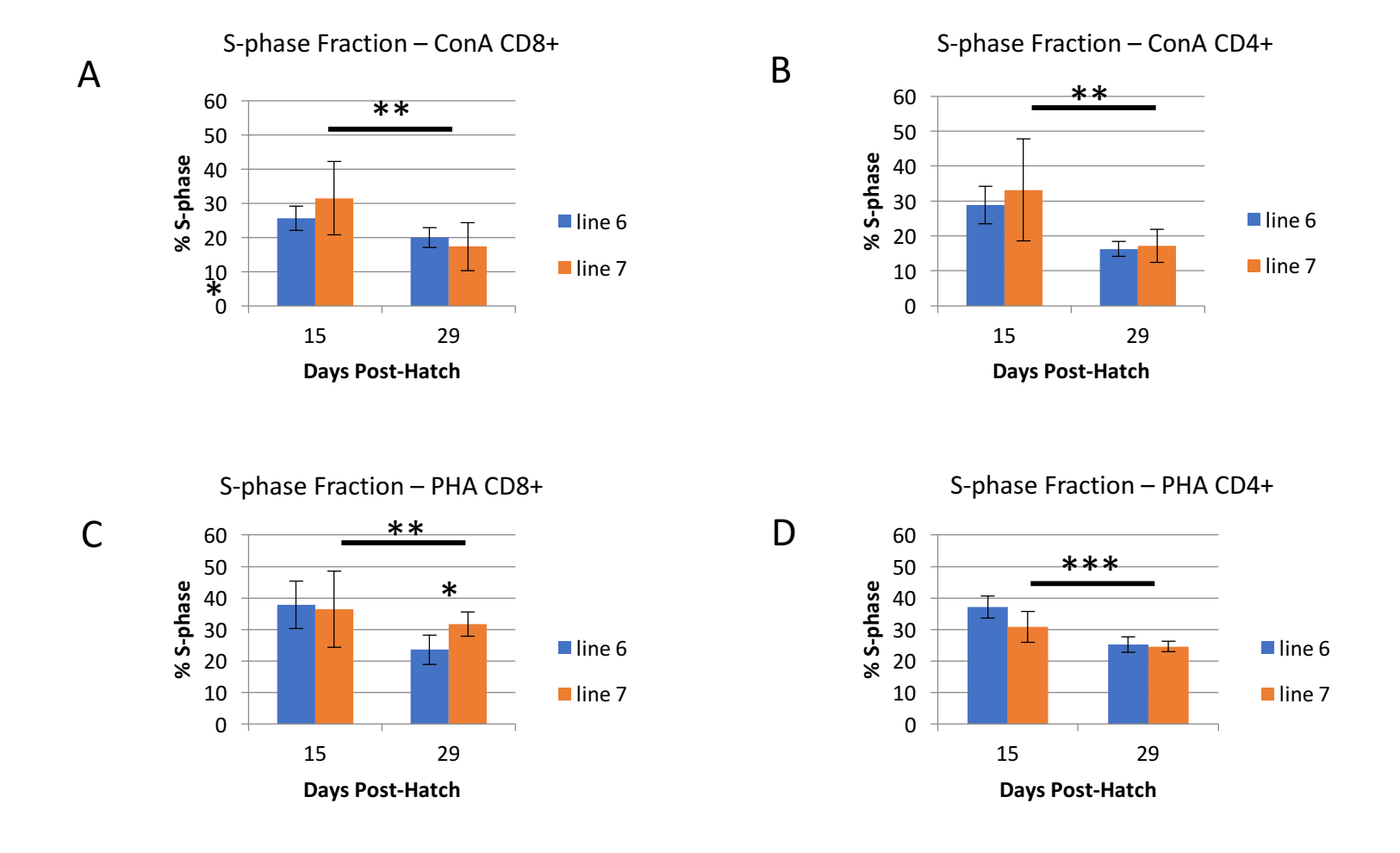
at one early timepoint for each mitogen in Line 7 (Figure 2.1A-D). In addition, we performed EdU-incorporation assays for cell cycle analysis and found that the percent of T cells entering S phase after 48 hours of stimulation were similar for both lines (Figure 2.2A-D; data representative of 2 replicates), again except for a mild increase in CD8+ T cells proliferating in Line 7 in response to PHA at 29 days of age (Figure 2.2C).

Lines 6 and 7 differentially express TCR $\alpha\beta$ Vb1 and TCR $\alpha\beta$ Vb2.

We examined the $\alpha\beta$ (classical) TCR repertoire of spleen cells in Line 6 and Line 7 chickens naively and during MDV infection over time. As shown in Figure 2.3A and 2.3B, CD3+ T cells from both lines used TCR $\alpha\beta$ Vb1 more frequently than TCR $\alpha\beta$ Vb2, (consistent with previous literature on TCR usage in the chicken; see Chen 1983); however, Line 6 splenocytes were more strongly biased towards TCR $\alpha\beta$ Vb1, with 50-65% of their cells expressing TCR $\alpha\beta$ Vb1, and only about 10% expressing TCR $\alpha\beta$ Vb2. In contrast, 20-30% of Line 7 splenocytes expressed TCR $\alpha\beta$ Vb2, with a proportional reduction in TCR $\alpha\beta$ Vb1 compared to Line 6. During infection, the proportion of TCRαβVb1-expressing CD3+ splenocytes expanded in Line 6 only in replicate 2 (p<0.026 at 8 days post infection), and in both lines in replicate 1 (p<0.05 for both lines by 21 days post infection) (Figure 2.3A); however, expression of TCR $\alpha\beta$ Vb2 was more tightly controlled and minimally affected by infection status, suggesting that $TCR\alpha\beta Vb2+$ cells may respond poorly to MDV antigens (Fig. 2.3B). In replicate 2, splenocytes were examined on day 0 of infectious challenge, i.e. 1 day of age; interestingly, TCR $\alpha\beta$ Vb1 was much lower in both lines at 1 day of age, while TCR $\alpha\beta$ Vb2 usage was intermediate between lines at this earliest timepoint and diverged within the first week of life (Figure 2.3A-B)



<u>Figure 2.1. Splenic T cell proliferation.</u> Proliferation of splenic T cells generally did not differ between Lines 6 and 7 in response to lectin mitogens, with the exception of early CD8+ T cells. Pooled white cell fractions from the spleens of chicks at the ages indicated were stimulated with 10 ug/ml of ConA or 100 ug/mL of PHA for 72 hours. For each assay (timepoint), N=4-6 sample pools per group. Groups were compared within assay by Student's t-test. * = p<0.05; ** = p<0.01.

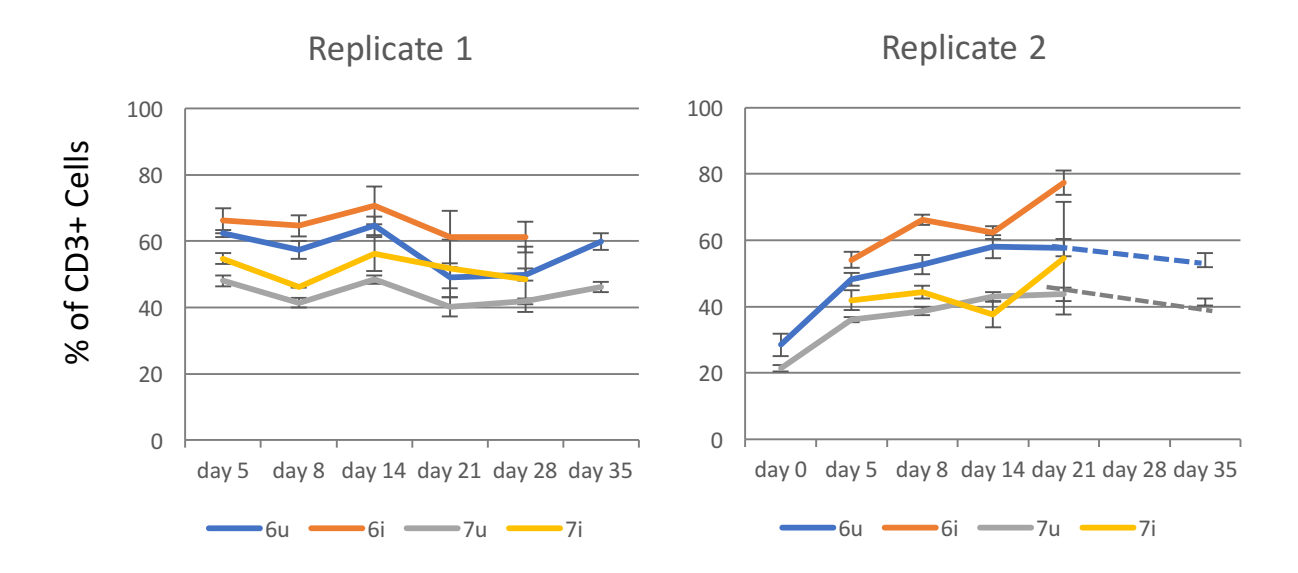


<u>Figure 2.2. S-phase fraction.</u> A,B: CD4+ and CD8+ lymphocytes from resistant and susceptible lines showed no difference in 1 hr Edupulsed S-phase fraction at 15 and 29 days of age in response to ConA. Both lines showed a similar reduction in S-phase fraction at 29 days of age (p< 0.01, 2-way ANOVA). C,D: At 29 days of age, more PHA-stimulated CD8+ lymphocytes were in S-phase in Line 7 than Line 6 (corrected p value = 0.026). Both lines showed a reduction in S-phase fraction at 29 days of age (p<0.01 and p<0.0001, 2-way ANOVA). For each assay (timepoint), N=4-6 sample pools per group. * = p<0.05; ** = p<0.01.

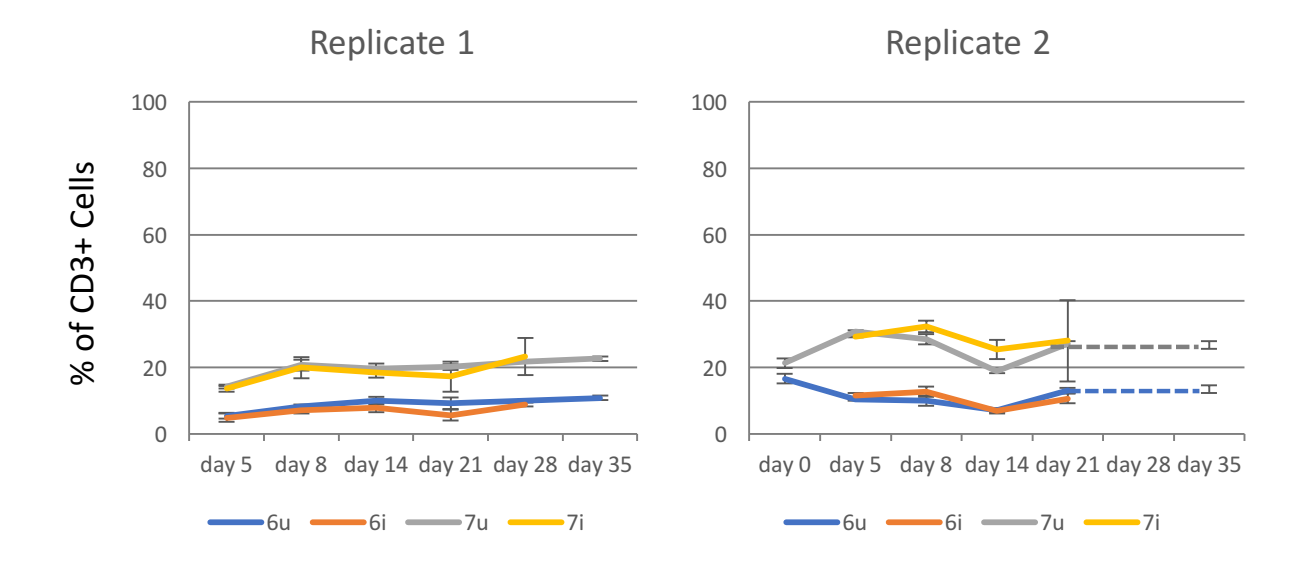
We additionally examined the TCR repertoire of CD8+ CD3+ T cells (cytotoxic T cells). In experiment 1, we included antibodies against both the CD8a and CD8b chains in our flow cytometry panel, which allowed us to examine the classical CD8ab T cell population, while in the second replicate we only used the CD8a antibody to identify CD8+ T cells, as CD8aa cells made up only 5-10% percent of the CD8+ population in replicate 1. The between-line differences were similar to in bulk T cells. However, upon infection, we observed a significant (p<0.05) bias toward higher TCR $\alpha\beta$ Vb1 usage in the CD8+ T cells of Line 6 birds in replicate 2, beginning on day 8; and in replicate 1, this bias was observed across both lines (p<0.001), but only day 21 in Line 6 was individually statistically significant (p=0.002) (Figure 2.3C). In contrast, TCR $\alpha\beta$ Vb2 usage in CD8+ cells was tightly controlled in Line 6 in both replicates, but was mildly expanded in Line 7 birds relative to controls after 2 weeks of age only in replicate 2 (p=0.025) (Fig. 2.3D).

We examined the TCR repertoire of CD4+ CD3+ T cells in replicate 2. In contrast to the CD8+ T cells, the CD4+ population showed no effect of MDV infection on TCR usage until day 14, at which time non-statistically significant reductions in TCR usage occurred in both $TCR\alpha\beta Vb1$ and $TCR\alpha\beta Vb2$ subsets. By 21 days post-infection, individual birds variably became highly biased toward one or the other subset, as is expected from the development of clonal T cell tumors. The lack of a $TCR\alpha\beta Vb1$ or $TCR\alpha\beta Vb2$ response in the CD4+ subset prior to day 21 suggests that highly focused CD4 T cell proliferation was not a component of the immune response to MDV infection (Figure 2.3E).

A CD3+ TCR $\alpha\beta$ Vb1 splenocytes



B CD3+ TCR $\alpha\beta$ Vb2 splenocytes

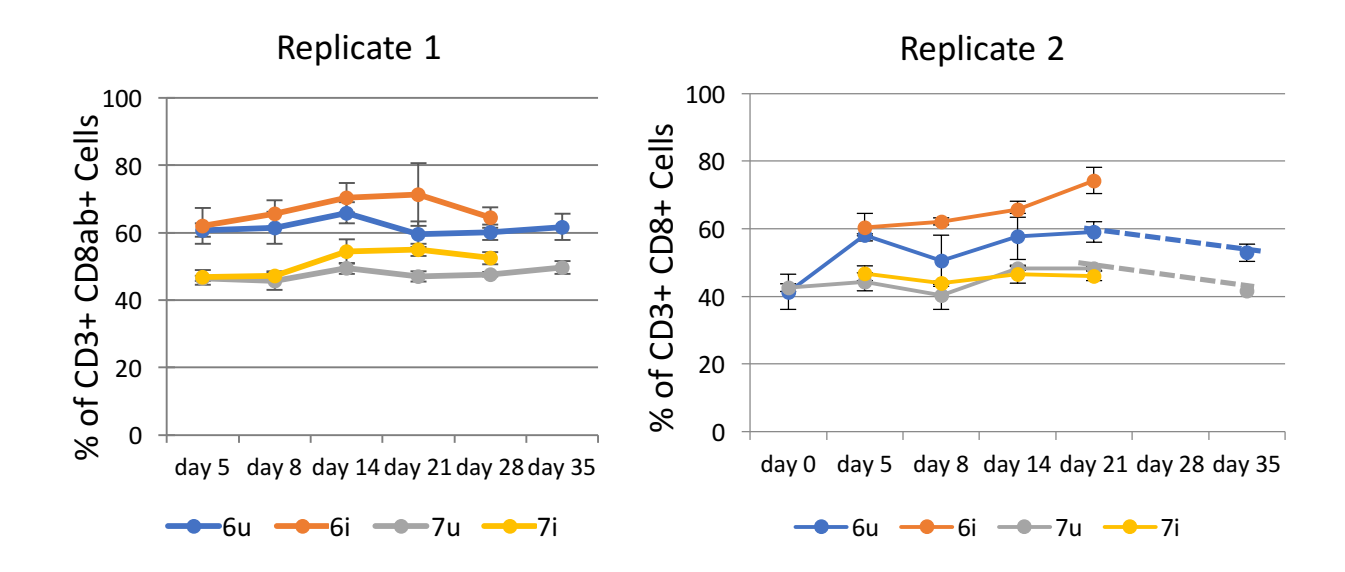


<u>Figure 2.3. TCR usage in MHC-matched lines.</u> Splenocytes from line 6 and 7 were analyzed at indicated times. Resistant birds used $TCR\alpha\beta Vb1$ at a greater frequency within the splenic T cell population than susceptible birds. A: $TCR\alpha\beta Vb1$ was responsive to MDV infection in splenic T cells of line 6 (resistant) birds in both replicates, and in line 7 (susceptible) birds in replicate 1. B: $TCR\alpha\beta Vb2$ was minimally responsive to infection in splenic T cells of either line 6 or line 7 birds.

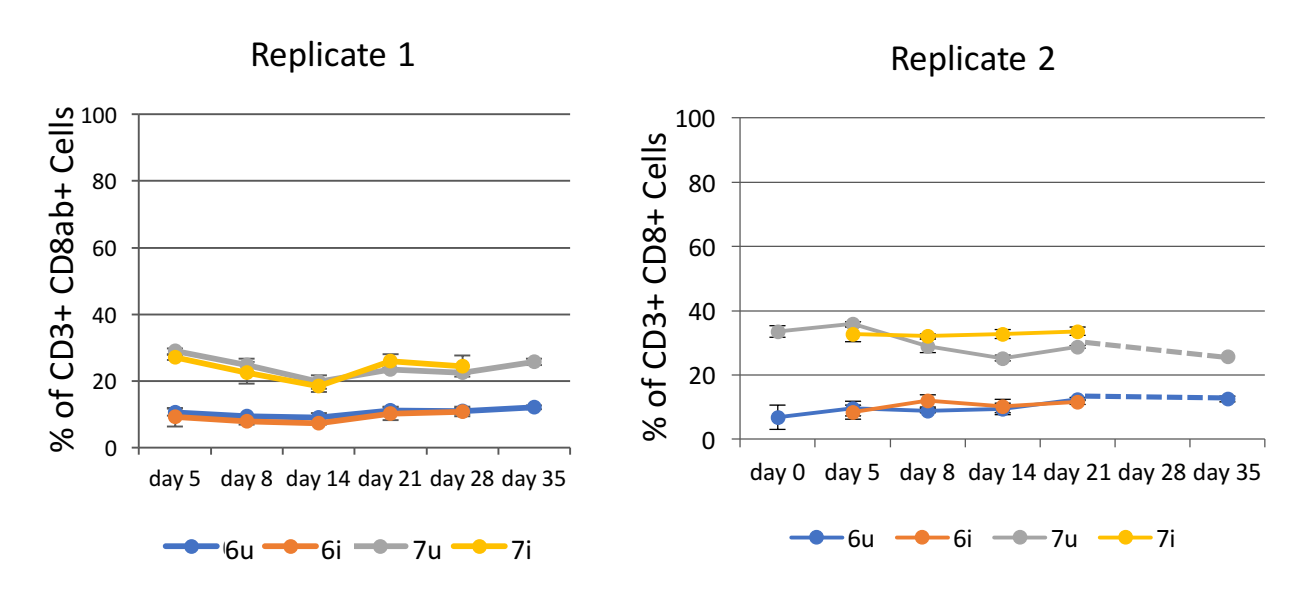
Figure 2.3 (cont'd).

C

CD3+ CD8+ TCR $\alpha\beta$ Vb1 splenocytes



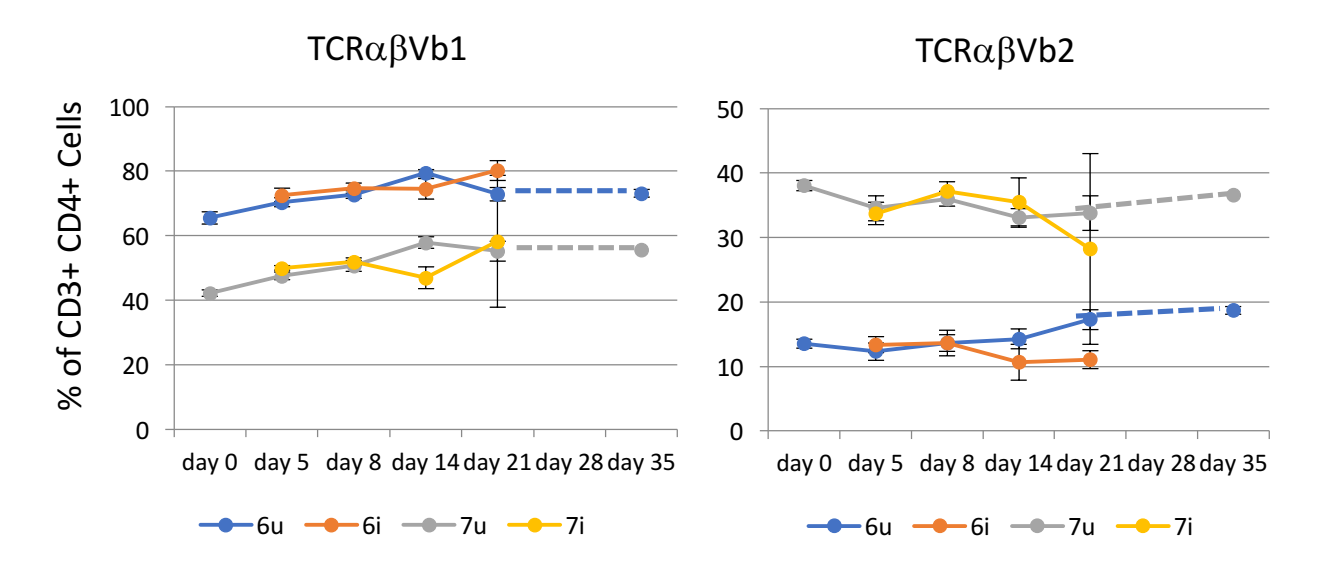
D CD3+ CD8+ TCR $\alpha\beta$ Vb2 splenocytes



C: $TCR\alpha\beta Vb1$ responds to MDV infection in CD8+ splenocytes of resistant birds (p<0.01), and also shows non-MHC-based genetic selection (p<0.001). D: $TCR\alpha\beta Vb2$ was minimally responsive to infection, but showed strong non-MHC-based selection in CD8+ splenocytes (p<0.001). In replicate 1, triple-staining CD3+ CD8ab+ T cells were measured, while in replicate 2, dual-staining CD3+ CD8a+ T cells were measured.

Figure 2.3 (cont'd).





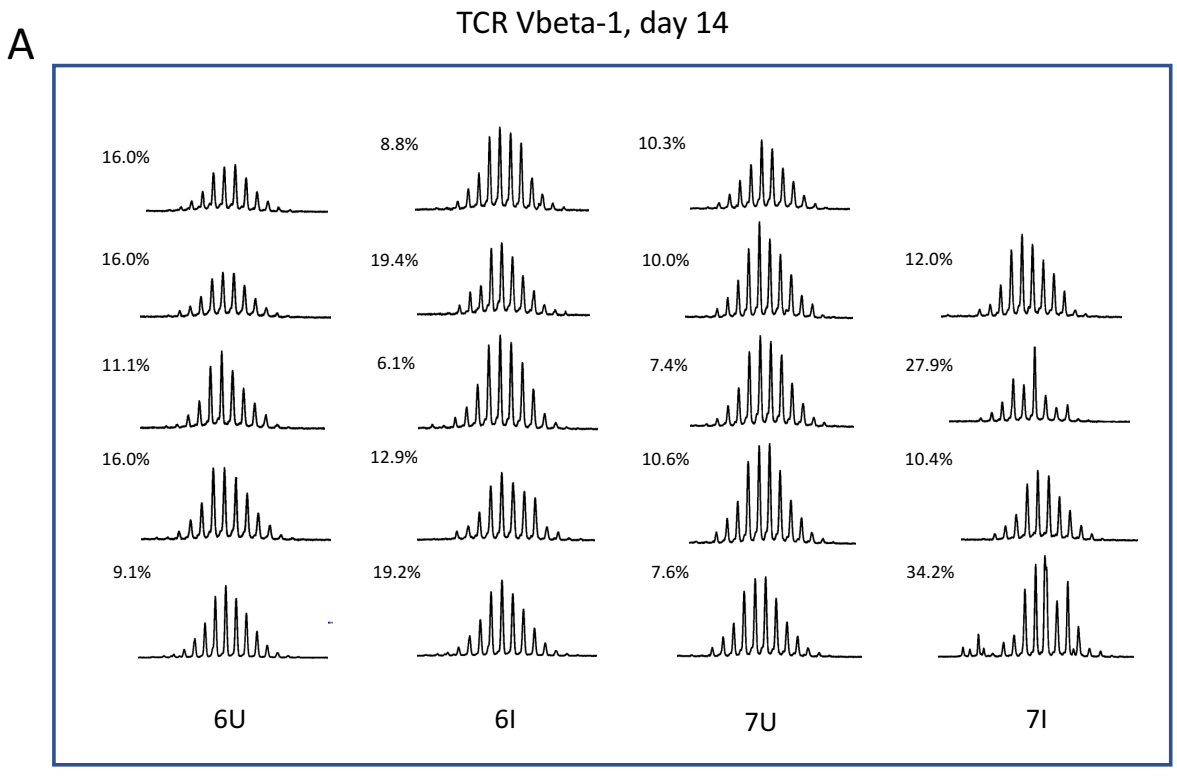
E: CD4+ splenocytes were examined in replicate 2. Neither TCR was responsive to early MDV infection in CD4+ splenocytes, but both showed non-MHC-based selection in CD4+ splenocytes (p<0.001). For replicate 1, N=4 sample pools of 3 birds each per group at day 5; N=4 birds per group at days 8-28; and N=6 birds per control group at day 35. For replicate 2, N=2-3 sample pools of 3 birds per group at each timepoint from days 0 and 5; N=5 birds per group from days 5-21; and N=5 and 8 birds per control group for lines 6 and 7, respectively, at day 35. U=uninfected, i=infected.

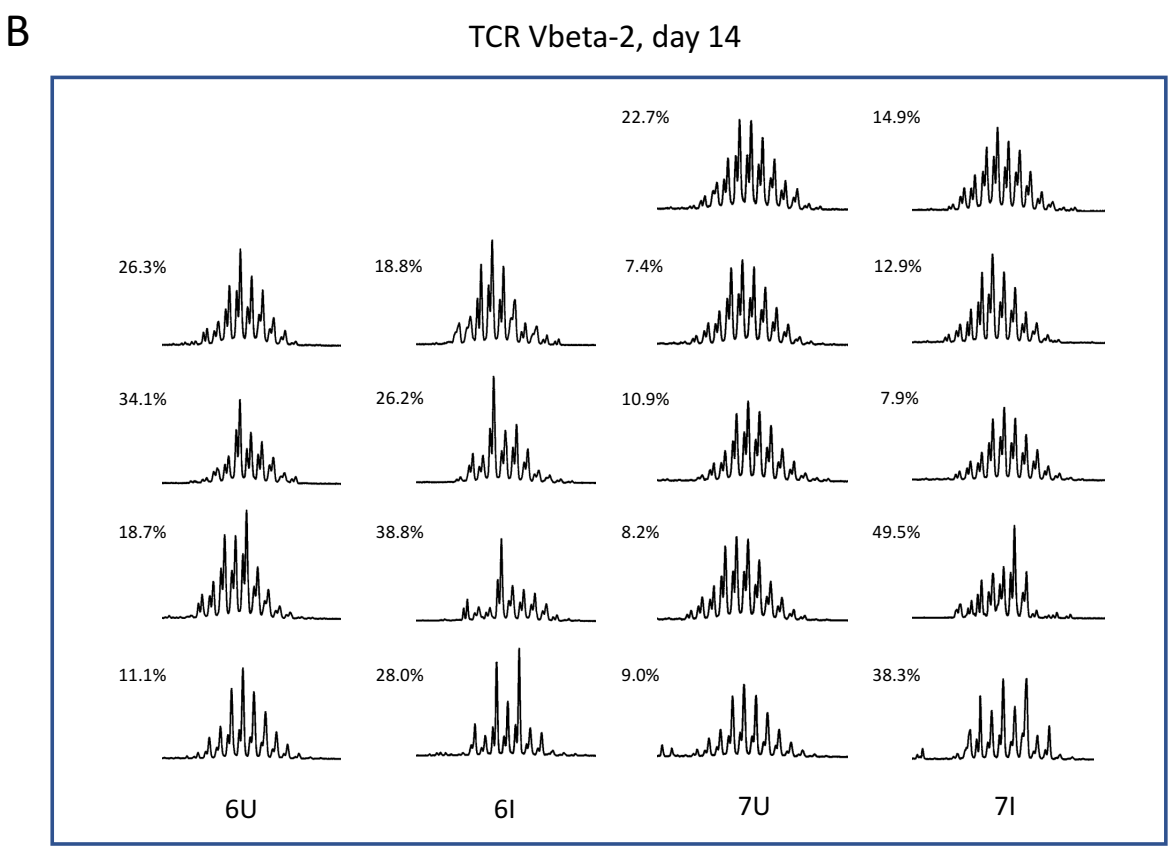
TCR spectratype analysis demonstrates early clonal responses to MDV infection in both resistant and susceptible birds.

We performed TCR spectratyping on spleen tissue from MD-resistant Line 6 and MD-susceptible Line 7 birds at multiple stages of MDV infection. We were able to identify clonal expansion in bulk TCR Vbeta-1 and TCR Vbeta-2 T cell populations in infected birds as early as 14 days post-infection (Figure 2.4A-B), which can be identified as an increase in total deviation score compared to the control samples, especially in the spleens of susceptible Line 7 birds, but also particularly in the TCR Vbeta-2 subset in resistant Line 6 birds. Both lines showed clonal expansion in TCR Vbeta-1 populations by day 21, but only Line 7 showed the development of strong individual clones, consistent with tumor formation occurring only in these birds (Figure 2.4C-D).

Lines B.21 and B.19 differentially express TCR $\alpha\beta$ Vb1 and TCR $\alpha\beta$ Vb2 in the CD8+, but not CD4+ splenocyte populations.

Our initial model of genetic host resistance to MD involved inbred bird lines that share the same MHC haplotype (B2) but differ at non-MHC loci. We also compared TCR usage in a genetic resistance model comparing two congenic lines that differ at the MHC locus but share the same genetic background (including TCR loci), in order to demonstrate whether MHC-TCR interactions are important for determining genetic differences in T cell immunity. As shown in Figure 2.5A we found that CD4+ T cells did not differ in usage of $TCR\alpha\beta Vb1$ and $TCR\alpha\beta Vb2$ receptors between congenic lines B.21 (genetically resistant to MD) and B.19 (genetically susceptible to MD), or in response to MDV infection. As in the Line 6 and Line 7 birds,

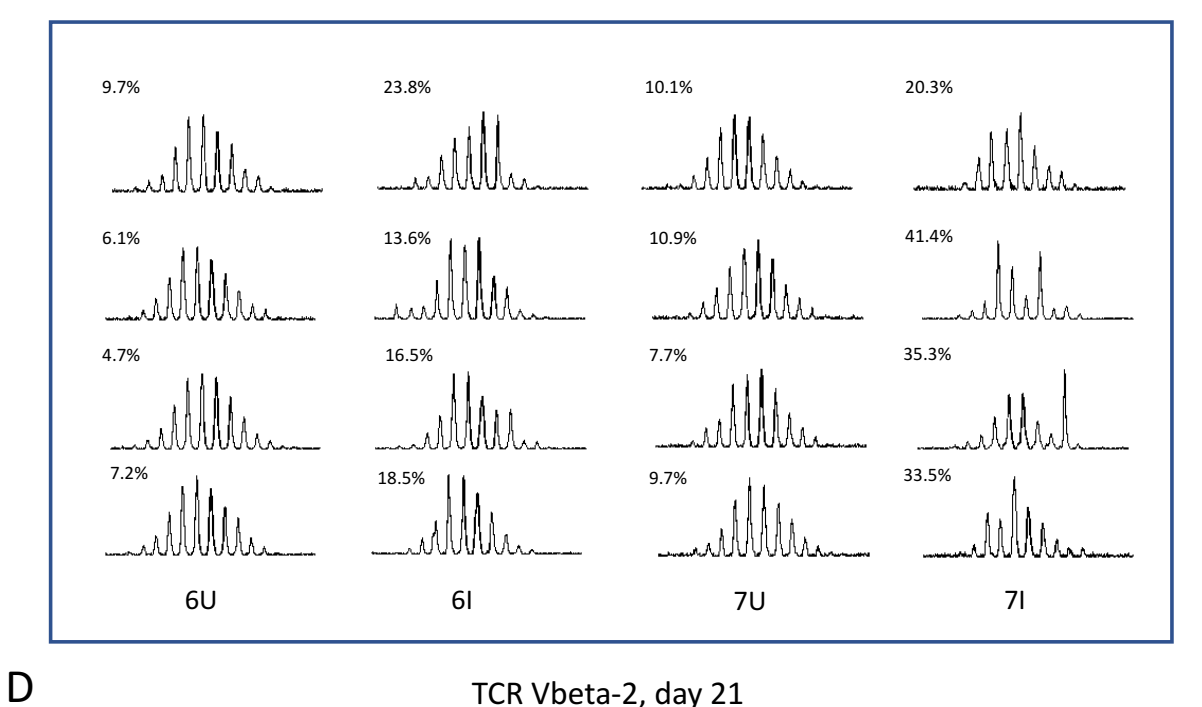




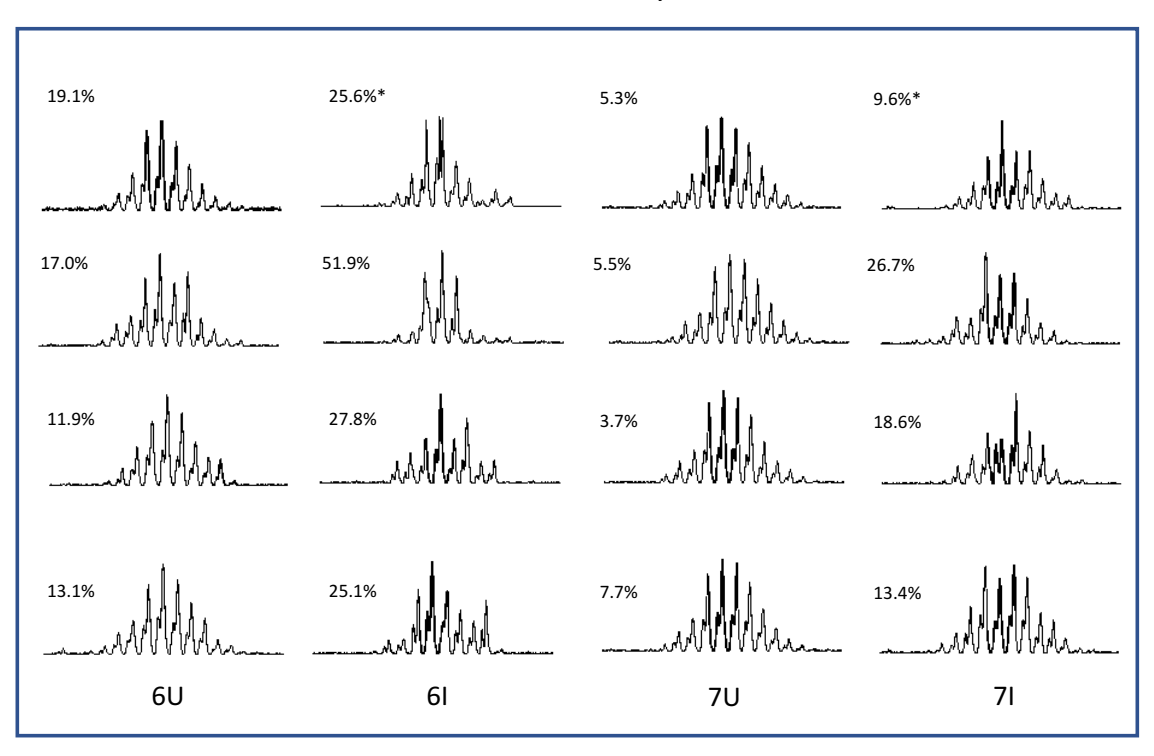
<u>Figure 2.4. TCR spectratyping of splenocytes from MHC-matched lines.</u> Divergence scores are indicated. A, B: TCR Vbeta-1 and 2 PCR fragments at 14 days post-infection with MDV.

Figure 2.4 (cont'd).





TCR Vbeta-2, day 21



C,D: TCR Vbeta-1 and 2 PCR fragments from 21 days post-infection with MDV. *=contains a saturating peak; divergence score is estimated. U=uninfected, I=infected.

TCR $\alpha\beta$ Vb1+ T cells make up a much greater percentage of splenic T cell populations (approximately 90% of CD4+ T cells) than TCR $\alpha\beta$ Vb2+ T cells (approximately 10% of CD4+ T cells). In contrast, TCR usage in splenic CD8+ T cells in the spleen differed mildly between lines, suggesting that intra-thymic MHC class I (but potentially not MHC class II) has a direct effect on establishing the TCR repertoire in this model of MD resistance. As in the MHC-matched resistance model, the MD-resistant line tended to use TCR $\alpha\beta$ Vb1 at a higher rate than the MDsusceptible line on CD8+ T cells. Within the CD8+ population, TCR $\alpha\beta$ Vb2 showed no significant response to MDV infection, as in the Line 6 and Line 7 model. However, the $TCR\alpha\beta Vb1$ population was responsive to MDV infection (p<0.001), with Line B.19 (susceptible) gradually increasing in TCR $\alpha\beta$ Vb1 usage in CD8+ T cells until day 21 post infection, at which time both lines were essentially using this receptor at the same level (Figure 2.5B). We also analyzed the TCR usage on peripheral blood lymphocytes in this model, and found that infection resulted in an approximately 10-15% decrease in TCRαβVb1 usage in blood CD8+ T cells within both lines during days 8-14 of infection (p<0.05) (Figure 2.5C).

TCR usage in Line 6C.7 congenic lines is tightly controlled and TCR $\alpha\beta$ V1+ lymphocyte fraction correlates with MD resistance.

We examined baseline TCR usage within the blood PBMCs of a panel of Line 6 x Line 7 recombinant congenic lines (RCS), which have been developed to allow linkage analysis of parental line phenotypes and have been characterized for lymphoid organ size (Zhang 2006), and in the case of several lines, for MD resistance (Yonash 1998). We found that TCR usage was tightly controlled, especially in the CD4+ population (Figure 2.6A-C). TCR usage did not correlate

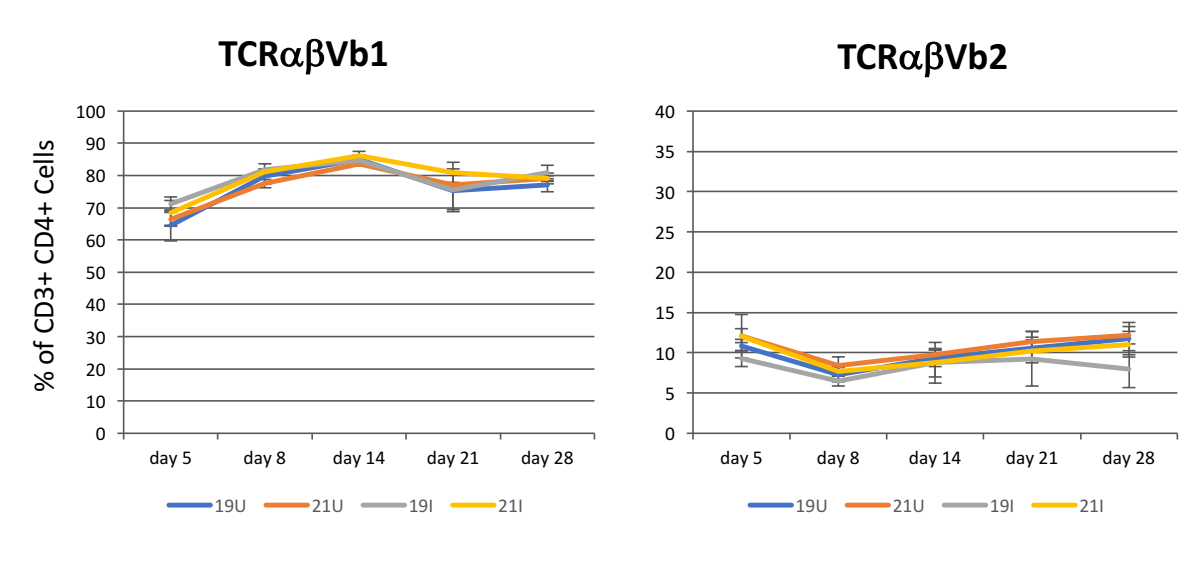
with organ size, which is known to vary strongly across these lines (Zhang 2006) but does not correlate directly with MD resistance. While TCR usage within the T cell population did not directly correlate with resistance in the lines with known relative resistance to MD, the fraction of TCRV $\alpha\beta$ Vb1+ T cells in the total PBMC population was highest in congenic lines known to be relatively resistant to MD (Figure 2.6D), suggesting that the role of TCR usage in MD resistance may involve interactions with other factors to determine the available immune repertoire. We were unable to uniquely identify a genomic region segregating across these lines in the same pattern as TCR usage within previously collected microarray data; however, several lines were not fixed at the time of genetic testing and several low-producing lines have been rescued with backcrossing to Line 6, so additional typing of genetic markers of these lines as they currently exist would be necessary to perform a valid linkage analysis.

Lines 6 and 7 encode differing TCR variable beta-1 genes.

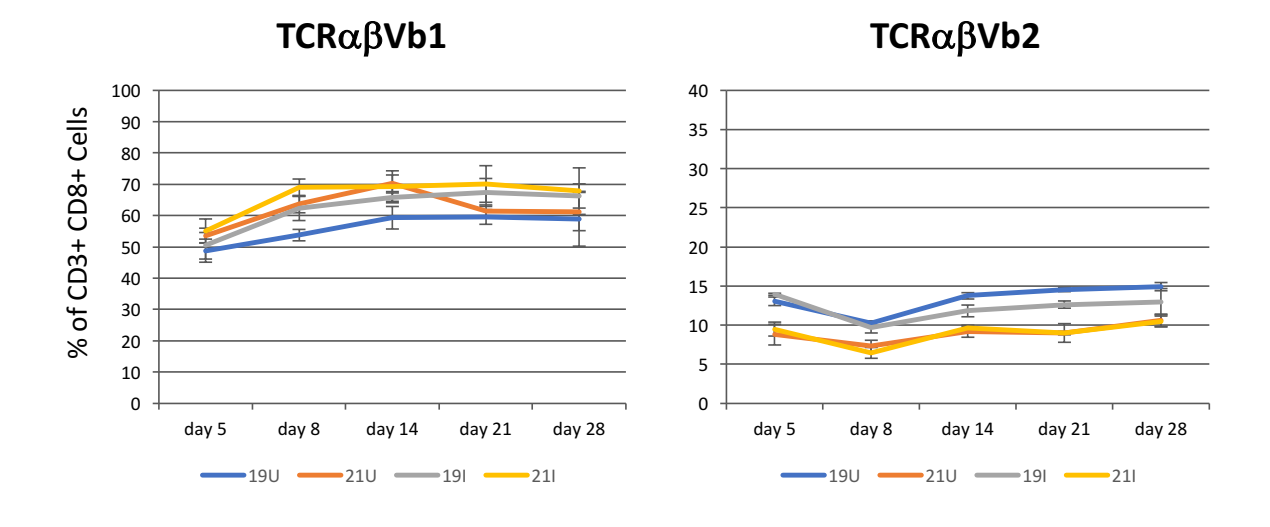
We compared the genomic TCR Vbeta-1 sequences from Illumina DNA-seq data generated from pooled blood collected from MD-resistant Line 6 and MD-susceptible Line 7. While short (92-bp) read Illumina data does not provide sufficient read-length to uniquely map reads to Vbeta genes, we estimated diversity at the Vbeta-1 locus by aligning all Vbeta-1-mapping reads to a single model Vbeta-1 gene and calling variants. Interestingly, 62 variants in Vbeta-1 could be identified in Line 6, in contrast to 46 variants in Line 7, using a short, 3-bp haplotype window in Freebayes. When more complex haplotypes were considered (10-bp haplotype window), a large proportion of variants (29% of 41 variants) in Line 6 were found to have more than 3 non-

Α

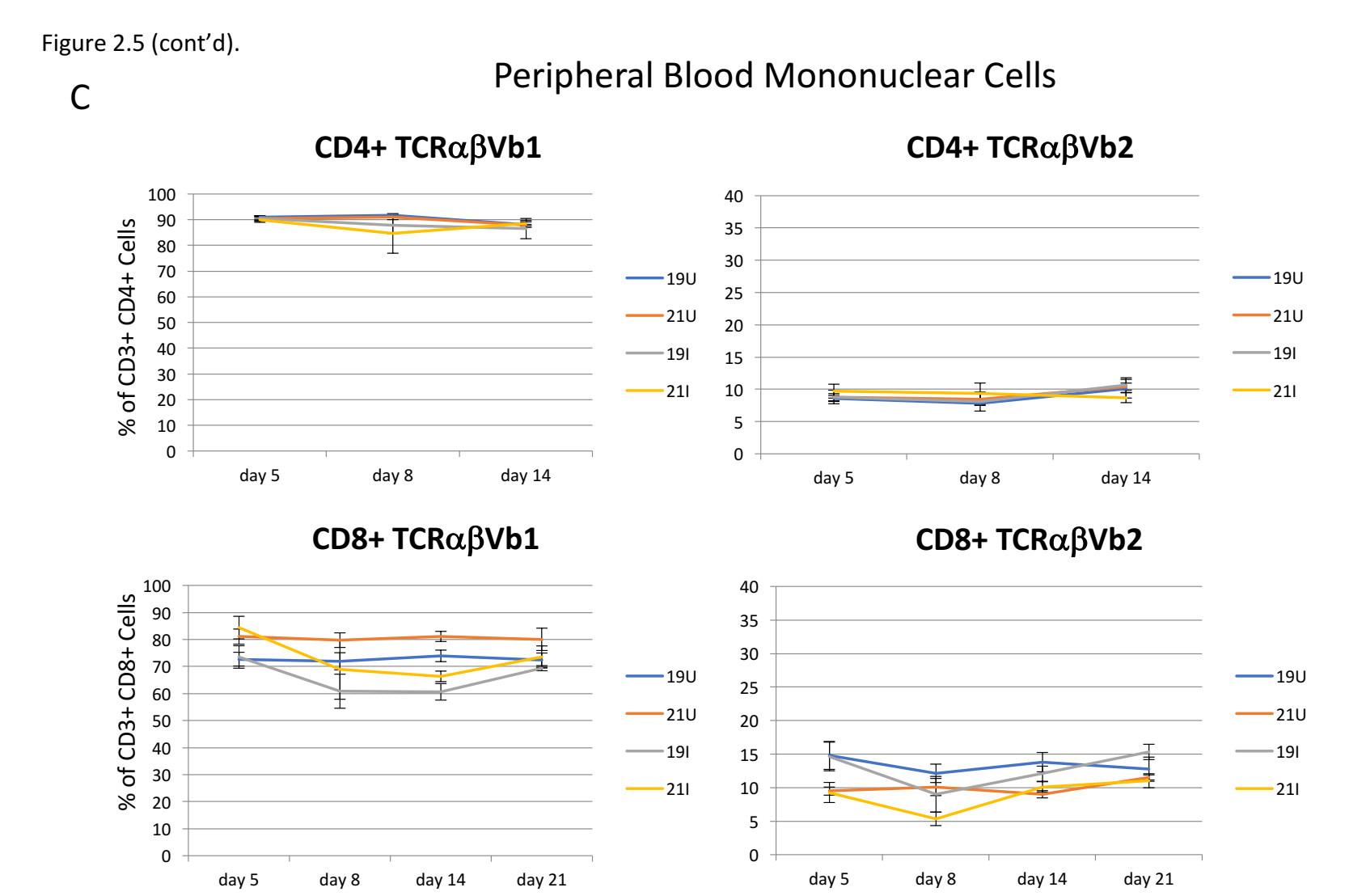
CD3+ CD4+ splenocytes



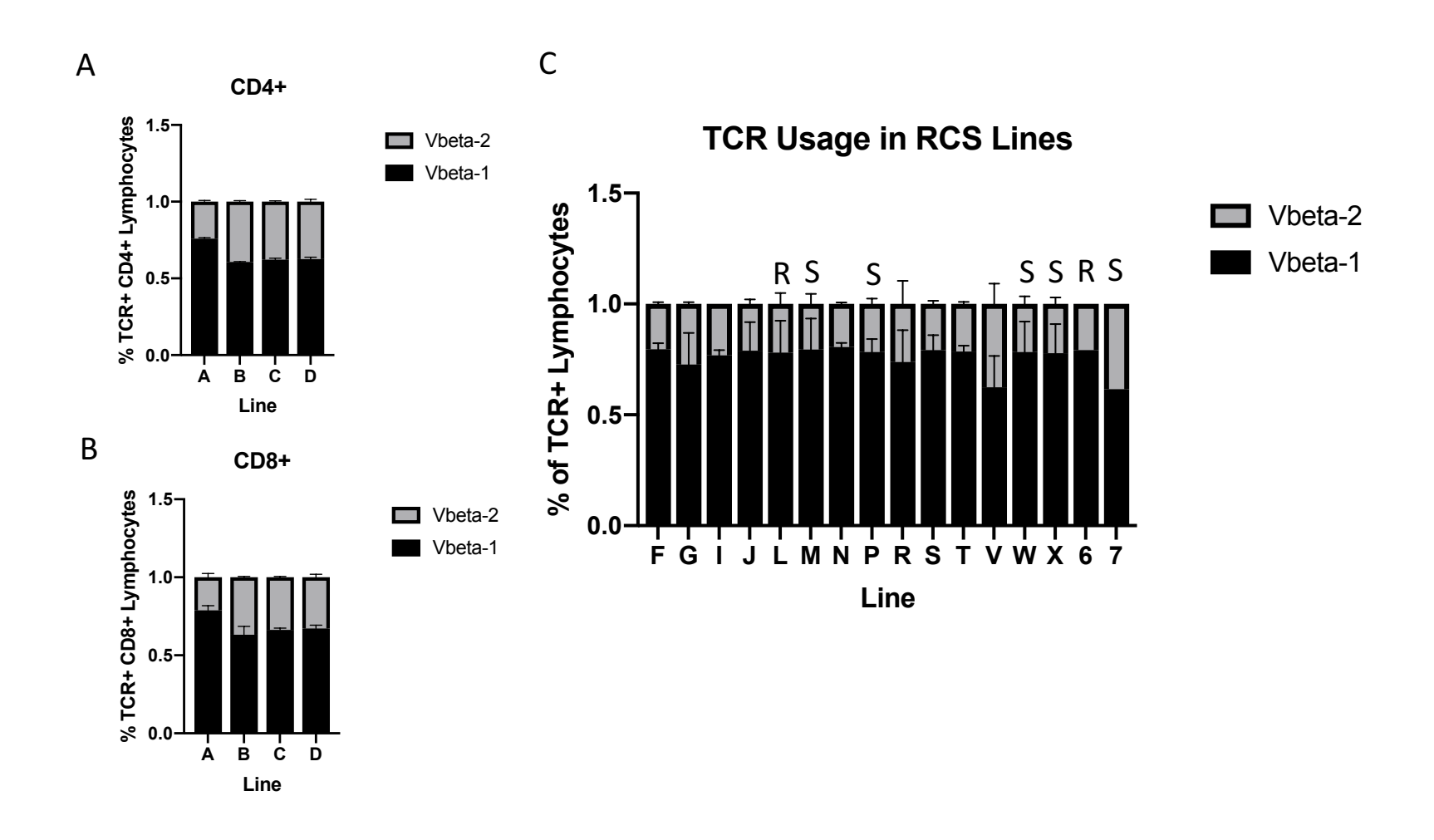
B CD3+ CD8+ splenocytes



<u>Figure 2.5. TCR usage in MHC congenics.</u> Days post-infection with MDV are indicated. A: TCR families are not differentially responsive to either MDV infection, or MHC haplotype, in CD3+ CD4+ splenocytes. B: $TCR\alpha\beta Vb1$ was mildly responsive to both MDV infection and line (p<0.001), while $TCR\alpha\beta Vb2$ responded primarily to MHC haplotype in CD3+ CD8+ splenocytes (p<0.001).

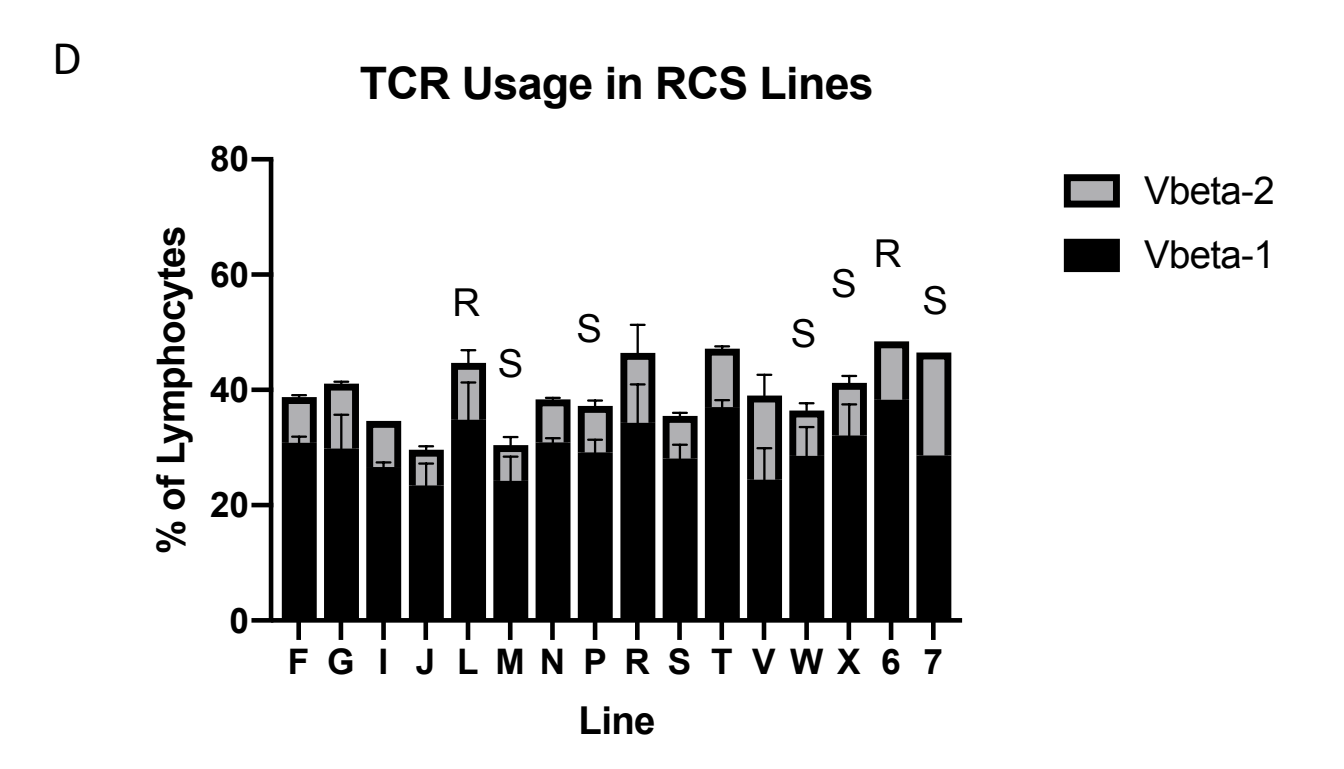


C: $TCR\alpha\beta Vb1+ CD8+ T$ cells, but not $TCR\alpha\beta Vb1+ CD4+ T$ cells, were reduced in peripheral blood during days 8-14 of acute MDV infection in both resistant B.21 and susceptible B.19 MHC-congenic birds (p<0.05). N=4 birds per group. U=uninfected, I=infected.



<u>Figure 2.6. TCR usage in RCS lines.</u> A-B: TCR usage in RCS lines A-D was compared within CD4+ and CD8+ peripheral blood mononuclear cell populations. C: TCR usage within RCS lines F-X was compared within all TCR+ cells falling within the lymphocyte gate on FSC vs SSC. Parental strains 6 and 7 are included as controls. Relatively resistant and susceptible lines are indicated where known.

Figure 2.6 (cont'd).



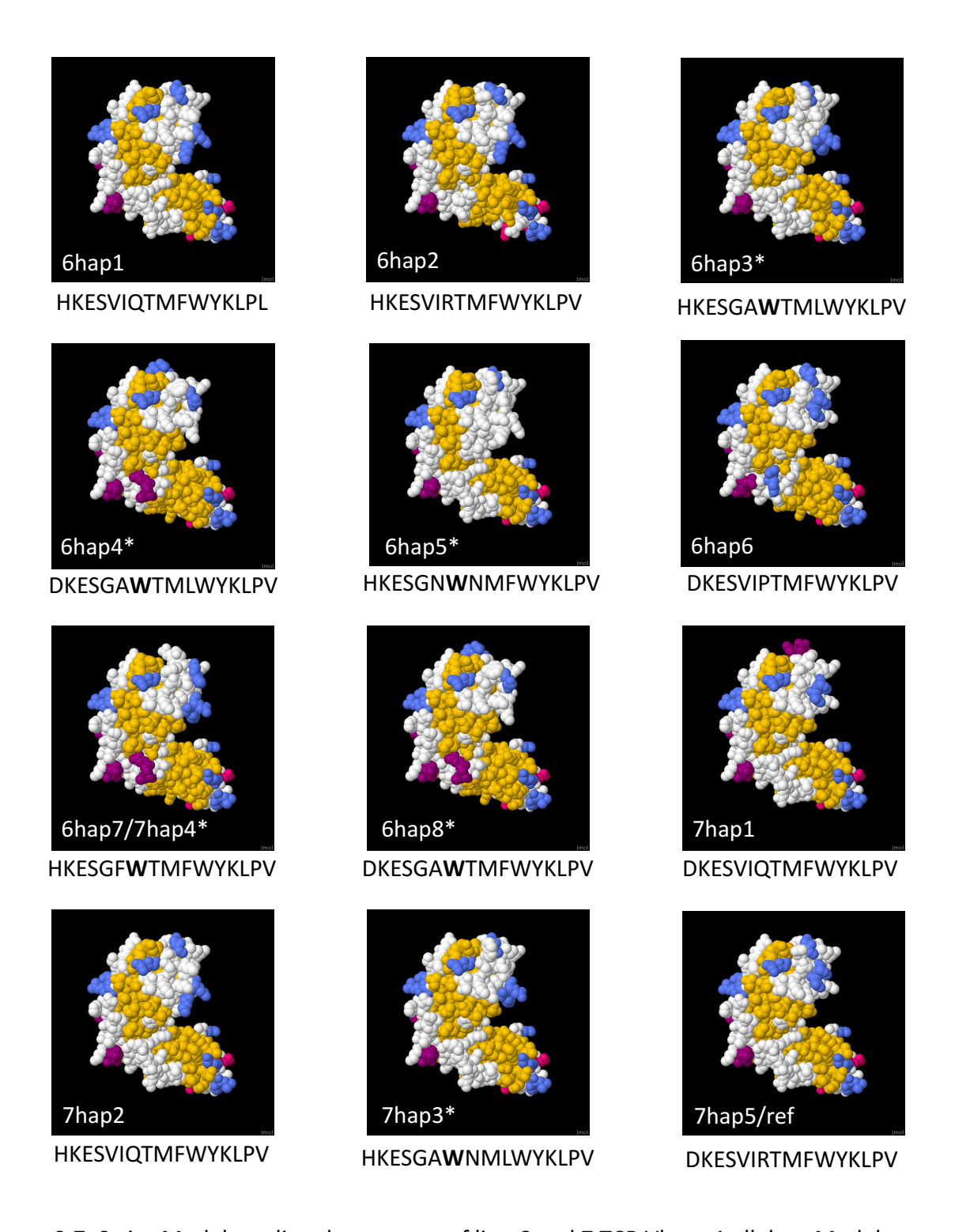
D: TCR usage within RCS lines F-X was compared within the total peripheral blood lymphocyte population as gated on FSC vs. SSC. Relatively resistant and susceptible lines are indicated where known. N=2 individuals per line.

reference alleles, while only 15% of 34 variants in Line 7 had this many non-reference alleles, indicating that there is greater variation present in the TCR Vbeta-1 sequences of Line 6₃.

A variant hotspot located at the CDR1 loop allowed manual identification of longer (85-bp; 27-amino acid) haplotypes in spanning reads; interestingly, 7 unique Vbeta-1 haplotypes could be identified in Line 6 (Figure 2.7), while only 4 unique haplotypes could be identified in Line 7 at this site, with 1 additional haplotype shared between lines. We modelled these CDR1 sequences in the context of a published TCR beta chain (GenBank ABU93634.1), using a crystallography-supported mouse TCR-pMHC complex as a modelling framework; chicken TCR beta adopted the expected two-immunoglobulin domain structure (suppl. Figure 2.S1). CDR1 sequence affected the predicted shape of the CDR1 loop and its interaction with the CDR3 loop (Figure 2.7, suppl. Figure 2.S1), and the aromatic amino acid Trp was substituted for Arg45 in the CDR1 loop of 5 out of 8 Vbeta-1 haplotypes in Line 6, versus 2 out of 5 haplotypes in Line 7.

In order to estimate TCR Vbeta-1 gene usage at the mRNA level, we compared the usage of Vbeta-1 CDR1 haplotypes in a pre-existing Illumina RNA-seq dataset from MDV-infected and uninfected spleens of first-generation (F1) hybrids of Line 6 and Line 7, at 4 days post-infection.

Using Freebayes, we identified 9 different 32-bp (10-amino acid) haplotypes within the CDR1 site, each uniquely identifiable as one of the 12 haplotypes identified by DNA sequencing; and estimated usage of each haplotype within sample (Figure 2.8). At 4 days post-infection, there was no significant change in usage of any TCR Vbeta-1 gene within the total TCR Vbeta-1 pool between infected and uninfected birds. However, the amino acid sequence "SHKESVIQTM" (with glutamine falling at position 45) was over-represented in both infected and uninfected samples, with a haplotype from the Line 7 parentage encoding this sequence comprising



<u>Figure 2.7. Swiss-Model predicted structures of line 6 and 7 TCR Vbeta-1 alleles.</u> Models were built by incorporating the indicated CDR1 haplotypes into a reference TCR Vbeta-1 sequence and predicting each structure against a murine template. One allele (6hap7/7hap4) was shared between lines. *=indicates the presence of a Trp-45 substitution (also indicated in bold within the CDR1 haplotype).

TCR Vb1 CDR1 Haplotypes

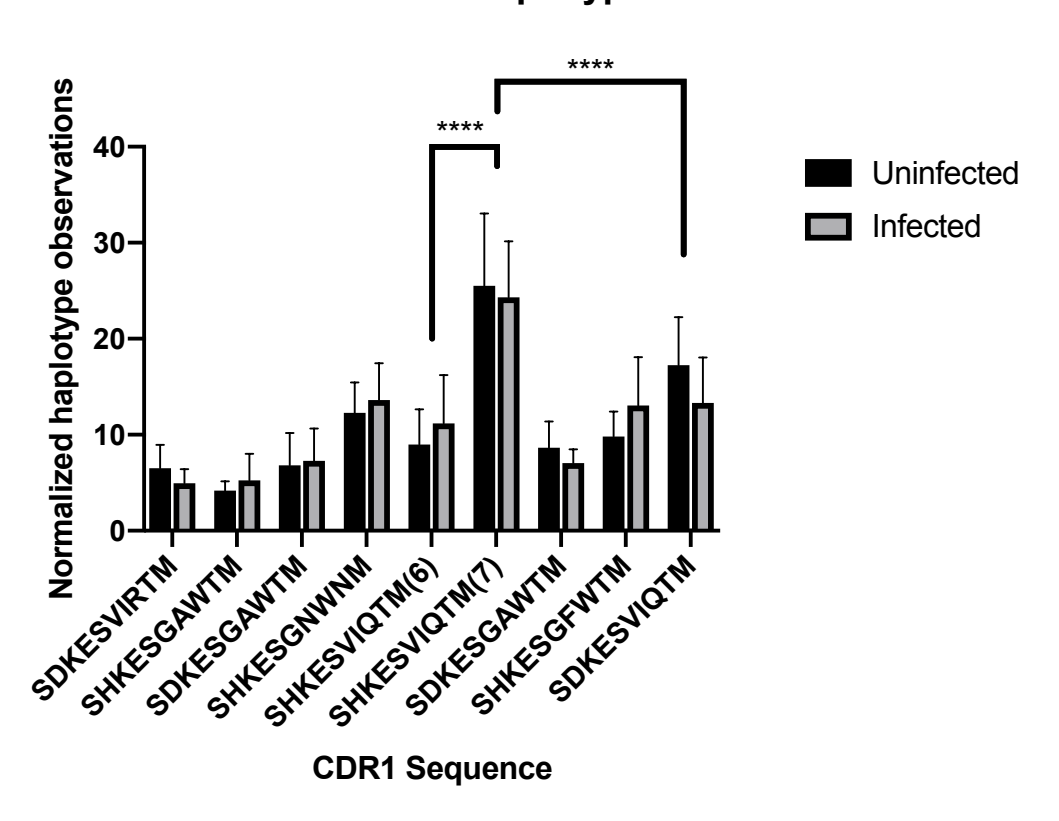


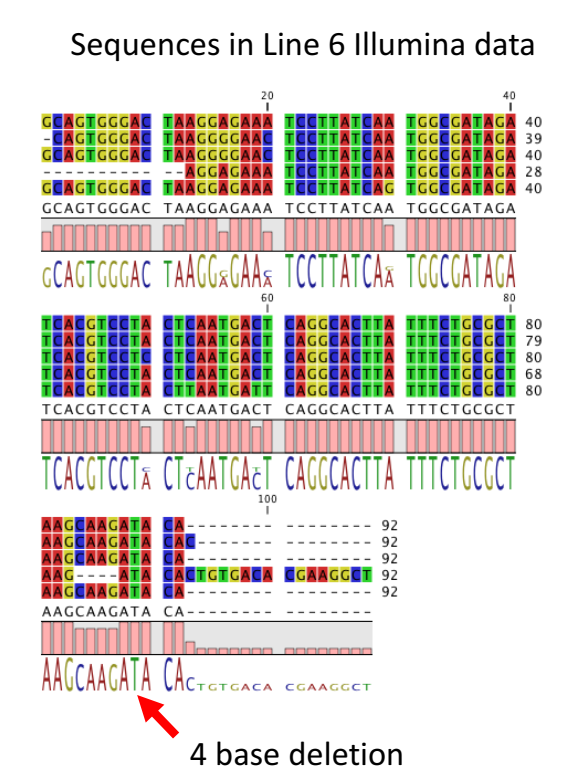
Figure 2.8. TCR Vbeta-1 CDR1 haplotypes in line 6x7 F1 RNA-seq data. RNA-seq was performed on splenocytes from uninfected birds or birds infected at 4 dpi with MDV. CDR1 haplotypes were predicted with Freebayes. Parental line 6 and 7 alleles contributing the SHKESVIQTM haplotype could be differentiated by a downstream Val-Leu-54 substitution in the C-C' loop. No significant difference was observed between uninfected and infected samples, so haplotypes were compared inclusive of infection status by Tukey's test. **** = p<0.0001.

approximately 25% of haplotype observations. Surprisingly, a Line 6 haplotype which also encoded this sequence (with a synonymous SNP) was observed less than half as frequently; the only definitive difference between these two haplotypes which could be inferred from the longer DNA-based haplotype is a Val-Leu substitution at position 54 in the variable region's C-C' loop (which is expected to form part of the Valpha-Vbeta interface), although it is possible that these TCR Vbeta-1 genes contain important sequence differences further from the CDR1 region, e.g. at the CDR2 or CDR3 loops. Three CDR1 haplotypes identified in the DNA sequence data (2 from Line 6 and 1 from Line 7) were not observed within the RNA sequence data, at the detection threshold used in our analysis.

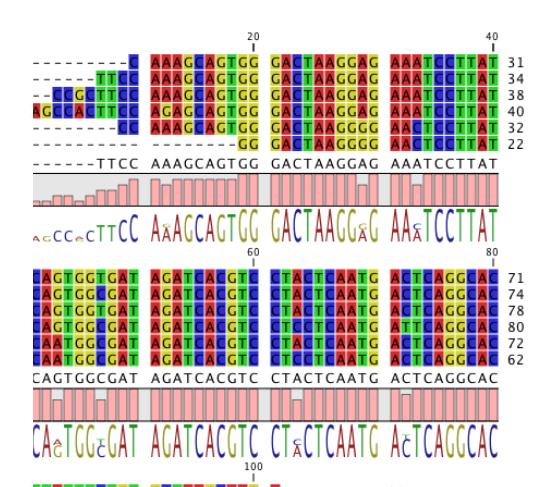
Additionally, one of the Line 6 TCR Vbeta-1 genes contained a 4-base deletion which introduces a Gln to Ile (polar to hydrophobic) amino acid change at position 112, just upstream to the V-D junction of the CDR3 loop (Figure 2.9A). Using the RNA-seq data set from splenocytes of 4-day old Line 6x7 F1 hybrid birds either uninfected or infected with MDV at hatch, we observed approximately 68% usage of the canonical Gln-112 if the upstream codon was unmodified, while Ile-95 was used 4% of the time. In this sequence context, usage of Gln-112 was reduced during early MDV infection, while Ile-112 usage remained stable, as did usage of a codon-initial adenine at this position, which was present in about 10% of sequences (Figure 2.9B).

Finally, we were able to obtain long-read (~20 kb at N50) PacBio DNA sequencing data from both lines 6 and 7. De novo assembly in Canu allowed reconstruction of the TCRbeta locus for each line (suppl. Figure 2.S2A-C). Despite the repetitive nature of the locus, Line 7 could be constructed successfully (with all TCRbeta genes in one contig) using stringent defaults for

3' TCR Vbeta-1 Sequences



Α



ULTAAGCAAG ATAGAGTGTG

Sequences in Line 7 Illumina data

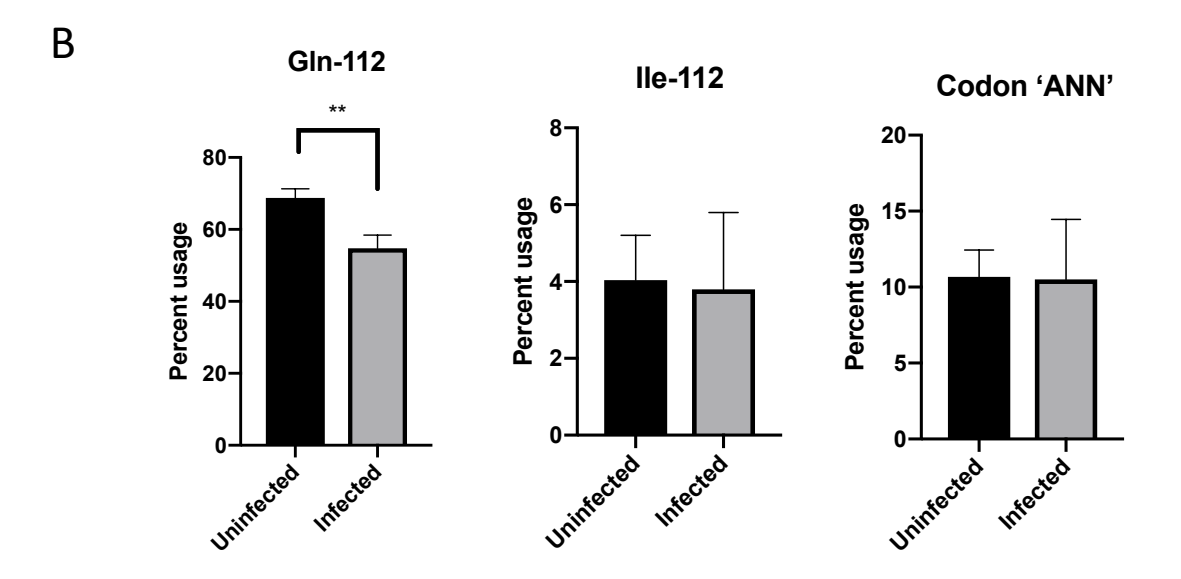


Figure 2.9. 3' TCR Vbeta-1 sequences in Illumina data. A: Illumina DNA-seq data from line 6 and line 7 birds were interrogated for conserved Vbeta-1 sequences upstream of the 3' RSS using a custom script (Appendix), and consensus sequences aligned. A 4-base deletion upstream of the RSS was identified in one line 6 sequence. N=1 pool of 7 birds per line. B: Illumina RNA-seq data from 6x7 F1 birds were interrogated for use of canonical (Gln-112), non-canonical (Ile-112), or adenine-initiated ('ANN') codons at the Vbeta-1-CDR3 junction in reads with canonical sequences through codon 111. **=p<0.01 by Student's T test. N=3 birds per group.

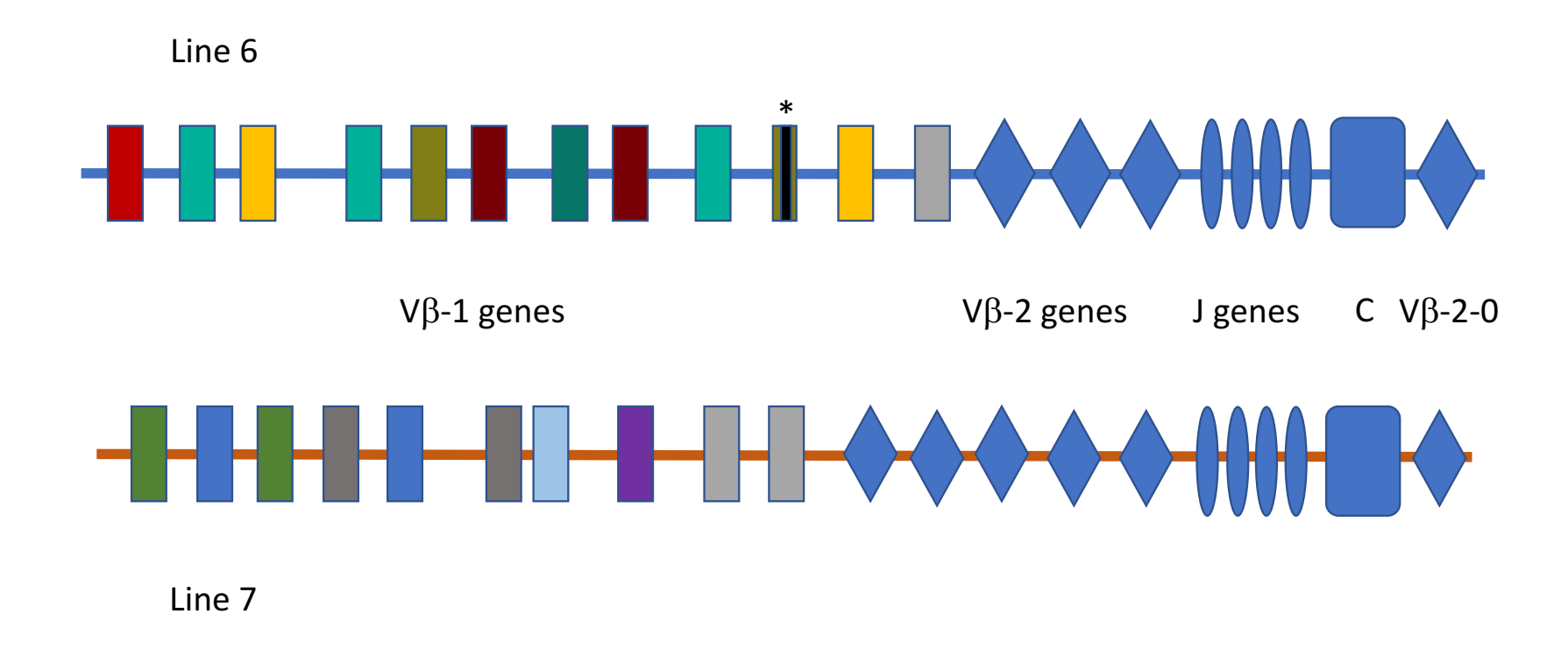
PacBio data (4.5% between-read allowable error rate), and contained 10 Vbeta-1 genes and 6 Vbeta-2 genes (Figure 2.10, suppl. Figure 2.S2C). In contrast, Line 6 required somewhat less stringent parameters to construct a single TCRbeta-containing contig (10.5% allowed error rate), and contained at least 12 Vbeta-1 genes and only 4 Vbeta-2 genes (suppl. Figure 2.S2A-B, Figure 2.10), consistent with the differential TCRbeta usage identified by flow cytometry. One Line 6 Vbeta-1 gene appeared to contain a large indel (14 novel bases replacing 171 bp of sequence), and is therefore most likely a pseudogene.

Similarly to the Illumina data, CDR1 haplotypes were identified for each Vbeta-1 gene in both lines (Figure 2.11); most previously identified haplotypes could be identified within the assembled PacBio data, with the exception of SHKESVIRTMF and SHKESGFWTMF in Line 6.

Conversely, genes containing the haplotypes SHKESGTWTMF in Line 6 and SDKESVILTMF in Line 7 were present in the assembled PacBio data but were not previously identified in the Illumina data; these may contain sequencing errors and their sequences should be confirmed by targeted resequencing. The most common CDR1 haplotypes in Line 7 were SDKESVIRTMF, SDKESVIQTMF, and SHKESVIQTMF, each of which was represented by two genes. In Line 6, SHKESVIPTMF was represented by 3 genes, and SDKESGAWTMF was represented by two; the "VIQT" motif was only represented by one gene in Line 6. Figure 10 shows the reconstructed model of the TCR beta loci in Line 6 and 7, with unique CDR1 haplotypes highlighted between the lines.

Contig locat	tion Sequence	CDR1 motif
Line 6	446733 GAGAGTGTAATCCCGACCATGTTCTGGTACAAGCTGCCAGTGGGGAAGAACGCCACT 458424 GAGAGTGGACCATGCTCTGGTACAAGCTGCCAGTGGGGAAGAACGCCACT 439637 GAGAGTGGAACATCTCTGGTACAAGCTGCCAGTGGGAAGAACACCACT 331698 GAGAGTGGAAACTGGAACATGTTCTGGTACAAGCTGCCACTGGGGAAGAACGCCACT 344213 GAGAGTGGAACATGTTCTGGTACAAGCTGCCAGTGGGGAAGAACACCTCT 354602 GAGAGTGGAACCATGTTCTGGT——————————————————	GAWT GNWN VIQT GNWN GTWT
Line 7	304791 GAGAGTGTAATCCTGACCATGTTCTGGTACAAGCTGCCAGTGGGGAAGAACGCCACT 333749 GAGAGTGTAATCCAGACCATGTTCTGGTACAAGCTGCCAGTGGGGAAGAACGCCACT 344271 GAGAGTGTAATCCAGACCATGTTCTGGTACAAGCTGCCAGTGGGGAAGAACGCCACT 266378 GAGAGTGGATTCTGGACCATGTTCTGGTACAAGCTGCCAGTGGGGAAGAACACCACT 303183 GAGAGTGTAATCCAGACCATGTTCTGGTACAAGCTGCCAGTGGGGAAGAACGCCACT 319688 GAGAGTGAACCCACTGTCTCTGGTACAAGCTGCCAGTGGGGAAGAACGCCACT 248038 GAGAGTGGACCCT-GAACCATGTTCTGGTACAAGCTGCCAGTGGGGAAGAACGCCACT 278045 GAGAGTGTAATCCAGACCATGTTCTGGTACAAGCTGCCAGTGGGGAAGAACACGCCACT 285914 GAGAGTGTAATCCAGACCATGTTCTGGTACAAGCTGCCAGTGGGGAAGAACGCCACT 2859021 GAGAGTGTAATCCGGACCATGTTCTGGTACAAGCTGCCAGTGGGGAAGAACGCCACT 303183 GAGAGTGTAATCCAGGACCATGTTCTGGTACAAGCTGCCAGTGGGGAAGAACGCCACT 319688 GAGAGTGTAATCCAGGACCATGTTCTGGTACAAGCTGCCAGTGGGGAAGAACGCCACT 3278045 GAGAGTGTAATCCAGGACCATGTTCTGGTACAAGCTGCCAGTGGGGAAGAACGCCACT 328914 GAGAGTGTAATCCAGGACCATGTTCTGGTACAAGCTGCCAGTGGGGAAGAACGCCACT 329021 GAGAGTGTAATCCGGACCATGTTCTGGTACAAGCTGCCAGTGGGGAAGAACGCCACT 329021 GAGAGTGTAATCCGGACCATGTTCTGGTACAAGCTGCCAGTGGGGAAGAACGCCACT 33784	VIQT VIQT GFWT VIQT GA* GFWT VIQT VIQT VIRT

Figure 2.10. Vbeta-1 CDR1 alignments from long-read Pacbio DNA-seq. Vbeta-1 sequences were extracted from long-read Pacbio DNA-seq assemblies and aligned for each bird line. CDR1-adjacent portions of alignments are shown only. CDR1 motifs are indicated. "GA*" indicates an apparent single base deletion falling within the CDR1 motif which may be due to sequencing error. The line 6 Vbeta-1 sequence at contig location 354602 is most likely a pseudogene due to the large deletion immediately downstream of the CDR1 region (indicated by dashes). Asterisks below alignments indicate 100% conserved bases.



<u>Figure 2.11. TCR beta locus model.</u> The TCR beta loci of lines 6 and 7 were reconstructed from long-read PacBio sequence data. Number of probable gene segments and approximate location with the locus is shown. Vbeta-1 genes are differentially colored to indicate unique CDR1 region haplotypes. One CDR1 haplotype (light grey; "SHKESVIQTMF") was shared between lines. * indicates pseudogene.

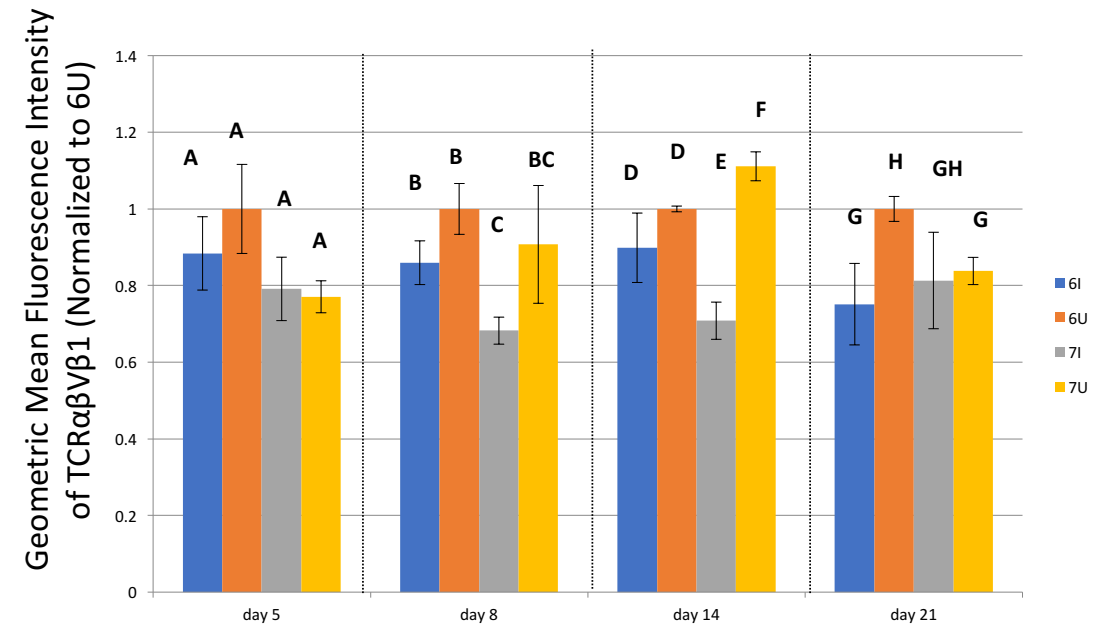
MDV downregulates TCR surface expression differentially in Lines 6 and 7.

Levels of TCR surface expression on gated TCR+ CD3+ T cells were examined by flow cytometry. In both lines, a mild reduction of TCR $\alpha\beta$ Vb1 surface expression was seen on day 8; however, this became statistically significant in Line 7 on day 14, while it was not significant in Line 6 until day 21 (Figure 2.12A). TCR $\alpha\beta$ Vb2 surface expression was significantly reduced in both lines by day 14 (Figure 2.12B).

TCR expression is reduced in an MDV-reactivated cell line.

We examined the levels of TCR $\alpha\beta$ Vb1 expression on the TCR $\alpha\beta$ Vb1+ CD4+ T cell line UAO4, which contains latent, reactivatable MDV and expresses GFP upon MDV reactivation with BrdU (a thymidine analogue), soluble anti-CD3 and anti-CD28 antibodies (through TCR-dependent signaling (Figure 2.13A), PMA (a potent PKC activator), or any of several interleukin cytokines (personal communication, Henry Hunt); but not anti-TCR $\alpha\beta$ Vb1 antibody alone (Figure 2.13A). We found that the small number of reactivating UAO4 cells present in the absence of any treatment also express lower levels of TCRαβVb1 (although our staining protocol for flow cytometry increased reactivation and thus can be considered a treatment). Either BrdU or the combination of soluble anti-CD3/CD28 antibodies reduced TCR $\alpha\beta$ Vb1 expression on UAO4 cells, with the GFP-expressing cells showing lower TCR $\alpha\beta$ Vb1 expression than GFP-negative cells (Figure 2.13B). In contrast, MHC class II was not significantly affected by either treatment or in GFP-expressing cells relative to GFP-negative cells (Figure 2.13C), and the TCR downregulation was not caspase-dependent, as the caspase inhibitor Z-VAD-FMK did not effect it (Figure 2.13D).





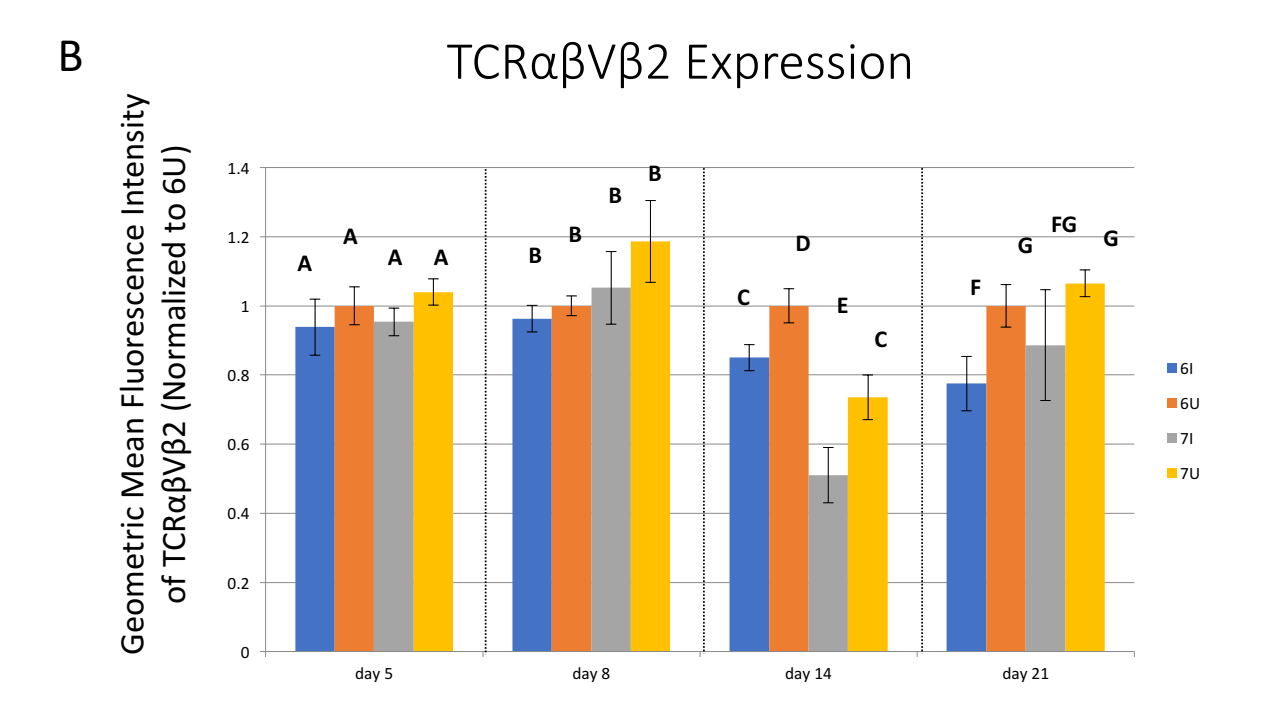
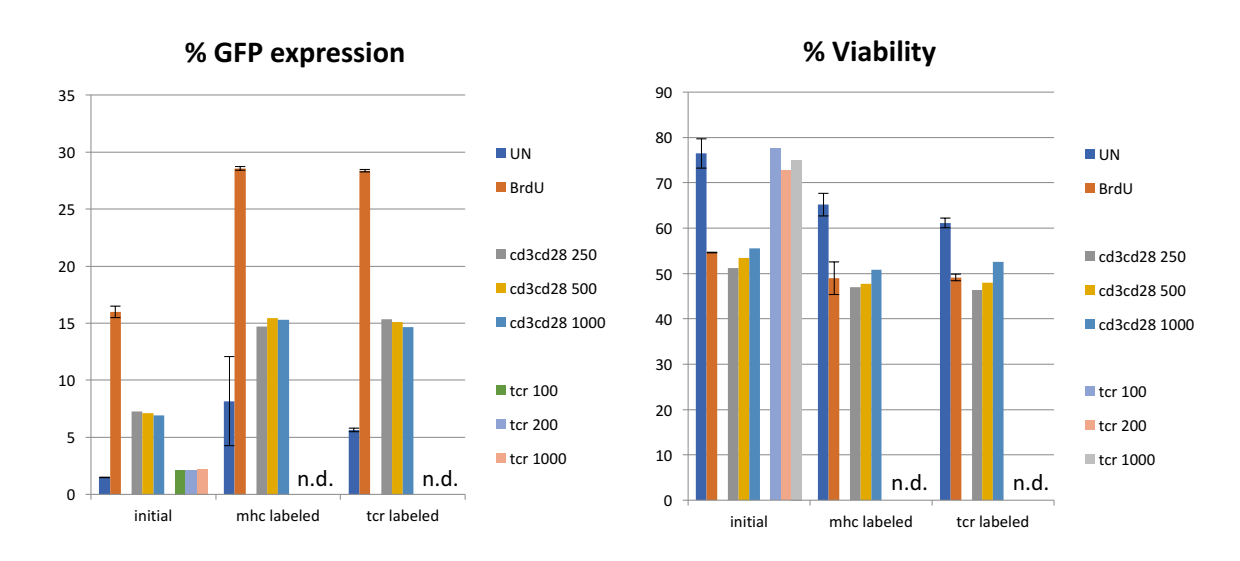
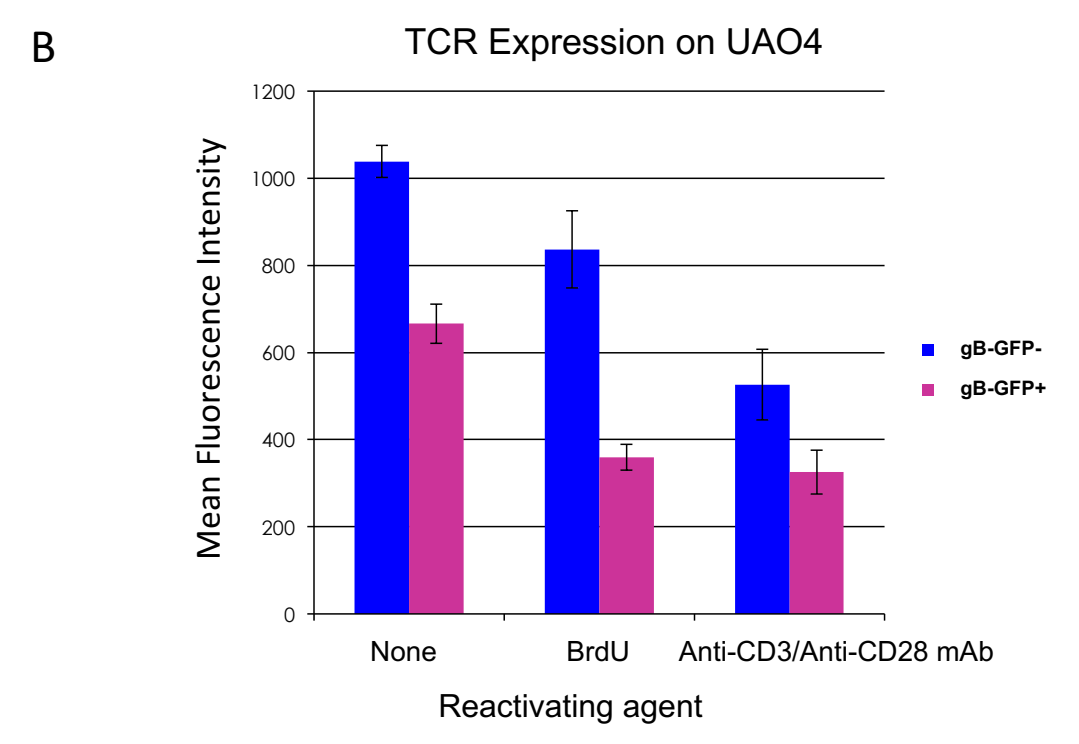


Figure 2.12. TCR Vbeta expression on CD3+ splenocytes. Geometric mean fluorescence intensity of TCR α βVb1 (A) and TCR α βVb2 (B) staining of gated CD3+ TCR+ cells from samples shown in Figure 1.3A-B. Non-overlapping letters indicate significant difference within dates by p<0.05 on Bonferonni-corrected Student's T tests.

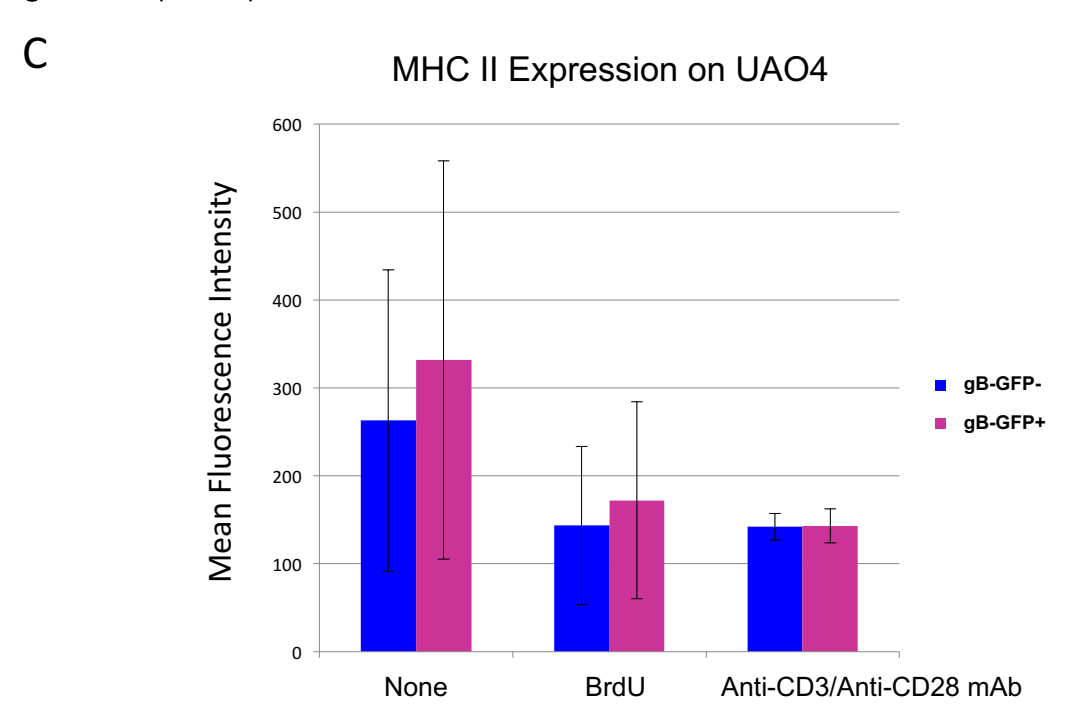


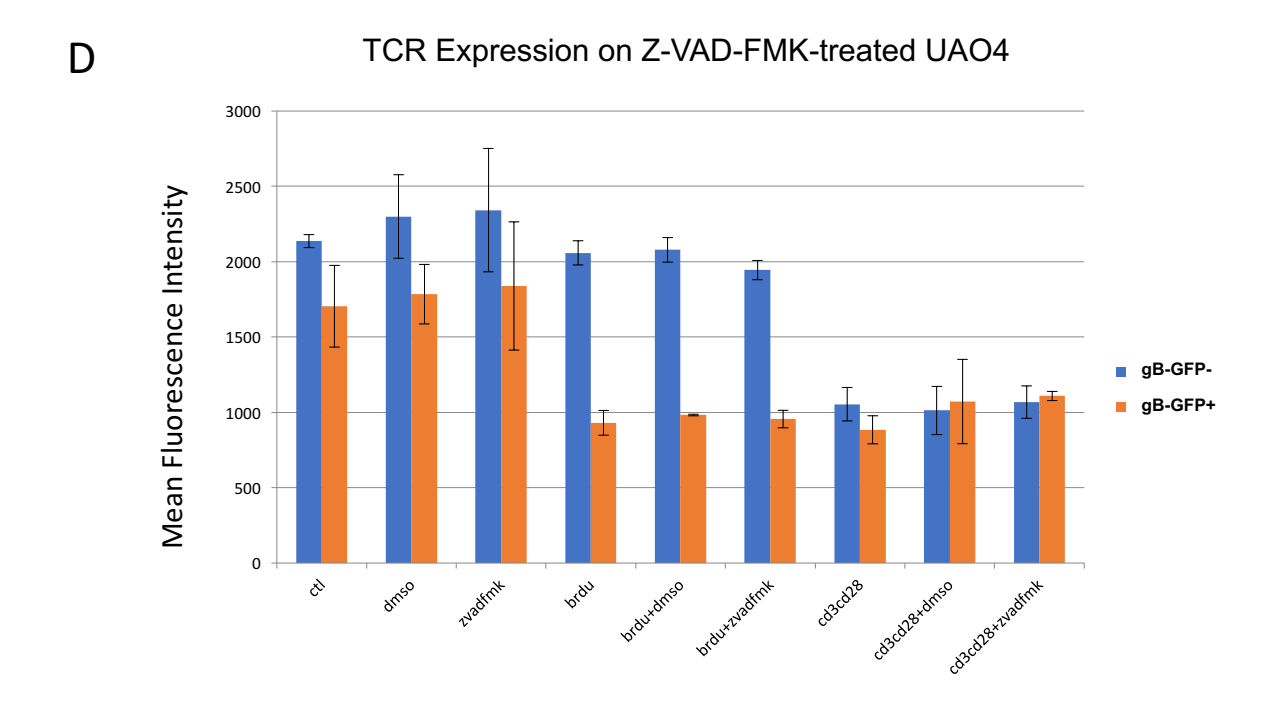




<u>Figure 2.13. UAO4 cell reactivation assays.</u> A: Stimulation with BRDU and CD3/CD28 antibodies, but not anti-TCR antibody alone, reactivates MDV (measured as gB-GFP expression) in latently infected UAO4 cells. Response to CD3/CD28 antibodies was not concentration-dependent across 3 dilutions (1:250, 1:500, 1:1000), therefore these dilutions were treated as replicates for analysis of TCR and MHC II expression. B. Reactivating gB-GFP+ UAO4 cells downregulate surface expression of TCR, measured by flow cytometry. gB-GFP+ and gB-GFP- cells were gated within untreated, BrdU-treated, and anti-CD3/CD28 antibody-treated samples.

Figure 2.13 (cont'd).





C: Reactivating gB-GFP+ UAO4 cells express similar levels of MHC class II to latently-infected gB-GFP- UAO4 cells within the same sample. D: Broad-acting caspase inhibitor Z-VAD-FMK did not rescue TCR expression in reactivating UAO4 cells. Cells were treated with 10uM, 25uM, and 50uM of Z-VAD-FMK or an equivalent volume of DMSO and reactivated; average of titrations is shown, as TCR expression was not concentration-dependent in reactivating samples.

Discussion

We broadly characterized the T cell repertoires and responses of MD-resistant and susceptible chickens using two pairs of inbred chicken lines, in order to identify immune responses that correlate with a resistant phenotype in vivo. Initially we hypothesized that base functionality in peripheral (i.e. splenic) T cells might differ between lines in our MHC-matched model, in accordance with an early hypothesis that T cell infection relies on activation (Calnek 1984) and thus susceptible birds may have more easily activated T cells in general. In all cases, CD4+ cells did not differ in proliferative response to mitogen stimulation, suggesting that neither tumorigenesis nor T helper response is impaired in one line by general activation/proliferation capacity. In contrast, CD8+ proliferative responses differed at early timepoints; however, the proliferative advantage was in the susceptible line, indicating that this phenomenon is not responsible for a more protective anti-viral or anti-tumor response in vivo. Total splenic lymphocyte proliferative responses were not different between lines, in contrast to previously reported whole blood assays (Frederickson 1983, Lee 1983) but in agreement with purified splenic lymphocyte mitogen responses reported in Lee et al., 1981. Strong differences in lymphocyte count between lines likely account for the differences between these assays. Our data, which extended previous findings about peripheral T cell proliferative capacity to CD4+ and CD8+ subpopulations, demonstrate that activation ability cannot explain differences in susceptibility between these lines. This suggests that either the numbers of lymphocytes present, interactions with non-lymphocyte cell populations, or the TCR repertoire itself is likely to be responsible for differences in response to MDV infection or development of lymphoid tumors.

In this paper, we identified differences in the usage of the two TCR Vbeta families in the T cell repertoire of both our MHC-matched and MHC-congenic MD-resistance models. In our MHC-matched model, in which the same MD-susceptible MHC haplotype has been maintained in inbred lines divergent for disease resistance, we infer these differences, which are as high as 25-30%, may be due to structural differences at the TCR beta locus itself, and in fact we were able to identify differences in number and sequence of genes at the TCR beta locus in these lines. In contrast, our MHC-congenic lines, which share the same genetic background (including TCR loci) but carry MHC haplotypes linked to different levels of MD resistance, showed mild (5-15%) differences in TCR usage in the CD8+ T cell population only, indicating that MHC class I, but not necessarily MHC class II in this model, selects for different T cell repertoires in the thymus that are recognizable at the bulk (gene family) expression level. This may help explain the critical importance of the MHC locus as the strongest genetic determinant of host resistance against MD, in addition to differences in quantity of MDV antigen presented by differing MHC alleles (Chappell 2015). Selection for MHC structures that efficiently present viral peptides is believed to be a critical aspect of immune locus evolution, and in the chicken it has been theorized that MHC class I and the TAP peptide transporter have co-evolved to optimize responses to pathogens such as herpesviruses in the context of a greatly reduced MHC locus. It is additionally likely that TCR loci, which are reduced in gene number in the chicken relative to mammalian loci, are also co-evolving along with their MHC binding partners, and selection for pathogen resistance or susceptibility may skew TCR repertoires towards or away from "best fit" receptors that recognize viral peptides as presented on MHC.

We were able to identify MDV-responsive populations of T cells in our flow analysis, based on expansions in TCR $\alpha\beta$ Vb1 or TCR $\alpha\beta$ Vb2+ subsets. In both our models, we saw little change in TCR usage within CD4+ populations prior to late infection when CD4+ T cell lymphomagenesis is likely to be occurring. This is explainable in part due to CD4+ T cells comprising a larger component of the lymphoid compartment. However, in our MHC-matched model, $TCR\alpha\beta Vb1+$ responses visible in the splenic lymphoid population as a whole could only be attributed to CD8+ and not CD4+ T cells, indicating that the TCR α β Vb1+ CTL TCR response in MD-resistant Line 6 was large. Prior literature suggests that TCR $\alpha\beta$ Vb1+, but not TCR $\alpha\beta$ Vb2+ T cells are important for the development of anti-MDV serotype 2 (non-oncogenic MDV) vaccinal immunity (Omar and Schatt, 1997). Our results indicate that TCR $\alpha\beta$ Vb1+ responses, specifically within the CD8+ T cell subset, are likely playing a key role in host immunity to MD as well. It is important to note, however, that the strength of such a response does not necessarily correlate with protection against disease. In fact, in replicate 2 of Experiment 1, in which we saw the strongest and longest-lasting expansion of TCRαβVb1+ CD8+ T cells in MD-resistant Line 6 birds, most of the Line 6 birds which were not euthanized for tissue collection succumbed to the acute phase of infection prior to the end of the experiment despite not developing gross MD tumors. It is possible that a particularly robust anti-viral or anti-tumor response in these birds led to mortality due to cytokine storm rather than providing complete protection from disease.

Additionally, we were able to identify clonality within the $TCR\alpha\beta Vb1+$ and $TCR\alpha\beta Vb2+$ subsets directly, using TCR spectratyping analysis. While both resistant and susceptible lines showed clonal expansions in MDV-infected birds by day 14 post-infection, these occurred primarily in the TCR Vbeta-2 subset in the resistant line, while the susceptible line showed early

clonality in both TCR subsets. The unusually high clonality in TCR Vbeta-2 in Line 6 birds that do not develop lymphoid tumors from MDV infection is likely due to the very low usage of $TCR\alpha\beta Vb2$ in this line, magnifying the effect of T cell expansion in response to viral antigens. By day 21 post-infection, very high clonality consistent with tumor development was visible in the spleens of susceptible Line 7 birds, while resistant birds showed a high deviation from discrete-normality but no strong clones in either TCR subset, more consistent with a robust T cell response.

We hypothesized that the relatively higher usage of TCR $\alpha\beta$ Vb1 in Line 6, visible both in the flow cytometry results and as reduction in clonal diversity in TCR Vbeta-2 in TCR spectratyping, may be due to heritable structural differences in the TCR Vbeta locus in this line. Therefore we attempted to genetically map the TCR usage trait using a panel of RCS strains between our two MHC-matched inbred lines; however, incomplete microsatellite typing in these RCS lines did not allow us to uniquely link phenotype to genotype. We were able to draw inferences about the heritability of the TCR usage trait (which was tightly controlled within lines and behaved similarly to a biallelic Mendelian trait) and also to compare the usage patterns with known MD susceptibilities in several of the RCS lines. While most lines followed the TCR usage phenotype present in the resistant line (unsurprisingly, as these RCS lines were developed through back-crossing to Line 6), the several lines known to be relatively susceptible to MD showed lower percentages of TCR $\alpha\beta$ Vb1+ lymphocytes regardless of the distribution of TCR usage within T cells. This could indicate that not only the TCR locus, but also factors that affect over-all T cell numbers, influence the availability of cells responsive to infection. A rigorous comparison of these RCS lines in MDV infection has not been completed, to our

knowledge, but would help answer questions about the relative contribution of these phenotypes to MD resistance.

Although we lacked a robust structural model of the TCR beta locus for Lines 6 and 7, we were able to compare the gene diversity present in the TCR Vbeta-1 family in our MHCmatched MD-resistant model, using both standard Illumina DNA-seq and long-read PacBio DNA-seq. We noted that in terms of single-nucleotide polymorphism (SNP) density, Line 6 was more divergent from the jungle fowl reference sequence for Vbeta-1, and also exhibited a larger number of multi-variant haplotypes, indicating more inter-gene diversity and potentially more variable gene blocks present within the Vbeta-1 family, and fewer within the Vbeta-2 family (suppl. Figure 2.S3) which was confirmed by long-read sequence analysis. Additionally, we also identified a 4-base deletion in one TCR Vbeta-1 gene in our MD-resistant line, which is likely to affect affinity and usage of that Vbeta-1 gene. As this deletion occurred just upstream of the V-D junction in the CDR3 loop of this TCR, it is likely to produce an in-frame product after VDJ recombination; however, unless nucleotides are deleted upstream of the V-D junction, the canonical Gln-112 which is present in all other TCR Vbeta-1 genes will be substituted with Ile-112. In TCR beta RNA sequence data from Line 6x7 F1 splenocytes, the canonical Gln-112 was maintained 68% of the time during codon end processing if the upstream codon was present (and greater than 50% of the time regardless of upstream codon modification). We modelled TCR beta-chains in the context of both the original sequence and the substituted Ile-112 in Swiss-Model (suppl. Figure 2.S4) and found that this substitution changes the predicted orientation of the CDR3 loop, which is consistent with comparatively rare usage of Ile-112 in normal spleen TCR beta RNA sequence data obtained from Line 6₃ x Line 7₂ F1 birds.

Surprisingly, usage of the canonical amino acid was decreased during early infection, indicating either that these cells make better targets for MDV infection or are less responsive than some other TCR subset(s) at this phase. We suggest that the Line 6 repertoire has been further shaped by inclusion of a non-canonical variant which is not outcompeted by other early responding T cells, or perhaps is less susceptible to lytic infection.

Additionally, we noted nearly twice as many variants present within the CDR1 hypervariable region of Vbeta-1 in Line 6 as Line 7, and noted changes in both the structure of haplotypes and their selection in the peripheral repertoire, suggesting that there are functional differences between the CDR1 regions in each line. The CDR1 region is thought to primarily bind to MHC, although it may also interact with bound peptide (Roomp 2011). Notably, Line 6 has an expanded repertoire of CDR1 loops containing a hydrophobic aromatic residue at position 45, which is not present in the most commonly selected variant in Line 6x7 F1 birds. Conversely, the most commonly used CDR1 variant (SHKESVIQTMF) in Line 6x7 F1 birds, which is overrepresented at 25% usage, is a line 7 haplotype; the corresponding line 6 haplotype is not similarly overrepresented and also contains a downstream substitution in the Valpha-Vbeta interface. While the presence of two genes in Line 7 containing that haplotype could explain its overusage in F1 birds, two other duplicated genes in Line 7 were not similarly overrepresented. These data suggest that the line 6 TCR Vbeta-1 repertoire has been selected away from a "bestfit" relationship between the SHKESVIQTMF motif and at least one of the B2-encoded MHC molecules; this could provide increased protection from MD either by maximizing the use of different TCRs which better recognize MD antigens, especially on MHC class I, or by reducing the availability of activated CD4+ target cells for MDV infection.

Lastly, we studied the influence of MDV on TCR expression. MDV has been shown to down-regulate TCR signaling pathways in MD lymphoblastic cell lines using transcriptome sequencing (Mwangi et al., 2017). Several other herpesviruses, including HHV-6 and HVS, have been demonstrated to directly downregulate expression of the TCR complex, through targeting TCR complex proteins to the lysosome (Lusso 1991, Sullivan 2008, Cho 2006). We demonstrate here that MDV down-regulates TCRbeta expression on splenic T cells during the early (cytolytic) phase of infection, to a greater degree in MD-susceptible birds than MD-resistant birds. As we could not differentiate between the several possible mechanisms of TCR down-regulation in our in vivo model (including direct viral effects, activation of T cells, or expansion of TCR-low tumor cells), we examined the levels of TCRalpha/beta expressed on an MD lymphoblastic cell line with and without viral re-activation. In this in vitro model, we found that MDV reactivation from latency leads to a drop in TCR expression, consistent with a viral evasion strategy that involves downregulating the TCR on infected T cells. This downregulation was stronger than the TCR downregulation that occurred in non-reactivating cells treated with anti-CD3/CD28 antibodies (Fig 9A); further work will be necessary to determine what cell pathways are affected by MDV to cause TCR downregulation, and whether differences in the TCR repertoire between Lines 6 and 7 play a role in the differential susceptibility to TCR downregulation in vivo.

While the MHC is the only single locus of large effect on MDV resistance found to date, we have examined an MHC-matched resistance model to identify other potentially interacting factors which may have been selected for in the development of highly MD-resistant chicken lines. The TCR repertoire is a complex trait which is shaped by TCRalpha, TCRbeta, and MHC loci; as well as self and environmental antigens. We have examined the most tractable of

these, TCRbeta, and found indications that selection for resistance and susceptibility to MDV in an MHC-matched model has modified the repertoire of MHC ligands, i.e. the TCR repertoire. Intuitively, rational breeding strategies to take advantage of MHC-linked resistance to MDV could also incorporate TCR repertoire optimization; further work will be required to develop these kinds of strategies for creating highly disease-resistant poultry stock.

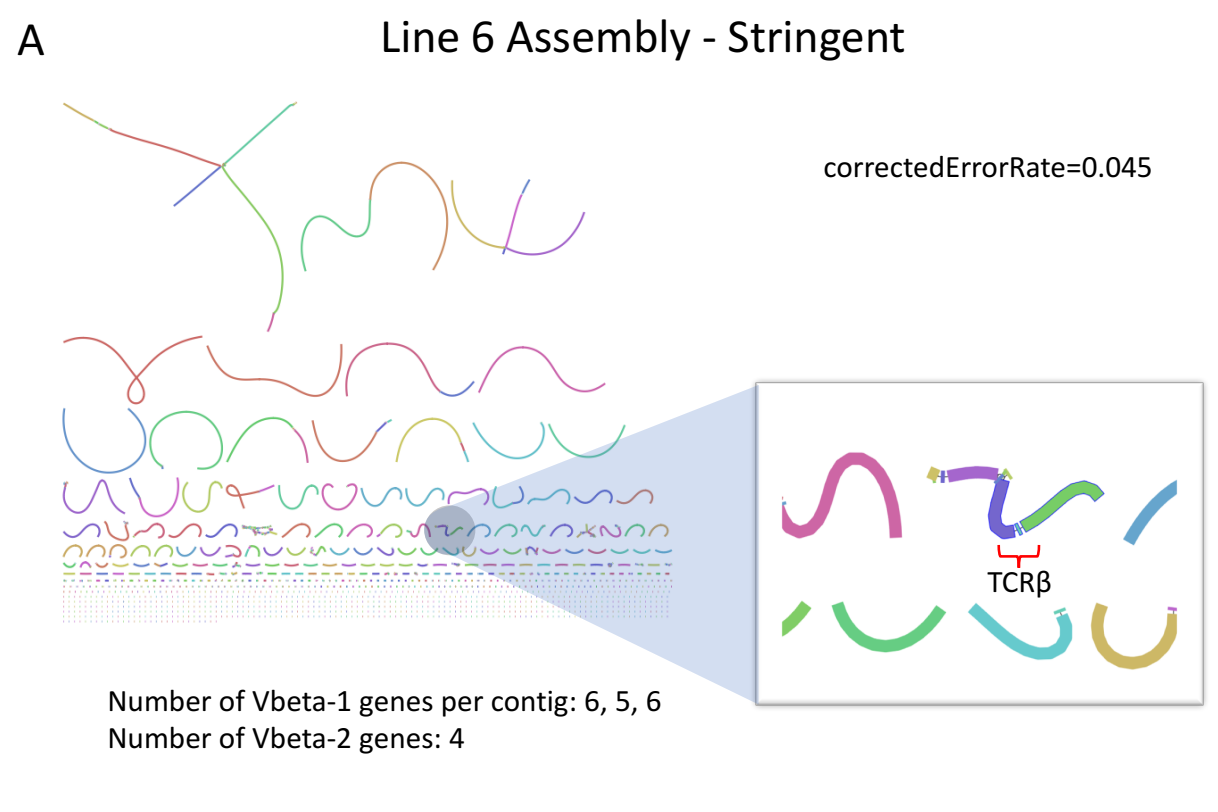
APPENDICES

APPENDIX A

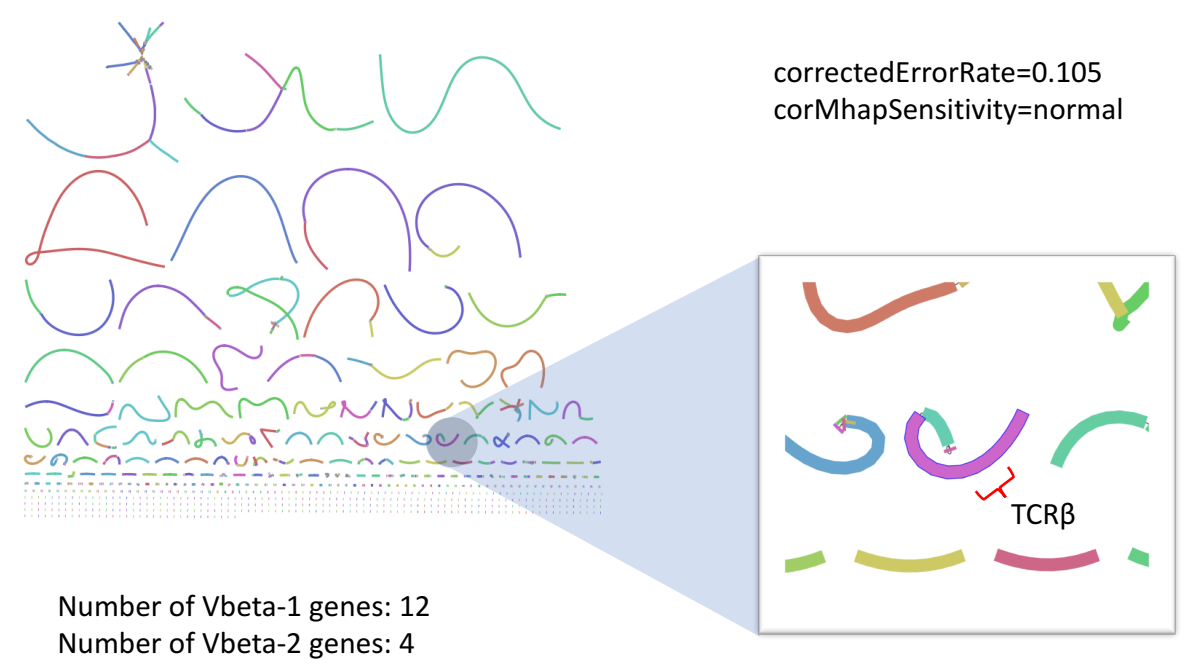
Supplemental Figures



<u>Figure 2.S1. Swiss-Model predicted ribbon models of TCR Vbeta-1 alleles.</u> Structures presented in Fig. 1.7 shown in ribbon-model form. The CDR3 loop is oriented uppermost and to the rear of the structure. Potential interactions between the reference CDR3 loop and the substituted CDR1 loops can be observed as changes in predicted loop orientation.

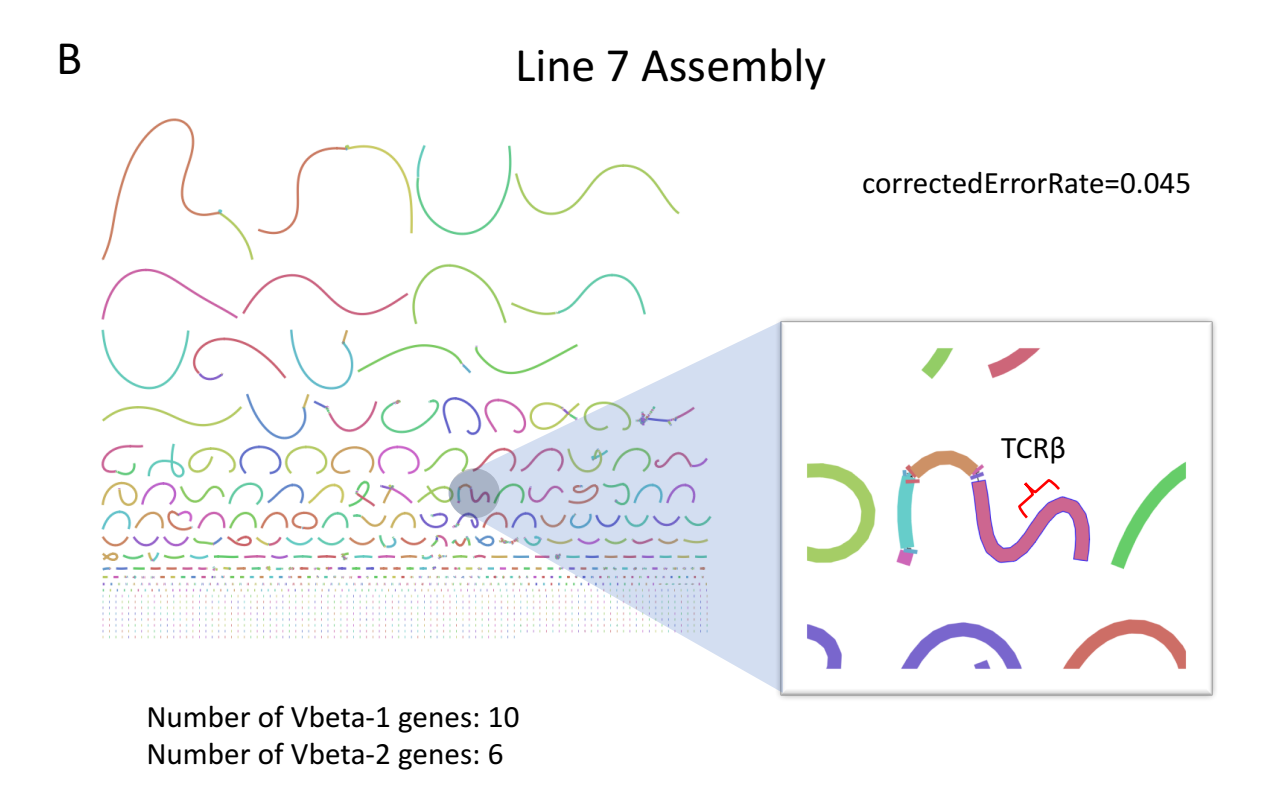


Line 6 Assembly - Relaxed



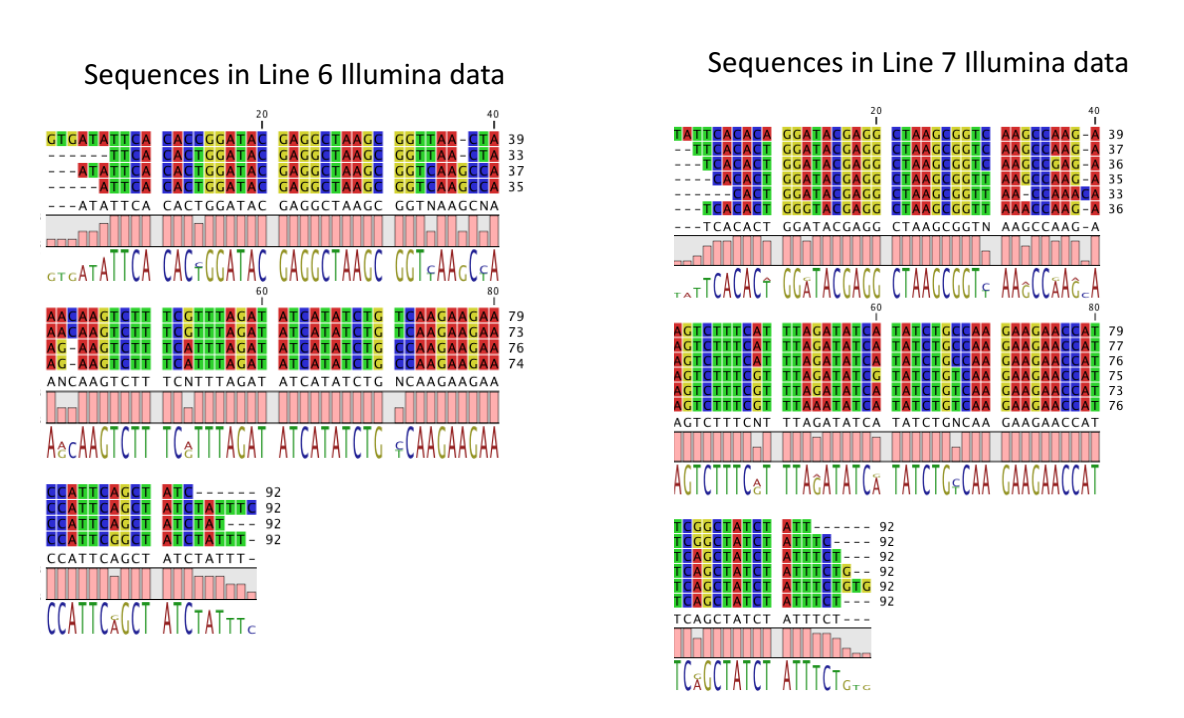
<u>Figure 2.S2. De novo assembly of line 6 and line 6 Pacbio DNA-seq in Canu.</u> TCR beta locus assembly was examined for contiguity in Bandage. A: Two line 6 assemblies. Relaxed stringency was required to assemble the complete line 6 TCR beta locus on one contig.

Figure 2.S2 (cont'd).



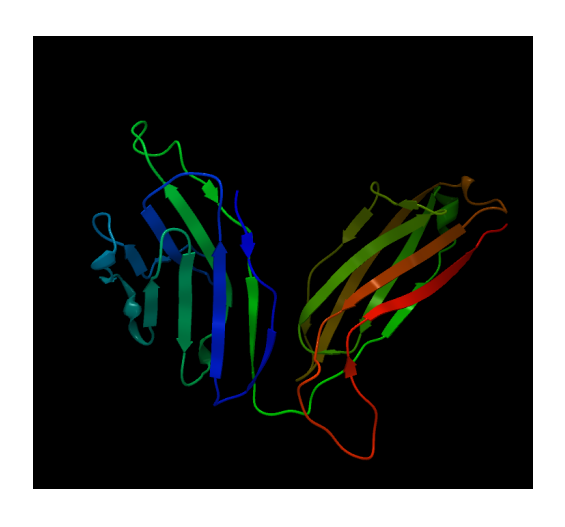
B: Line 7 assembly. Assembly with default stringency parameters produced a contiguous TCR beta locus. Stringency parameters used and number of TCR variable genes resolved by each assembly are indicated.

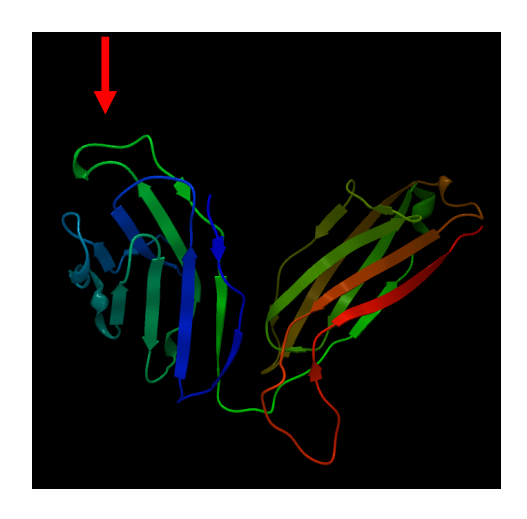
3' TCR Vbeta-2 Sequences



<u>Figure 2.S3. 3' TCR Vbeta-2 sequences identified in Illumina DNA-seq.</u> Illumina DNA-seq data from line 6 and line 7 birds were interrogated for conserved Vbeta-2 sequences upstream of the 3' RSS using a custom script (Appendix), and consensus sequences aligned.

Line 6 TCR Vbeta-1 3' Deletion Variant





Gln-112 (Reference)

Ile-112 (Variant)

Figure 2.S4. Swiss-Model predicted structure of line 6 3' deletion variant. A reference chicken TCR beta incorporating Vbeta-1 was folded in silico using a mouse TCR beta molecule as the folding template. Chicken TCR beta formed a 2-barrel structure homologous to mouse TCR beta; substitution of Ile-112 into the reference sequence induced a predicted conformational change in the orientation of the CDR3 loop (red arrow).

APPENDIX B

tcr analysis: a simple script for analysis of TCRs in chicken transcriptomics data

The following Bash script was made publically available at https://github.com/steepale/tcr_analysis on July 18, 2018. It was run on the Michigan State University High Performance Computer Cluster (HPCC), atop the CentOS 6.6 operating system and Moab 9.1.1/TORQUE 6.1.1.1 resource scheduler. Line numbers are indicated at the left margin.

```
1
    2
    #
3
             FILE:
    /mnt/research/ADOL/OutsideCollaborations/20160201 Cheng_Steep_Xu_Zhang/tcr_analysis/
    tcr analysis main documentation.txt
4
5
    #
            USAGE: for documentation purposes, scripts inside
6
      DESCRIPTION: This script serves as a step by step documentation script for T-cell
    receptor analysis
8
    # REQUIREMENTS: ---
10
            NOTES: ---
11
           AUTHOR: Cari Hearn, DVM
    #
12
             EDITOR: Alec Steep
                  PI: Hans Cheng, PhD
13
           CONTACT: hearncar@msu.edu, alec.steep@gmail.com
14
15
    # AFFILIATION: Michigan State University (MSU), East Lansing, MI, United States
16
17
        USDA ARS Avian Disease and Oncology Lab (ADOL), East Lansing, MI, United States
        Technical University of Munich (TUM), Weihenstephan, Germany
18
19
          VERSTON: 1.0
20
          CREATED: 2017.07.18
21
         REVISION:
```

```
22
23
24
    # PROJECT DIRECTORY (MSU Cluster)
    MDV DIR='/mnt/research/ADOL/OutsideCollaborations/20160201 Cheng Steep Xu Zhang'
25
    PROJ DIR='/mnt/research/ADOL/OutsideCollaborations/20160201 Cheng Steep Xu Zhang/tcr
26
    analysis'
27
    cd ${PROJ DIR}
28
    # make appopriate directories
29
    mkdir -p ./{data,scripts,analysis,jobs}
30
31
32
    #Data Set:
33
    #130 fastq files including 26 tumors and 2 normal spleen samples
34
    # Location of original files: ${MDV DIR}/RNA seq/data/reads
35
36
    # Download fastq-tools v 0.8
    wget http://homes.cs.washington.edu/~dcjones/fastq-tools/fastq-tools-0.8.tar.gz \
37
    -O ${HOME}/Apps/fastq-tools-0.8.tar.gz
38
39
    tar xfvz ${HOME}/Apps/fastq-tools-0.8.tar.qz
40
    rm ${HOME}/Apps/fastq-tools-0.8.tar.qz
    cd ${HOME}/Apps/fastq-tools-0.8
41
42
    ./configure --prefix ${HOME}/Apps/fastq-tools-0.8
    make install
43
    # Export to PATH
44
    export PATH="${HOME}Apps/fastq-tools-0.8/bin:${PATH}"
45
46
    #loop through local fastq file set and collect sequences for further analysis with
47
    CLC
    for file in `ls -1 ${MDV DIR}/RNA seq/data/reads/*.fastq.qz | head -n1`
48
49
    gsub -v Var=${file} -N "tcr analysis"${file} ./scripts/tcr analysis.sh
50
51
    done
52
    # ./scripts/tcr analysis.sh
53
    54
```

```
55
    #!/bin/bash -login
    ### Job name
56
57
    ### Resources
    #PBS -l nodes=1:ppn=1,walltime=00:03:59:00,mem=1gb
58
    ### Send email if the job encounters an error
59
60
    #PBS —m a
    ### Output files to where you submitted your batch file
61
    #PBS -e ./jobs/${PBS JOBNAME} ${Var} ${PBS JOBID}.err
62
    #PBS -o ./jobs/${PBS_JOBNAME} ${Var}_${PBS_JOBID}.log
63
    #PBS -j oe
64
65
    # Change to working directory
66
    cd ${PBS O WORKDIR}
67
68
69
    # Directories
    MDV DIR='/mnt/research/ADOL/OutsideCollaborations/20160201 Cheng Steep Xu Zhang'
70
71
72
    #load program modules
    module load FASTX/0.0.14
73
74
    module load ClustalO/1.1.0
    fastq-grep='${HOME}Apps/fastq-tools-0.8/bin/fastq-grep'
75
76
77
    # Create name for unzipped file
    unzipped=`echo ${Var} | sed "s/.gz//g" | xargs -i basename {}`
78
    # Gunzip the file
79
    gunzip -c ${Var} > ./data/${unzipped}
80
81
    #each line calls fasts-grep in fastq-tools and searches for known primer sequence
82
    variants for a given tcrb gene family
    #each orientation (forward or reverse) are handled separately
83
    #reads are piped through fastx collapser to unique them
84
    fastq-grep
85
     "AATGGTTCAGACACTTATTT | AATGATTCAGACACTTATTT | AATGGCTCAGACACTTATTT | AATGACTCAGACACTTATTT
     | AATGGTTCAGGCACTTATTT | AATGATTCAGGCACTTATTT | AATGGCTCAGGCACTTATTT | AATGACTCAGGCACTTATTT
      ./data/${unzipped} | fastx collapser > ./data/${unzipped}.vbl.dirl.fasta
```

```
fastq-grep
86
     "AAATAAGTGCCTGAGTCATT | AAATAAGTGCCTGAGCCATT | AAATAAGTGCCTGAATCATT | AAATAAGTGCCTGAACCATT
     AAATAAGTGTCTGAGTCATT AAATAAGTGTCTGAGCCATT AAATAAGTGTCTGAATCATT AAATAAGTGTCTGAACCATT
      ./data/${unzipped} | fastx collapser > ./data/${unzipped}.vb1.dir2.fasta
     fastq-qrep "AGAAGAACCATTCAGCTAT | AGAAGAACCATTCGGCTAT" ./data/${unzipped}
87
     fastx collapser > ./data/${unzipped}.vb2.dir1.fasta
     fastq-grep "ATAGCTGAATGGTTCTTCT | ATAGCCGAATGGTTCTTCT" ./data/${unzipped} |
88
     fastx collapser > ./data/${unzipped}.vb2.dir2.fasta
     fastg-grep "TTTGATGGTGAAAAGATGACC" ./data/${unzipped} | fastx collapser >
89
     ./data/${unzipped}.j.dir1.fasta
     fastq-grep "GGTCATCTTTTCACCATCAAA" ./data/${unzipped} | fastx collapser >
90
     ./data/${unzipped}.j.dir2.fasta
91
    #reverse-direction reads are reverse-complemented
92
     fastx reverse complement -i ./data/${unzipped}.vb1.dir2.fasta >
93
     ./data/${unzipped}.vb1.dir2.revd.fasta
     fastx reverse complement -i ./data/${unzipped}.vb2.dir2.fasta >
94
     ./data/${unzipped}.vb2.dir2.revd.fasta
     fastx reverse complement -i ./data/${unzipped}.j.dir2.fasta >
95
     ./data/${unzipped}.j.dir2.revd.fasta
96
97
    #don't need these; we will handle the two orientations separately
98
    #cat ./data/${unzipped}.vb1.dir1.fasta ./data/${unzipped}.vb1.dir2.revd.fasta >
99
     ./data/${unzipped}.vbl.combined.fasta
    #cat ./data/${unzipped}.vb2.dir1.fasta ./data/${unzipped}.vb2.dir2.revd.fasta >
     ./data/${unzipped}.vb2.combined.fasta
101 #cat ./data/${unzipped}.j.dir1.fasta ./data/${unzipped}.j.dir2.revd.fasta >
     ./data/${unzipped}.j.combined.fasta
102 #clustalo -i ./data/${unzipped}.vbl.combined.fasta -o ./data/${unzipped}.vbl.aligned
    #clustalo -i ./data/${unzipped}.vb2.combined.fasta -o ./data/${unzipped}.vb2.aligned
103
    #clustalo -i ./data/${unzipped}.j.combined.fasta -o ./data/${unzipped}.j.aligned
104
105
    #this was run as a separate shell command after the fact but you could include it
106
     here
```

```
107 #loop through the newly created files
108 for file in `ls -1 ./data/${unzipped}*dir*.fasta`
109 do
110 clustalo -i ${file} -o ${file}.aligned
111
    done
112
    # Remove the redundant unzipped file
113
    rm ./data/${unzipped}
114
115
116 # Collect stats on run
    qstat -f ${PBS JOBID}
117
118
    119
120 #CLC Analysis:
121 #Import clustalo output file.
122 #Files that should contain directionally correct data (sufficient quantity of reads,
    probably cDNA):
123 #* R1 001.fastq.vb*.dir1.*
124 #* R2 001.fastg.vb*.dir2.*
125 #Files containing inverse-directional data (few reads, probably genomic
    contamination, ultimately not analyzed):
126 #* R1 001.fastq.vb*.dir2.*
127 #* R2 001.fastg.vb*.dir1.*
128 #Sort sequences by similarity.
129 #Manually remove sequences which end prior to the CDR3 splice sites:
130 #Vb1: ...TATTTCTGCGCTAA(G)
131 #Vb2: ...TATTTCTGTGCCA(G)
132 #For files which contain 20+ unique, CDR3-identifiable reads:
133 #Identify dominant clone as:
134 #-More than 50% of unique reads
135 #Identify moderately dominant clone as:
136 #-More than 30% of total reads
137 #Remove all non-dominant clone reads and obtain consensus sequence (separately for
    dominant or moderately dominant clones)
138 #For tumors represented by more than one file:
```

- 139 #Align related consensus sequences from individual files and obtain overall consensus sequence
- 140 #CLC alignment default settings:
- 141 #Gap open cost = 2
- 142 #Gap extension cost = 0
- 143 #End gap cost = free
- 144 #Alignment set to very accurate (slow)

REFERENCES

REFERENCES

Andrews, S. FastQC: a quality control tool for high throughput sequence data. (2010).

Atkins, K. E. et al. Vaccination and reduced cohort duration can drive virulence evolution: Marek's disease virus and industrialized agriculture. Evolution 67, 851–860 (2013).

Bacon, L. D., Hunt, H. D. & Cheng, H. H. A review of the development of chicken lines to resolve genes determining resistance to diseases. Poult. Sci. 79, 1082–1093 (2000).

Berry, R. et al. Structure of the chicken CD3 $\epsilon\delta/\gamma$ heterodimer and its assembly with the $\alpha\beta T$ cell receptor. J. Biol. Chem. 289, 8240–8251 (2014).

Bienert, S. et al. The SWISS-MODEL repository—new features and functionality. Nucleic Acids Res. 45, D313–D319 (2017).

Briles, W. E., Stone, H. A. & Cole, R. K. Marek's disease: effects of B histocompatibility alloalleles in resistant and susceptible chicken lines. Science 195, 193–195 (1977).

Calnek, B. W., Adene, D. F., Schat, K. A. & Abplanalp, H. Immune response versus susceptibility to Marek's disease. Poult. Sci. 68, 17–26 (1989).

Calnek, B. W., Schat, K. A., Ross, L. J. & Chen, C. L. Further characterization of Marek's disease virus-infected lymphocytes. II. In vitro infection. Int. J. Cancer 33, 399–406 (1984).

Chappell, P. E. et al. Expression levels of MHC class I molecules are inversely correlated with promiscuity of peptide binding. eLife 4, e05345 (2015).

Chen, C. H. et al. TCR3: a third T-cell receptor in the chicken. Proc. Natl. Acad. Sci. U.S.A. 86, 2351–2355 (1989).

Chen, C.-I. H., Cihak, J., Lösch, U. & Cooper, M. D. Differential expression of two t cell receptors, tcr1 and tcr2, on chicken lymphocytes. Eur. J. Immunol. 18, 539–544 (1988).

Cheng, H. H. et al. Fine mapping of QTL and genomic prediction using allele-specific expression SNPs demonstrates that the complex trait of genetic resistance to Marek's disease is predominantly determined by transcriptional regulation. BMC Genomics 16, 816-824 (2015).

Cho, N.-H. et al. Association of herpesvirus saimiri tip with lipid raft is essential for downregulation of T-cell receptor and CD4 coreceptor. J. Virol. 80, 108–118 (2006).

Churchill, A. E. & Biggs, P. M. Agent of Marek's disease in tissue culture. Nature 215, 528–530 (1967).

Cole, R. K. Studies on genetic resistance to Marek's disease. Avian Dis. 12, 9 (1968).

Fredericksen, T. L. & Gilmour, D. G. Ontogeny of con A and PHA responses of chicken blood cells in MHC-compatible lines 6(3) AND 7(2). J. Immunol. 130, 2528–2533 (1983).

Garrison, E. & Marth, G. Haplotype-based variant detection from short-read sequencing. arXiv:1207.3907 [q-bio.GN] (2012).

Gimeno, I. M. Marek's disease vaccines: a solution for today but a worry for tomorrow? Vaccine 26, C31-41 (2008).

Gordon, A. FASTX-toolkit. (2009).

Hearn, C. J., Steep, A. & Cheng, H. H. tcr_analysis. (2017).

Jones, D. C. fastq-tools. (2012).

Kaufman, J. The simple chicken major histocompatibility complex: life and death in the face of pathogens and vaccines. Philos. Trans. R. Soc. Lond., B, Biol. Sci. 355, 1077–1084 (2000).

Koch, M. et al. Structures of an MHC class I molecule from B21 chickens illustrate promiscuous peptide binding. Immunity 27, 885–899 (2007).

Koren, S. et al. Canu: scalable and accurate long-read assembly via adaptive k-mer weighting and repeat separation. Genome Res. 27, 722–736 (2017).

Kumar, S., Buza, J. J. & Burgess, S. C. Genotype-dependent tumor regression in Marek's disease mediated at the level of tumor immunity. Cancer Microenviron. 2, 23–31 (2009).

Lahti, J. M., Thompson, C. B. & Cooper, M. D. Two distinct alpha-beta T-cell lineages can be distinguished by the differential usage of T-cell receptor V beta gene segments. Proc. Natl. Acad. Sci. U.S.A. 88, 10956–10960 (1991).

Lee, L. F. & Bacon, L. D. Ontogeny and line differences in the mitogenic response of chicken lymphocytes. Poult. Sci. 62, 579–584 (1983).

Lee, L. F., Powell, P. C., Rennie, M., Ross, L. J. & Payne, L. N. Nature of genetic resistance to Marek's disease in chickens. J. Natl. Cancer Inst. 66, 789–796 (1981).

Li, H. Aligning sequence reads, clone sequences and assembly contigs with BWA-MEM. arXiv:1303.3997 [q-bio.GN] (2013).

Li, H. et al. The Sequence Alignment/Map format and SAMtools. Bioinformatics 25, 2078–2079 (2009).

32. Liu, H.-C., Cheng, H. H., Tirunagaru, V., Sofer, L. & Burnside, J. A strategy to identify positional candidate genes conferring Marek's disease resistance by integrating DNA microarrays and genetic mapping. Anim. Genet. 32, 351–359 (2001).

Luhtala, M. Chicken CD4, CD8alphabeta, and CD8alphaalpha T cell co-receptor molecules. Poult. Sci. 77, 1858–1873 (1998).

Luo, J. et al. Histone methylation analysis and pathway predictions in chickens after MDV Infection. PLoS ONE 7, e41849 (2012).

Luo, J. et al. DNA methylation fluctuation induced by virus infection differs between MD-resistant and -susceptible chickens. Front. Genet. 3, doi:10.3389/fgene.2012.00020 (2012).

Luo, J. et al. Genome-wide copy number variant analysis in inbred chickens lines with different susceptibility to Marek's disease. G3-Genes Genom. Genet. 3, 217–223 (2013).

Lusso, P. et al. Productive infection of CD4+ and CD8+ mature human T cell populations and clones by human herpesvirus 6. Transcriptional down-regulation of CD3. J. Immunol. 147, 685–691 (1991).

Ma, J., Wang, S., Zhao, F. & Xu, J. Protein threading using context-specific alignment potential. Bioinformatics 29, i257–i265 (2013).

MacEachern, S., Muir, W. M., Crosby, S. & Cheng, H. H. Genome-wide identification of allele-specific expression (ASE) in response to Marek's disease virus infection using next generation sequencing. BMC Proc. 5, S14-S16 (2011).

MacEachern, S., Muir, W. M., Crosby, S. D. & Cheng, H. H. Genome-wide identification and quantification of cis- and trans-regulated genes responding to Marek's disease virus infection via analysis of allele-specific expression. Front. Genet. 2, doi:10.3389/fgene.2011.00113 (2012).

Marek, J. Multiple Nervenentzündung (Polyneuritis) bei Hühnern. DTW. Dtsch. Tierarztl. Wochenschr. 15, 417–421 (1907).

Miller, M. M. & Taylor, R. L. Brief review of the chicken Major Histocompatibility Complex: the genes, their distribution on chromosome 16, and their contributions to disease resistance. Poult. Sci. 95, 375–392 (2016).

Mwangi, W. N. et al. Clonal structure of rapid-onset MDV-driven CD4+ lymphomas and responding CD8+ T cells. PLoS Pathog. 7, e1001337 (2011).

Nair, V. Evolution of Marek's disease—a paradigm for incessant race between the pathogen and the host. Vet. J. 170, 175–183 (2005).

Omar, A. R. & Schat, K. A. Characterization of Marek's disease herpesvirus-specific cytotoxic T lymphocytes in chickens inoculated with a non-oncogenic vaccine strain of MDV. Immunology 90, 579–585 (1997).

Parham, P. Immunogenetics. Soaring costs in defence. Nature 401, 870–871 (1999).

Perumbakkam, S., Muir, W. M., Black-Pyrkosz, A., Okimoto, R. & Cheng, H. H. Comparison and contrast of genes and biological pathways responding to Marek's disease virus infection using allele-specific expression and differential expression in broiler and layer chickens. BMC Genomics 14, 64-73 (2013).

Robinson, J. T. et al. Integrative genomics viewer. Nat. Biotechnol. 29, 24–26 (2011).

Sherman, M. A. et al. Mass spectral data for 64 eluted peptides and structural modeling define peptide binding preferences for class I alleles in two chicken MHC-B haplotypes associated with opposite responses to Marek's disease. Immunogenetics 60, 527–541 (2008).

Sievers, F. & Higgins, D. G. Clustal Omega, accurate alignment of very large numbers of sequences. Methods Mol. Biol. 1079, 105–116 (2014).

Stone, H. A. USDA Tech. Bull. No. 1514, United States Department of Agriculture, Boca Raton. (1975).

Sullivan, B. M. & Coscoy, L. Downregulation of the T-cell receptor complex and impairment of T-cell activation by human herpesvirus 6 U24 protein. J. Virol. 82, 602–608 (2008).

Thorvaldsdóttir, H., Robinson, J. T. & Mesirov, J. P. Integrative Genomics Viewer (IGV): high-performance genomics data visualization and exploration. Brief. Bioinformatics 14, 178–192 (2013).

Tian, F. et al. DNMT gene expression and methylome in Marek's disease resistant and susceptible chickens prior to and following infection by MDV. Epigenetics 8, 431–444 (2013).

Vainio, O., Lassila, O., Cihak, J., Lösch, U., and Houssaint, E. Tissue distribution and appearance in ontogeny of alpha/beta T Cell Receptor (TCR2) in Chicken. Cell. Immunol. 1245, 254–260 (1990).

Vallejo, R. L. et al. Genetic mapping of quantitative trait loci affecting susceptibility to Marek's disease virus induced tumors in F2 intercross chickens. Genetics 148, 349–360 (1998).

Wang, Z. & Xu, J. Predicting protein contact map using evolutionary and physical constraints by integer programming (extended version). Bioinformatics 29, i266–i273 (2013).

Warren, W. C. et al. A new chicken genome assembly provides insight into avian genome structure. G3-Genes Genom. Genet. 7, 109–117 (2017).

Waterhouse, A. et al. SWISS-MODEL: homology modelling of protein structures and complexes. Nucleic Acids Res. 46, W296–W303 (2018).

Wick, R. R., Schultz, M. B., Zobel, J. & Holt, K. E. Bandage: interactive visualization of de novo genome assemblies: Fig. 1. Bioinformatics 31, 3350–3352 (2015).

Witter, R. L. Increased virulence of Marek's disease virus field isolates. Avian Dis. 41, 149-163 (1997).

Xu, S., Yonash, N., Vallejo, R. L. & Cheng, H. H. Mapping quantitative trait loci for binary traits using a heterogeneous residual variance model: an application to Marek's disease susceptibility in chickens. Genetica 104, 171–178 (1998).

Yonash, N., Bacon, L. D., Witter, R. L. & Cheng, H. H. High resolution mapping and identification of new quantitative trait loci (QTL) affecting susceptibility to Marek's disease. Anim. Genet. 30, 126–135 (1999).

Yu, Y. et al. Temporal transcriptome changes induced by MDV in marek's disease-resistant and susceptible inbred chickens. BMC Genomics 12, 501-512 (2011).

Zhang, H. M., Hunt, H. D., Kulkarni, G. B., Palmquist, D. E. & Bacon, L. D. Lymphoid organ size varies among inbred lines 6(3) and 7(2) and their thirteen recombinant congenic strains of chickens with the same major histocompatibility complex. Poult. Sci. 85, 844–853 (2006).

Zhang, Z., Schwartz, S., Wagner, L. & Miller, W. A greedy algorithm for aligning DNA sequences. J. Comput. Biol. 7, 203–214 (2000).

CHAPTER 3

Neurovirulence of a Meq-deleted MDV in Early In Ovo Challenge

Abstract

Marek's disease virus is an important pathogen of chickens which causes neuropathic as well as lymphoproliferative disease. Virulent MDV strains include an oncogene, Meq, while avirulent MDV and closely related viruses are nononcogenic and apparently non-neuropathic, thus allowing their use as vaccine strains. Here, we describe a fatal neuropathy of chicks induced by early in ovo injection (prior to 15 days of embryogenesis) of non-oncogenic Meq-deleted MDV, which induces severe bursa and thymic atrophy as well as mild lymphocytic peripheral nerve lesions. We suggest that the previously identified correlation between neuropathogenicity and a single MDV gene (pp14) presents a strong case for an immune-mediated component to MDV neuropathy, and that other vaccine strains may be capable of inducing neuropathic disease in immune-disregulated birds.

Introduction

Marek's disease (MD) was first identified by Dr. Josef Marek in 1907, and was originally described as a polyneuritis of chickens (Marek, 1907). In subsequent decades, lymphoma was also identified as a component of the disease, and MD was grouped with other lymphomagenic diseases of chickens as part of the 'avian leucosis complex'; by the 1950's, lymphomas due to MD had become a significant problem for the poultry industry, although neurologic lesions were still noted (Witter 1998). In 1967, the causative agent of the neuropathogenic member of

this disease complex was isolated and identified as a herpesvirus (Churchill and Biggs, 1967). In the latter half of the 20th century, Marek's disease was associated with several increases in virulence that necessitated introduction of vaccines for disease control, beginning with the use of the closely related apathogenic Herpesvirus of Turkeys (HVT), followed by non-oncogenic MDV serotype 2 strains and bivalent HVT/serotype 2 vaccination, and most recently including the in-vitro passaged, attenuated serotype 1 strain, CVI988/Rispens (reviewed in Biggs 1975). Virulent wild-type strains currently cause pathology ranging from visceral, skin and ocular lymphomas to several different neurologic syndromes (e.g., transient paralysis, chronic demyelinating polyneuritis), and can cause high morbidities and mortalities in unvaccinated flocks (reviewed in Osterrieder 2006).

Two types of neuropathic lesions have been identified on histopathology of peripheral nerves in classical MD. Type A is considered to be neoplastic/proliferative and also demyelinating in Payne and Bigg's early classification system, while the second lesion, "type B," is described as a lymphocytic inflammatory lesion (Payne 1967), although tracking the prevalence of each lesion over time suggested that proliferative lesions preceded inflammatory lesions, which might be regressing or repairing "type A" lesions (Lawn 1979, Payne 1979). It is not yet known what process directly leads to nerve injury in MD, although speculated possibilities have included direct infection of nerve tissue, neurolymphomatosis, or an autoimmune response.

A case for immune-mediated injury to peripheral nerves in MD was made in the 1970's by Lampert and others (Lampert 1977, Pepose 1981, reviewed in Lampert 1978). Histological and ultrastructural similarities between an iatrogenic autoimmune neuropathy, experimental

allergic neuritis (EAN), induced by vaccinating chickens with adjuvanted human nerve tissue, and MD neuropathy, included active demyelination by infiltrating mononuclear cells. No MDV virions could be detected within either neurons or myelinating Schwann cells, although supporting cells including mononuclear cells and nonmyelinating Schwann cells were found to be infected after 2-3 days of ex vivo culture (Lampert 1977). Most interestingly, infection with MDV was found to sensitize birds to healthy peripheral nerve homogenates, as demonstrated by a lymphocytic infiltrative response to dermal injection. This suggests that at least a component of MD neuropathic disease is mediated by cellular autoimmunity (Pepose 1981).

In addition to the classical chronic polyneuritis of MD, an acute transient paralysis has been described as an early (8-12 days post challenge) neurologic syndrome in which birds develop paralytic symptoms for 1 or 2 days and often recover, although they later develop 'classical MD' symptoms (Kenzy 1973, Swayne 1989). During the transient paralytic phase, the primary lesion appeared to be encephalitis characterized by lymphocytic vasculitis and perivascular cuffing, although scattered lymphocytes were also observed in the nerves during this phase (Kenzy 1973). The proximate cause of the paralytic symptoms in this syndrome has been identified as vasogenic edema (Swayne 1989), but it is unknown whether there is a local infection component or the response is primarily immune-mediated, although it has been suggested that antibody production may be necessary for this syndrome to occur, as bursectomy abrogates transient paralysis (Parker 1983). Virus virulence and host genetics are both known to contribute to susceptibility to transient paralysis, with more susceptible birds developing a more pro-inflammatory cytokine response within CNS tissue (Swayne 1989, Xu 2012).

Vaccination with HVT, while not associated with clinical disease, has been associated with the development of "Type B" neuropathic lesions. In ovo vaccination with HVT at 18 days of embryonation could cause mild vagus nerve lesions in week-old birds, although no lesions were detectable in 6-week old birds (Scharma 1982). Additionally, mild, regressing nerve lesions have been detected in birds vaccinated at hatch with HVT (indicating that nononcogenic strains are known to be capable of producing at least histopathologic neuropathy), although no mention of clinical signs was made. Immunosuppression with cyclophosphamide enhanced the nerve lesions and in these animals the lesions failed to regress after 10 weeks (Witter 1976). It was suggested that HVT may have a slight oncogenic potential on the basis of these lesions. Microscopic lesions have also been seen in birds vaccinated with very large doses of HVT at up to 20 weeks post-vaccination, but again were apparently not correlated with gross lesions or disease (Okazaki 1970). The same group also reported minor nerve lesions in birds treated with cyclophosphamide alone, or in one experiment, controls (although they did not report on virus isolation from these birds that tested negative for MDV antibodies) (Purchase 1974). When HVT is injected prior to 15 days of embryonation in ovo, before the first wave of lymphoid precursor cells enters the thymus, central tolerance to HVT can be induced and chicks exhibit a reduced vaccinal response against MDV; however, nerve lesions have to our knowledge not been studied in this model (Scharma 1982). Importantly, HVT replication in ovo in this model greatly reduces hatchability, so the chicks hatched may not be those most representative of the effect of immune tolerance on neuropathogenicity of HVT.

At least one neurovirulence factor in MDV has been described. The nonessential MDV gene pp14 was studied in knockout and revertant experiments, and was found to be necessary for neuropathology; birds challenged with the pp14 knockout virus failed to develop either type A or type B lesions, and survived to end of experiment at 42 days. Surprisingly, pp14 was not necessary for oncogenesis, as these birds had non-neurologic tumor involvement at the same rate as birds challenged with wild type virus (Tahiri-Alaoui, 2013). This finding would suggest that either oncogenesis is not involved in the development of neurologic lesions in MD at all, or, more probably, that pp14 predisposes challenged birds to intraneural tumorigenesis through lymphoid trafficking into inflammatory lesions within the nervous system.

An apparently spontaneous syndrome of polyradiculoneuritis bearing similarity to MDV has been described as affecting up to 1% of commercial White Leghorn layer chickens (Bader 2010). In this syndrome which was characterized in a MD-vaccinated (Rispens strain) flock, lymphohistiocytic inflammation and demyelination widely affected the peripheral nervous system of affected animals, and an IFN-y-driven cytokine response indicated robust TH1 activation in the affected nerves. Interestingly, the phenotype was found to correlate with MHC haplotype, similarly to MDV, and the most susceptible haplotype in the study (as identified by the linked genetic marker LEI0258) shared the same marker size (539 bp) with the MD-susceptible B19 haplotype (Fulton, 2016). The authors suggested that exposure to viral or other pathogens or vaccines could be responsible for this syndrome, although field strains of MDV were ruled out as the causative agent.

Recently, rational vaccine design methods have been sought in order to develop MDV vaccine strains for MDV that provide the most protective immunogenic stimulus while still

remaining avirulent in vivo. One strategy is deletion of specific virulence factor(s) from the viral genome that delete pathogenic effects directly or decrease viral replication to nonpathogenic levels. An example of this strategy was the development of the Meq-deleted strain of MDV (Lupiani 2004). Meg is the MDV-encoded oncogene; removal of Meg is sufficient to prevent the development of lymphomas, and the Meq-deleted strain (MDV-delta-Meq) is a highly effective vaccine that can protect against challenge with very virulent strains of MDV (Lee 2008). MDV-delta-Meq does not cause pathogenic effects in maternal-antibody-protected chicks; however, it causes thymic and bursal atrophy in chicks lacking maternal antibody unless serially passaged (Lee 2013). This indicates that MDV-delta-Meg is capable of supporting a robust cytolytic infection in these birds, and raises concerns about potential immunosuppressive effects of vaccination with this strain, at least in chicks lacking maternal antibodies. We tested the pathogenicity of this strain in a tolerized-embryo model, in which chicks were injected in ovo prior to 15 days of embryonation. In this report, we show that MDV-delta-Meq is both lethal and neuropathogenic when used as a tolerizing agent in ovo, and formally demonstrate that Meq-driven oncogenicity is not required for the development of nerve lesions secondary to MDV infection; i.e., the "type A" lesion is not a prerequisite for the "type B" lesion. Additionally, we believe this supports the hypothesis that vaccination with serotype 1 strains of MDV may be responsible for spontaneous paretic disease in commercial flocks, particularly in susceptible or immunocompromised animals, and that the potential for neuropathogenicity in susceptible animals should be considered as part of the safety profile in novel MD vaccine design.

Materials and Methods

<u>Animals</u>

The line of chickens used was $15I_5x7_1$ SPF white leghorn chickens, an F1 hybrid of MD susceptible $15I_5$ males mated to 7_1 females; both lines are highly inbred. Maternal antibodynegative embryos were used for all experiments. All experimental animal work was performed in accordance with USDA ADOL Animal Care and Use Committee-approved protocols.

Viruses

Md5 MDV was generated from the infectious BAC clone B40 which contains the entire Md5 genome (Niikura 2011). Md5-delta-Meq was generated from a Meq-deleted B40 BAC clone as previously described (Lupiani 2004) and has both copies of the Meq oncogene deleted. Viruses were propagated in duck embryo fibroblasts (DEFs), cryopreserved in liquid nitrogen and titrated on DEF monolayers to determine plaque-forming units per mL of frozen stock.

Tolerization Experiments

In Experiment 1, 90 embryos per group were inoculated on embryo incubation day (EID) 11 or 14 with 2,000 plaque-forming units of MDV-delta-Meq (propagated in DEFs) in 100 uL of sterile Lebowitz-McCoy media. In ovo injections were performed with a 1 inch, 22 g needle injected downward through the air sac to reach the chorioallantois. In the majority of eggs, injection could be performed vertically through the center of the large end of the egg. Embryos were incubated normally for the remainder of the 21-day incubation period. Groups of 17 hatched chicks per group were housed in Horsfall-Bauer (HB) units and challenged with 2,000 pfu of the

parental strain Md5 MDV at 3 days post-hatch, or maintained without further challenge.

Additional groups of 17 chicks were inoculated at hatch with 2,000 pfu of MDV-delta-Meq, inoculated at hatch with 2,000 pfu of MDV-delta-Meq and at 3 days post-hatch with Md5 MDV, inoculated at 3 days post-hatch with Md5 MDV, or left unchallenged; and housed in parallel.

In Experiment 2, 61 embryos per group were inoculated on EID 11 with either 2,000 pfu of MDV-delta-Meq (propagated in DEF) in 100 uL of sterile Lebowitz-McCoy media, or an equivalent number (approximately 3,000 cells) DEF in the same volume (mock treatment), using the same inoculation methods as in Experiment 1. Embryos were incubated normally for the remainder of the 21-day incubation period and 35 hatched chicks per group were housed in HB units. Additional groups of 35 chicks were inoculated at hatch with 2,000 pfu of MDV-delta-Meq, or the parental virus, Md5 MDV and housed in parallel. Humane euthanasia and tissue sampling of 6 chicks per group was performed at days 4, 8, 14, 21, and 28 post-hatch. Birds showing clinical signs on sampling days were selectively included within the sampling groups, as these birds were otherwise likely to die or require euthanasia prior to the next sampling date.

In both experiments, clinical signs were scored twice daily on a scale used in our facility to stage severity of MD, where a score of 0 indicates no symptoms, 1 indicates mild behavioral abnormalities, 2 indicates mild neurologic symptoms, 3 indicates partial or transient paralysis, 4 indicates significant morbidity including reduced responsiveness and unlikeliness to eat or drink, and 5 indicates a down/fully paralyzed bird. Scores of 4 and 5 are considered end-stage disease and require euthanasia.

Immunohistochemistry

Immunohistochemistry was performed at the Michigan State University Diagnostic Center for Animal Health. Samples for immunohistochemistry were flash-frozen in Tissue-Tek Optimal Cutting Temperature compound (Sakura Finetek) on liquid nitrogen and stored at -80 °C. Antibodies used for Immunohistochemistry included H19 anti-pp38 antibody (Lee 1983, Cui 1991), anti-Meq antibody (Lee 1997) and anti-CD4 antibody (Southern Biotech).

DNA extraction

From blood samples, peripheral blood leukocytes (PBLs) were isolated over Histopaque-1077 (Sigma) according to the manufacturer's instructions and stored at -20 °C until processing for DNA extraction. DNA was extracted from 5 uL of pelleted WBCs by resuspension in 300 ul lysis buffer (1% SDS, 10 mM Tris, 0.5 mM EDTA) and overnight incubation at 56 °C with shaking on a thermomixer. Samples were treated with 2 ug RNase A at room temperature for 30 minutes and precipitated with 100 ul of Qiagen Protein Precipitation Solution for 10 minutes on ice.

Centrifuged sample supernatants were loaded on a 96-well DNA column plate, centrifuged for DNA binding, and washed three times with WS buffer (GenCatch, Inc.), spun-dry for 5 minutes and air-dried overnight before elution with 100 uL of distilled water. Nerve tissue samples were processed similarly with the addition of 400 ug proteinase K to 500 ul of lysis volume for approximately 10 mg of tissue.

Quantitative PCR

Viral load was quantified from DNA extracted from WBCs or nerve tissue using Taqman qPCR on an ABI 7500 system. Primers and probes are listed in Table 1. DNA samples were diluted to 2 ng/ul and 2 ul of sample per 25 ul reaction was used, with Taqman Fast Universal 2x Master Mix and standard reaction conditions. GAPDH was used as an internal housekeeping gene (Gimeno 2008), and absolute quantitation for Meq, gB, and GAPDH was performed using serial dilutions of control DNA to generate a standard curve.

Table 3.1. Quantitative PCR primers and probes

Primer/Probe	Sequence			
Meq TM.5	5'-TGACCCTTGGACTGCTTACCA-3'			
Meq TM.3	5'-GAGCCAACAAATCCCCTGAC-3'			
Meq-TMP	5'-Fam-CCGCACGATCCCGTTCCTGAA-BHQ-3'			
gB TM.5	5-CGGTGGCTTTTCTAGGTTCG-3			
gB TM.3	5-CCAGTGGGTTCAACCGTGA-3			
gB TM probe	5'-Fam-CATTTTCGCGGCGGTTCTAGACGG-BHQ-3'			
DKGAPDH-TMF	5'-CAACGGTGACAGCCATTCCT-3'			
DKGAPDH-TMR	5'-ATGGTCGTTCAGTGCAATGC-3'			
DKGAPDH-TMP	5'-Vic-CCTTTGATGCGGGTGCT-BHQ-3'			

Statistics

For qPCR data, standard curves were used to calculate absolute concentrations of target genes and GAPDH, and ratios of target to GAPDH were calculated and averaged. Samples with target genes too low to quantify were counted as zero as long as GAPDH was quantifiable, and censored otherwise. Averaged ratios were compared by 2-way ANOVA in Prism 7 followed by post hoc Tukey's tests for multiple comparisons. A p-value of <0.05 was considered significant.

Survival curve analysis was performed in Prism 7, and log-rank comparisons were performed to assess between-group significance. A Bonferonni-corrected p-value of <0.05 was considered significant.

Bursa and thymic atrophy scores were analyzed in Jamovi v. 0.8.0.10. Groups were compared by Kruskall-Wallace's test, followed by Dwass-Steel-Critchlow-Fligner pairwise comparisons to control for multiple comparison of non-parametric data.

Results

Experiment 1

In Experiment 1, hatchability was 69% in uninjected controls, 64% in eggs injected at EID 11, and 69% in eggs injected at EID 14. Chicks injected at either day 11 or day 14 of embryonation, or at hatch with Md5-delta-Meq, and controls (unchallenged, challenged at 3 days with Md5, or vaccinated at hatch with Md5-delta-Meq and challenged at 3 days with Md5), were housed for 57 days and monitored for morbidity and mortality. As shown in the Kaplan-Meier analysis in Figure 1, Md5-delta-Meq at hatch was avirulent (Figure 3.1A) and fully protective against challenge 3 days later with virulent Md5 (Figure 3.1B); 100% of birds in these groups survived

with no clinical signs. In contrast, survival rate to 8 weeks was 60% in birds inoculated at 14 days of embryonation with Md5-delta-Meq, and survival rate in birds inoculated at 11 days of embryonation with Md5-delta-Meq was 30%, which was not significantly different than virulent Md5 given at hatch (21% estimated survival rate) (Figure 3.1A).

Clinical scores were recorded in each cage throughout the course of the experiment as described above. The scoring system used is specific to MD and tracks neurobehavioral abnormalities, with a score of 3 indicating partial paralysis (typically presenting as gait abnormalities, wing droop and/or torticollis.) Figure 3.1C shows the number of live birds scoring 3 or higher over time present in the single-challenged groups; no birds showed clinical signs scoring 3 or higher in the control group or hatch-vaccinated groups (and no mortalities occurred in these groups). In contrast, birds injected with Md5-delta-Meq at EID 11 or EID 14 showed sporadic clinical signs beginning at 14 days post-infection, followed by acute mortality of affected birds within 1-3 days, while the Md5-infected group also showed an early acute phase, which was followed by a late peak in clinical scores typical of oncogenic MD.

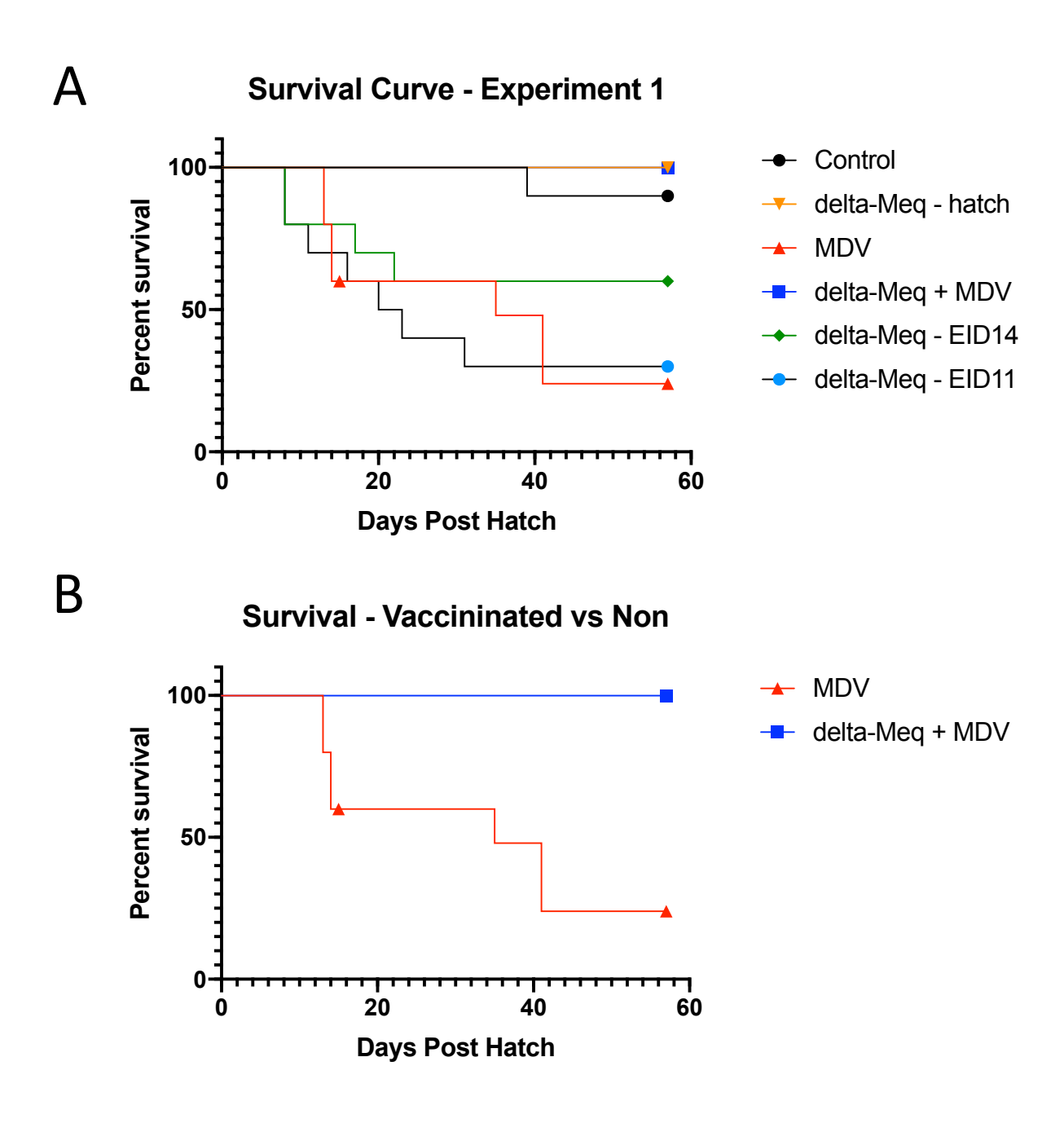
At necropsy, most birds injected either at hatch or in ovo with Md5-delta-Meq were found to have bursal and/or thymic atrophy (see Table 2); only groups injected at EID 14 had less than 100% of birds affected (Figures 3.2A, 3.S1). Bursa and thymic atrophy was scored visually on a 0-4 scale, and was extremely severe in birds injected at EID 11 with Md5-delta-Meq, either with or without Md5 challenge (Figure 3.3A-B). No tumors were found in birds injected only with Md5-delta-Meq, while visceral tumor involvement was present in two-thirds of Md5-challenged birds. Tumor incidence and nerve enlargement was reduced in birds inoculated at day 14, and especially day 11 of embryonation and challenged post-hatch with

Md5 (Table 2). Additionally, chick stunting was noted at similar levels between in chicks in ovo injected with Md5-delta-Meq at EID 11 (37%) and chicks injected at 3 dph with Md5 (33%), while stunting was not observed in chicks injected with Md5-delta-Meq at hatch (Table 3). Conversely, 66% of chicks injected with Md5-delta-meq at hatch were visually noted to have reduced spleen size, while 37.5% of chicks injected at EID11 had reduced spleen size, and this did not overlap with the stunting observed in this group; however, among chicks injected with both Md5-delta-Meq at EID11 and Md5 at 3 dph, stunted chicks also were found to have small, pale spleens (Table 3). One bird from the Md5-delta-Meq at EID 14 group lived to the end of the experiment but showed neurologic signs of wing droop and hunching (Figure 3.2); at necropsy, this bird was severely stunted and also had a dramatically atrophied pancreas (Figures 3.2, 3.S1).

Table 3.2. MD lesions from Experiment 1

	At risk ¹	Nerves ²	BTA ³	Visceral ⁴
Control	10	0%	0%	0%
Md5-delta-Meq at hatch	10	0%	100%	0%
Md5	9	67%	100%	67%
Md5-delta-Meq at hatch plus	10	0%	100%	0%
Md5				
Md5-delta-Meq at EID14	10	0%	70%	0%
Md5-delta-Meq at EID14 plus	9	22%	89%	44%
Md5				
Md5-delta-Meq at EID11	8	0%	100%	0%
Md5-delta-Meq at EID11 plus	9	0%	100%	0%
Md5				

- 1. Number of birds examined at necropsy
- 2. Indicates enlargement of vagal nerve, brachial or sciatic plexus
- 3. Indicates bursal and/or thymic atrophy
- 4. Indicates presence of visceral tumors or diffuse splenomegaly



<u>Figure 3.1. Experiment 1 survival and clinical scores.</u> A: Kaplan-Meier curves showing survival probabilities over time for each group in Experiment 1. B: Kaplan-Meier curves for MDV-infected and hatch-vaccinated, MDV-infected groups. Vaccination at hatch with MDV-delta-Meq was 100% protective.

Figure 3.1 (cont'd).



C: Clinical scores of 3 or higher were recorded for Experiment 1. Numbers of birds over time scoring at 3 or above are indicated for groups infected at hatch with Md5 strain MDV, or challenged in ovo with MDV-delta-Meq at either EID 11 or EID 14.

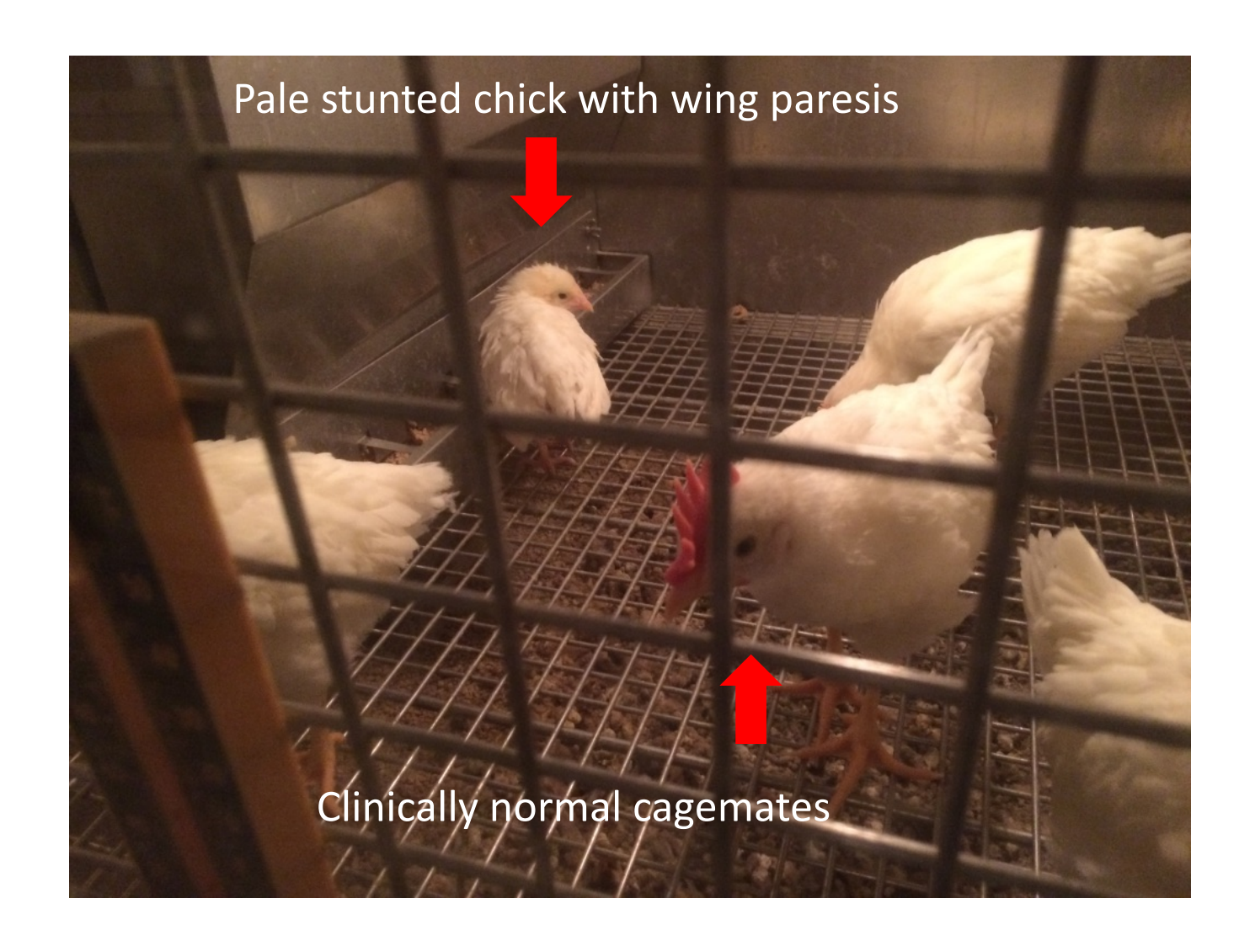
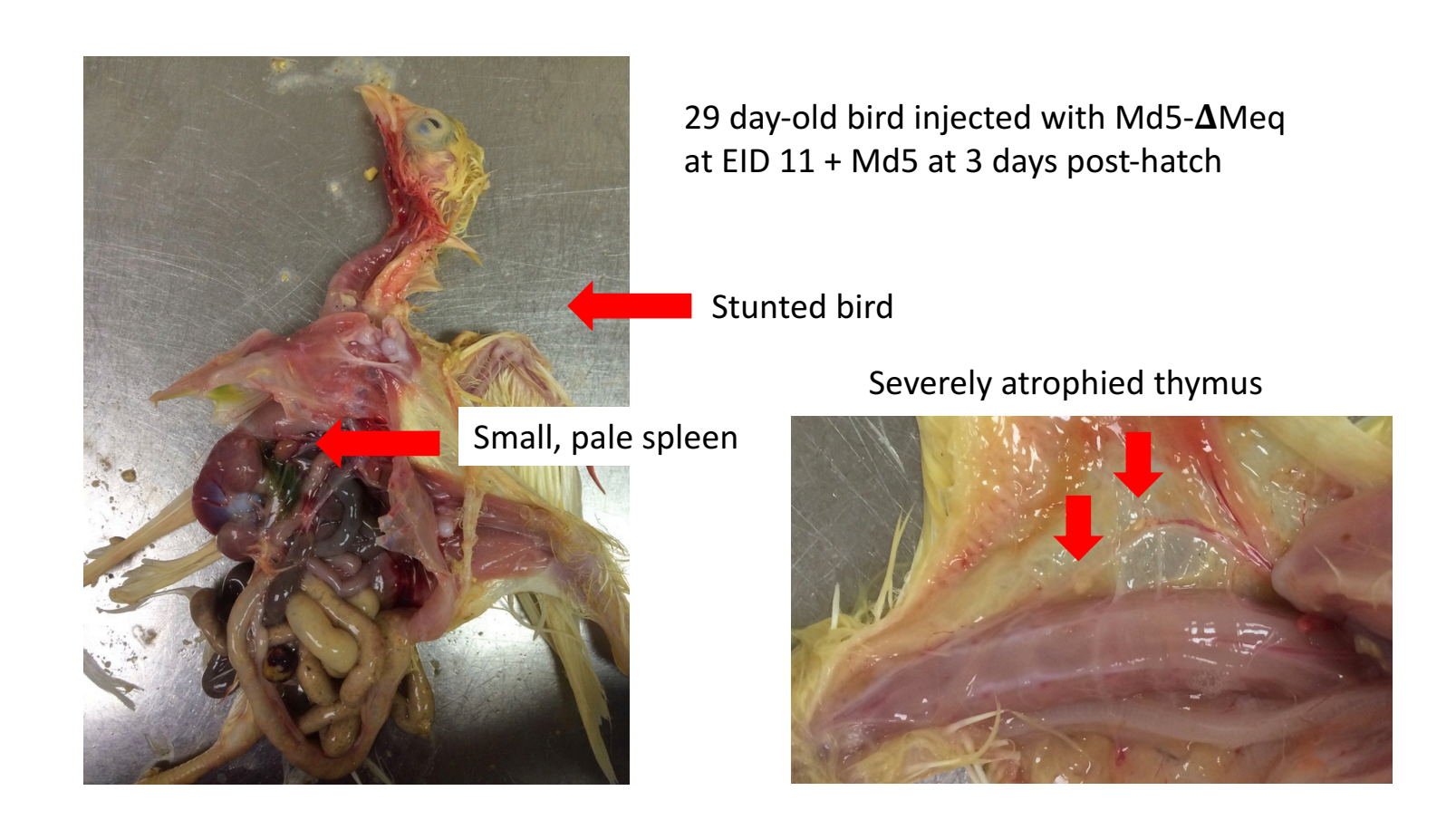


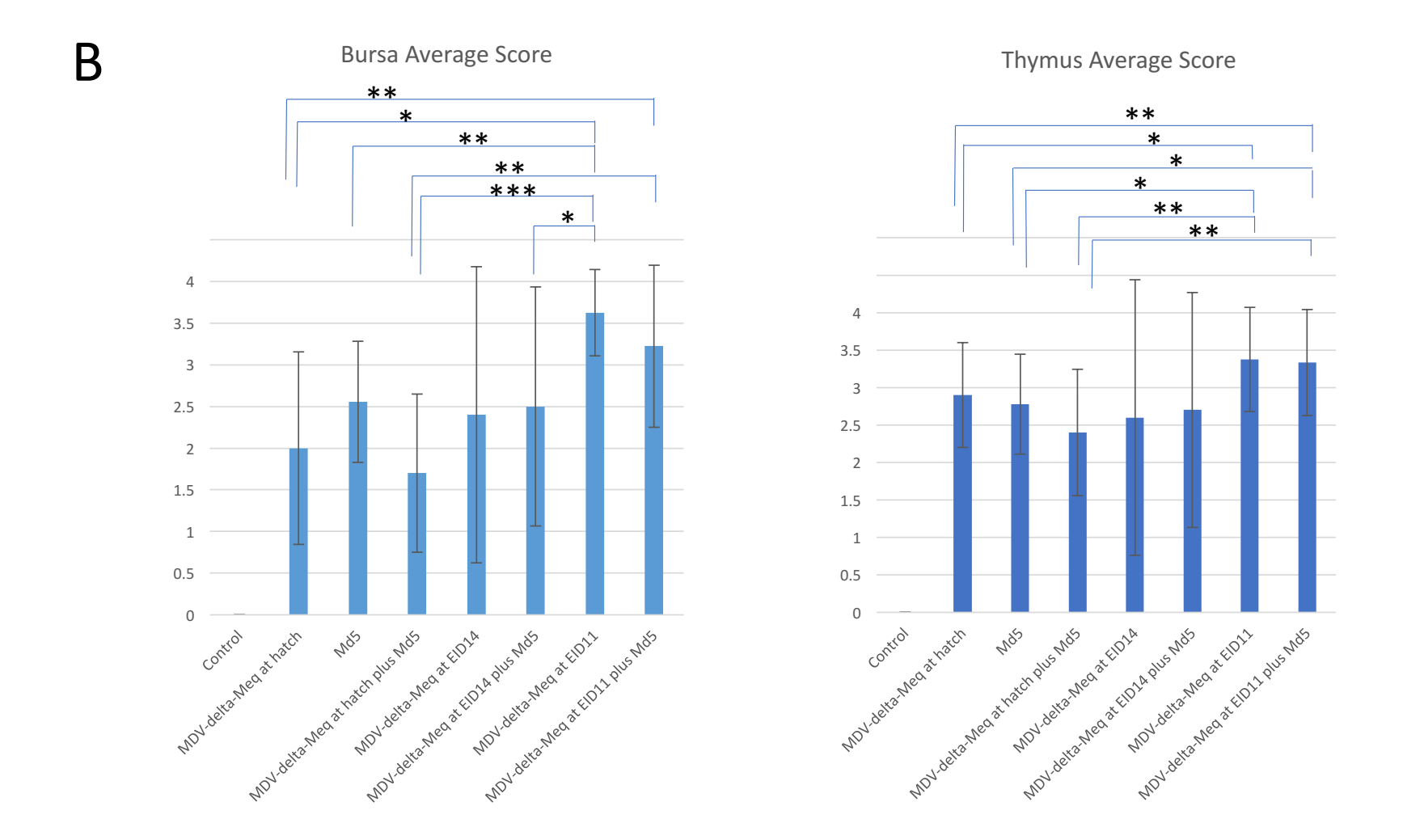
Figure 3.2. Variable results from in ovo injection of MDV-delta-Meq at EID 14. Photo of surviving birds at 34 days post-hatch.

Α



<u>Figure 3.3. Gross pathology.</u> A: Photos show necropsy findings associated with early (EID 11) injection of MDV-delta-Meq in a bird also infected with Md5 MDV at 3 days post-hatch. Necropsy of this bird was performed at 29 days of age.

Figure 3.3 (cont'd).



B: Bursal and thymic atrophy scores at necropsy. Ranked scores were compared by Dwass-Steel-Critchlow-Fligner's test. *=p<0.05, **=p<0.01, **=p<0.001.

Table 3.3. Additional necropsy findings from Experiment 1

	At risk ¹	% Small spleen	% Stunted
Control	10	0%	0%
Md5-delta-Meq at			
hatch	10	60%	0%
Md5	9	0%	33%
Md5-delta-Meq at			
hatch plus Md5	10	56%	0%
Md5-delta-Meq at			
EID14	10	10%	20%
Md5-delta-Meq at			
EID14 plus Md5	9	0%	11%
Md5-delta-Meq at			
EID11	8	38%	38%
Md5-delta-Meq at			
EID11 plus Md5	9	33%	33%

1. Number of birds examined at necropsy

Viremia was measured by quantitative PCR of white blood cell DNA, in single-challenge only groups, at 21 dph for MDV antigens Meq and glycoprotein B (gB), in order to demonstrate that lethality from Md5-delta-Meq was not due to cross-contamination of isolators with wild-type Md5. Meq was not detected in controls or in Md5-delta-Meq only groups, while it was detectable in Md5-challenged birds (Figure 3.4A). Conversely, gB was detectable at very low levels in birds injected at hatch or in ovo at EID 11 with Md5-delta-Meq, while it was more robustly present in birds challenged with Md5, and not detected in uninjected controls or in birds injected at EID 14 (Figure 3.4B).

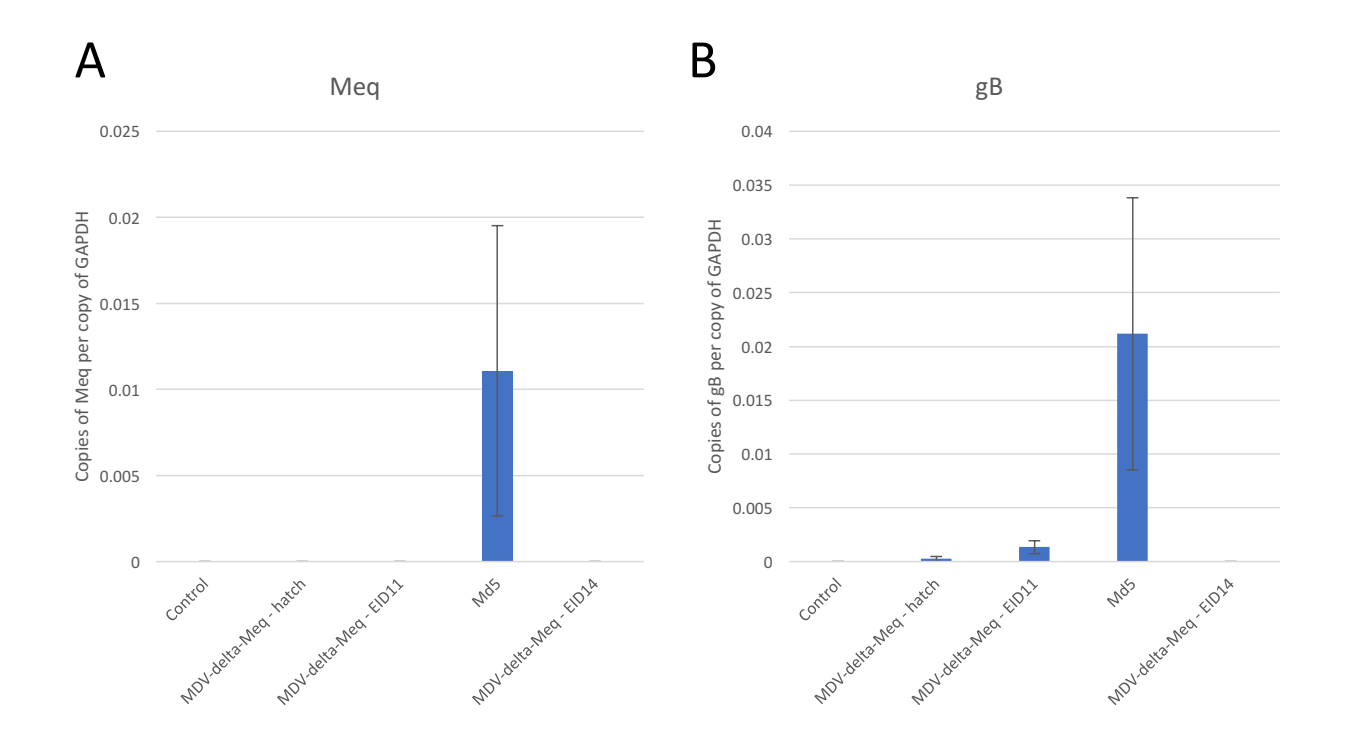
Due to the unexpected mortality and observation of neurologic signs in birds that were injected in ovo with Md5-delta-Meq, we performed histology on the sciatic nerve of 1 bird necropsied at 14 days from the EID 11 Md5-delta-Meq group. We observed moderate

lymphocytic infiltration in this sample which tended to form linear lesions within the nerve bundle (Figure 3.5).

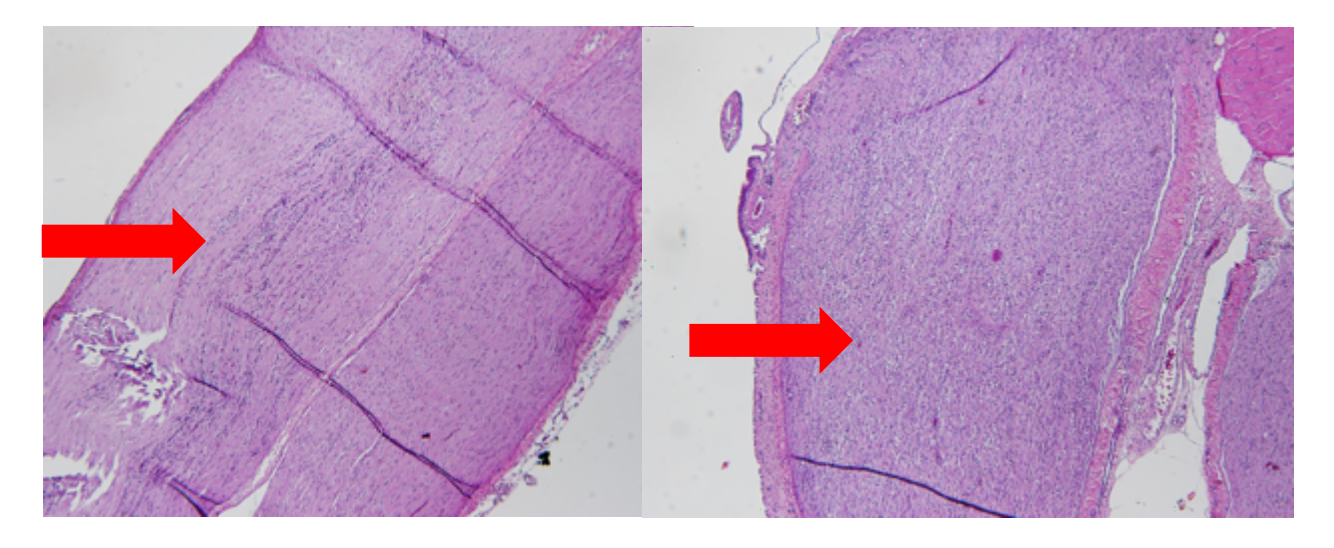
Experiment 2

In experiment 2, *in ovo* injection of Md5-delta-Meq at 11 days of embryonation did not significantly alter hatchability as 67% of embryos hatched in comparison to 69% of uninjected embryos. Eighty percent of mock-injected embryos hatched, indicating that the dose of DEF was not detrimental to hatchability. Based on the necropsy findings of Experiment 1, lack of thymic atrophy was used as an exclusion criterion in downstream analysis, as all birds without thymic atrophy in the in ovo-only injected groups lived to the end of the eight weeks and were suspected to be unsuccessfully inoculated. Survival curve analysis was not performed for this experiment, due to the early sampling performed; however, three birds out of 23 remaining non-sampled birds challenged with Md5 at hatch required euthanasia on day 11 post hatch, and within the group challenged with Md5-delta-Meq at EID 11, 1 bird each died on days 6 and 7 post hatch (out of 29 non-sampled birds) and on days 10 and 11 post hatch (after sampling on day 8, and thus out of 21 remaining non-sampled birds); thus, losses among non-sampled birds were similar in these two groups. No birds died or were euthanized for clinical symptoms in groups that were mock-injected, or vaccinated with Md5-delta-Meq at hatch.

Quantitative PCR of white blood cell DNA was used to compare viremia between sampling groups over the course of the experiment. Meq was not detected above background in any group except for the Md5-challenged birds, and peaked in this group by 2 weeks post-hatch (Figure 3.6A), while gB was detectable above background in birds hatch-vaccinated with



<u>Figure 3.4. Viremia in Experiment 1.</u> Viremia was measured by quantitative PCR of MDV genes Meq (A) and gB (B) at 21 days post-hatch. Data are shown normalized to genomic copies of GAPDH.

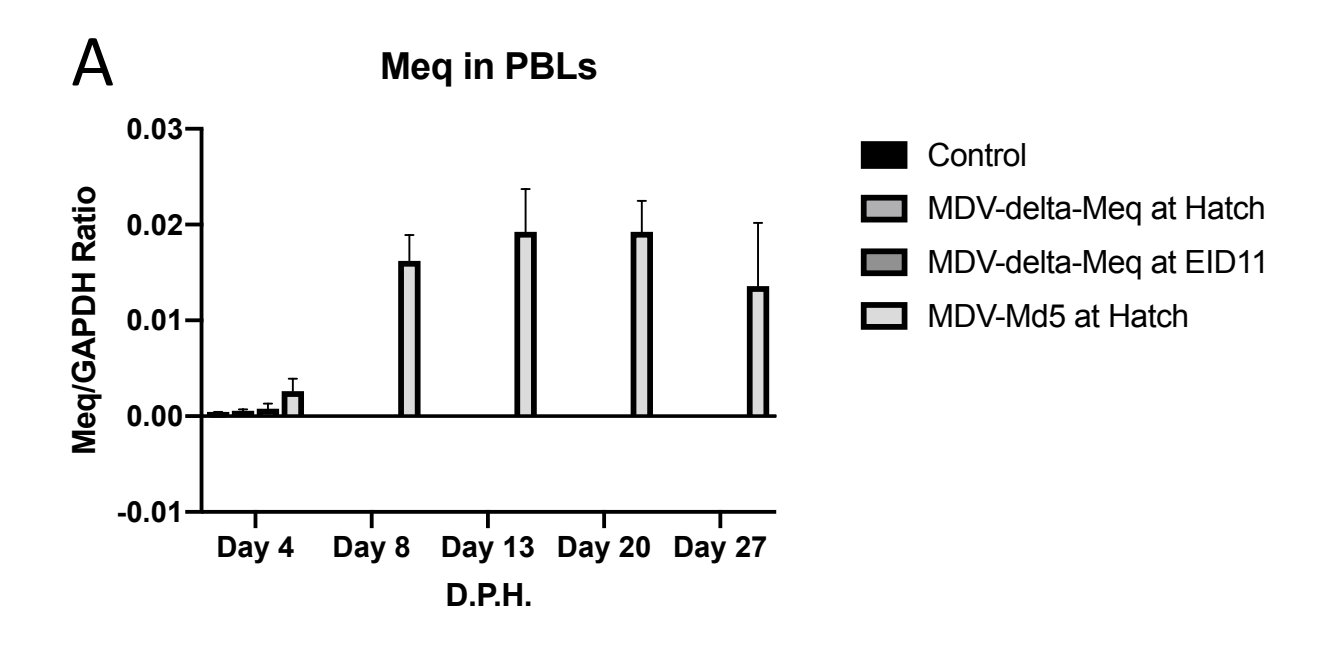


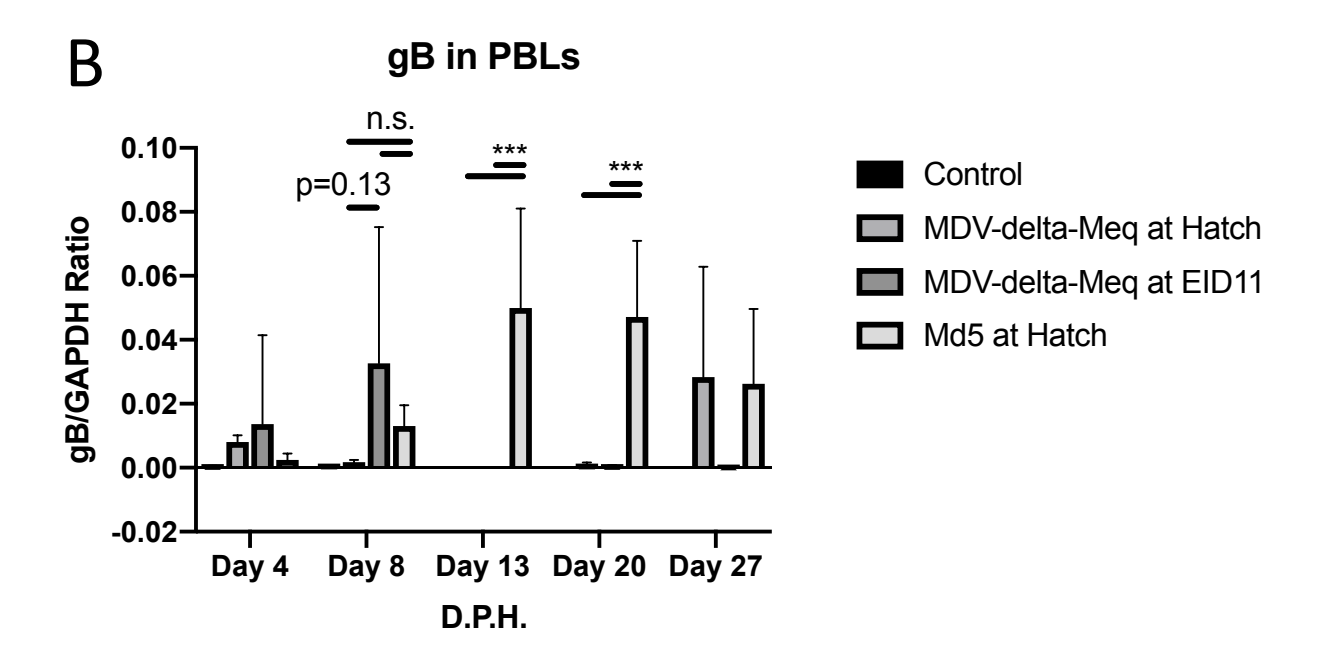
<u>Figure 3.5. Nerve Histopathology in Experiment 1.</u> Photomicrographs show lymphocytic infiltration in the sciatic nerve of a 2-week-old bird injected with Md5- Δ Meq at EID 11. Arrows indicate areas of infiltration within the nerve bundle.

Md5-delta-Meq at a higher level at day 4 than in birds challenged with wildtype Md5; as previously published, gB levels dropped rapidly in hatch-vaccinated birds (Hildebrandt 2015) but peaked at 2 weeks in Md5-challenged birds (Figure 3.6B). Conversely, in the group inoculated at EID 11 with Md5-delta-Meq, only a subset of birds had viremia above background at days 4 and 8 (Figure 3.52, Figure 3.6B), and subsequent time-points did not detect levels of viremia above background the in ovo-injected Md5-delta-Meq groups, although hatch-vaccinated birds variably demonstrated a second phase of viremia at day 27 (Figure 3.6B).

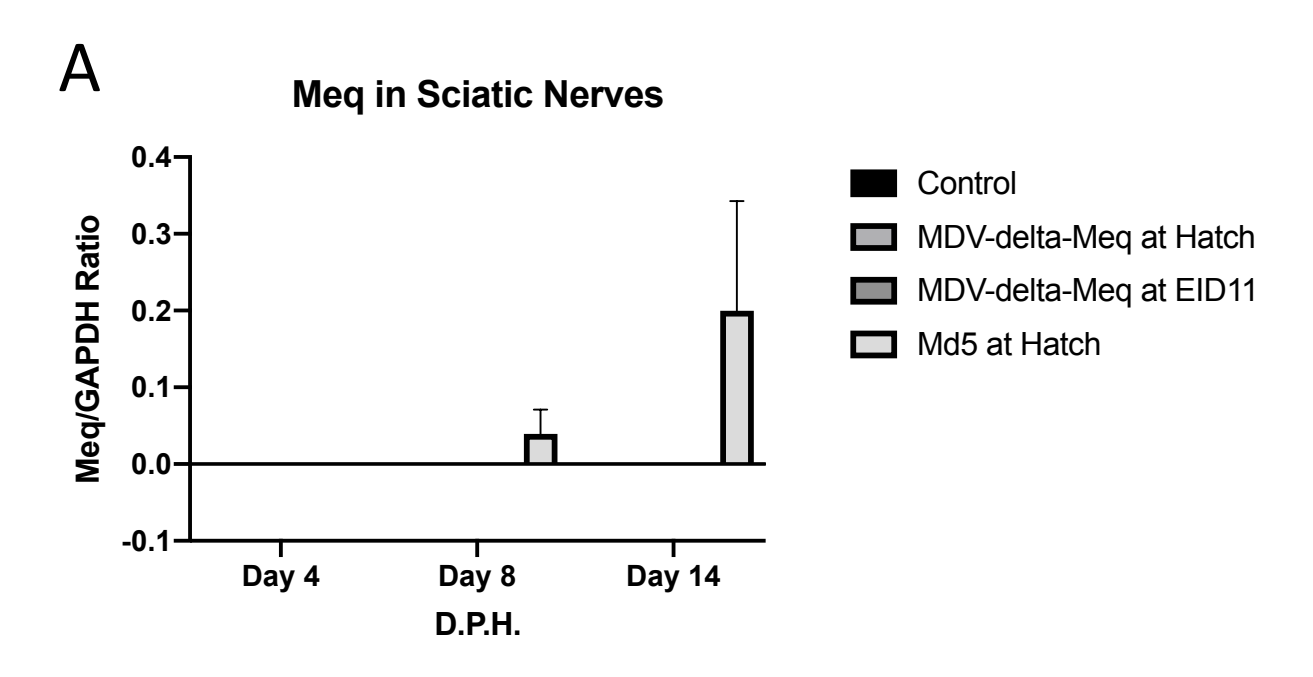
Sciatic nerves were also examined for the presence of virus using quantitative PCR. In both the Md5 and EID 11 Md5-delta-Meq groups, gB was detectable by 8 days, while very little gB was detected in nerves of birds injected with Md5-delta-Meq at hatch; however, by day 14, lytic virus was no longer detected in sciatic nerves of birds in the EID Md5-delta-Meq group, while it was maintained at approximately the same level in the Md5 group (Figure 3.7B). As expected, Meq was not detected in the sciatic nerves of either Md5-delta-Meq group. In contrast, Meq was expressed by day 8 in the sciatic nerves of the Md5 group, and increased in expression through 14 days post infection (Figure 3.7A).

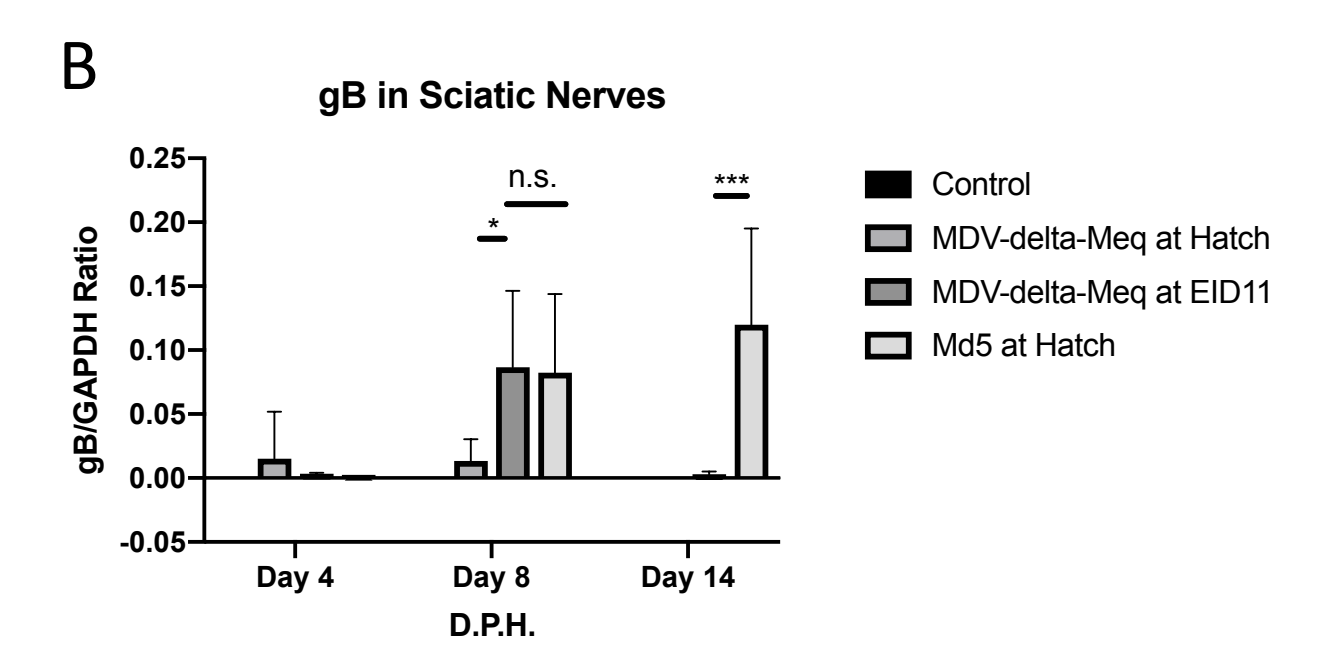
On histopathology, we examined peripheral nerve samples (brachial, vagal and sciatic) from 4 birds from each group of infected with Md5 at hatch, Md5-delta-Meq in ovo at EID 11, or uninfected, at days 8 and 14 post-hatch, and also immunostained samples from day 8 for either Meq or the lytic antigen, pp38. At 8 dph, which corresponded to the highest infection rate in sciatic nerves by qPCR, as expected, Md5-delta-Meq samples were negative for Meq protein expression, while Meq was observed in rare infiltrating cells in nerve samples from birds infected with wild-type Md5 only. Additionally, pp38 positive cells were very rare in both





<u>Figure 3.6. Viremia in Experiment 2.</u> Viremia was measured by quantitative PCR of MDV genes Meq (A) and gB (B) at the indicated days post-hatch. Data are normalized to genomic copies of GAPDH. N=6 birds per group per timepoint. ***=p<0.001; n.s.=no significant difference.





<u>Figure 3.7. Viral replication in peripheral nerve tissue, Experiment 2.</u> Viral replication in sciatic nerve tissue was measured by quantitative PCR of MDV genes Meq (A) and gB (B) at the indicated days post-hatch. Data are normalized to genomic copies of GAPDH. N=6 birds per group per timepoint. *=p<0.05; ***=p<0.001; n.s.=no significant difference.

Md5 and Md5-delta-Meq infected samples at day 8, and staining was localized to infiltrating lymphocytes. At day 14, occasional "type B" lesions were seen in one out of four birds infected with Md5-delta-Meq, with lymphocytes typically arranged linearly around a single nerve fiber. No "type A" lesions were observed in any early samples.

Discussion

Our in ovo model was initially developed to take advantage of the induction of immunological tolerance that can occur when antigens (including viruses) are introduced into the chicken embryo prior to the influx of prethymocytes into the embryonic thymus (Le Douarin et al., 1996; Payne et al., 1992, Zhang 2003). Interestingly, in our model, viremia was not maintained over time, in contrast to tolerance induction by HVT (Zhang 2003); and suggests that either tolerance was not successfully induced, allowing eventual immunological clearance; the herpesvirus latency program was intact (despite the deletion of Meq); or the cytolytic phase of infection reduced circulating target immune cells to very low levels. Two points favor the latter hypothesis; first, the in-ovo-injected birds did replicate virus for four days longer than birds injected at hatch (in PBLs, p-value approaching significance at 0.13; in sciatic nerves, p-value 0.05); and secondly, the extreme thymic atrophy seen in in ovo injected birds suggests that early cytolytic replication proceeded to thymic ablation in these birds. Finally, the induction of clinical signs and mortality only in birds injected with Md5-delta-Meq in ovo indicates that a competent immune system normally prevents neuropathic disease from the Md5-delta-Meq virus.

However, despite the suspected induction of central thymic tolerance in this model, an immune reaction evidently occurred in at least some chicks infected in this model, as inflammatory, but not tumorous, lesions were observed in two birds at a very early timepoint. Since lytic-phase virus was not seen on immunohistochemistry, except within infiltrating inflammatory cells, and viral loads in nucleated (non-axonal, e.g. supporting or inflammatory) cells were similar to that found in blood, we believe that primary replication in peripheral nerve tissue is not the mechanism involved in MDV neuropathogenicity, although we have yet to characterize central nervous tissue. Additionally, by using a Meq-deficient virus that does not promote tumor cell transformation, we have shown that primary lymphomagenesis occurring within the nerve tissue is not required for MDV neuropathy. A potential mechanism for virusinduced secondary damage to nerve tissues is autoimmunity, which may be promoted by chronic viral infection in this model (i.e. inability to clear viral replication through adaptive immunity). Long-term exposure to antigens that mimic self-antigens in the context of inflammation can overcome normal tolerance to self proteins. If this model does indeed induce central tolerance to MDV, this may be a case in which induced tolerance is ultimately overcome by the innate inflammatory response to generate autoimmunity (similarly to autoimmune reactions that are thought to occur subsequent to chronic carrier-state-inducing pre- or neonatal infections such as HBV; reviewed in Tran 2011), although we do not yet have direct evidence to support this hypothesis.

This study raises the possibility that MD vaccines, which are avirulent in immune-competent birds, may be neuropathic in immune-compromised hosts. A correlation was found between increased incidence of idiopathic Leghorn paralysis and the use of vaccines in young

pullets, suggesting that immune modulation by vaccine agents is a risk factor, although comparisons between groups treated with MDV vaccines alone and multivaccine combinations lacking MDV has not yet been done. Additionally, a link between the presence of an MHC haplotype (B19/B19) known to confer susceptibility to MD and development of idiopathic Leghorn paralysis was identified (Fulton 2016), further supporting MDV vaccines as a potential causative agent, and a single gene not linked to oncogenesis (pp14) is known to be required for MDV neuropathogenicity (Tahiri-Alaoui et al., 2013), suggesting a potential role for antigenic mimicry in MDV and any vaccine-induced neuropathy. We anticipate testing the neuropathic potential of commercial vaccine strains using our tolerance model. If commercial vaccine strains are indeed found to induce neuropathogenicity in the tolerized chick model, then it may be of benefit to the poultry industry to consider neuropathogenicity in immune-compromised animals when new MDV vaccines are designed, in order to mitigate the risk of causing vaccine-related disease in a subpopulation of vaccinated animals.

APPENDIX

APPENDIX

Supplemental Figures

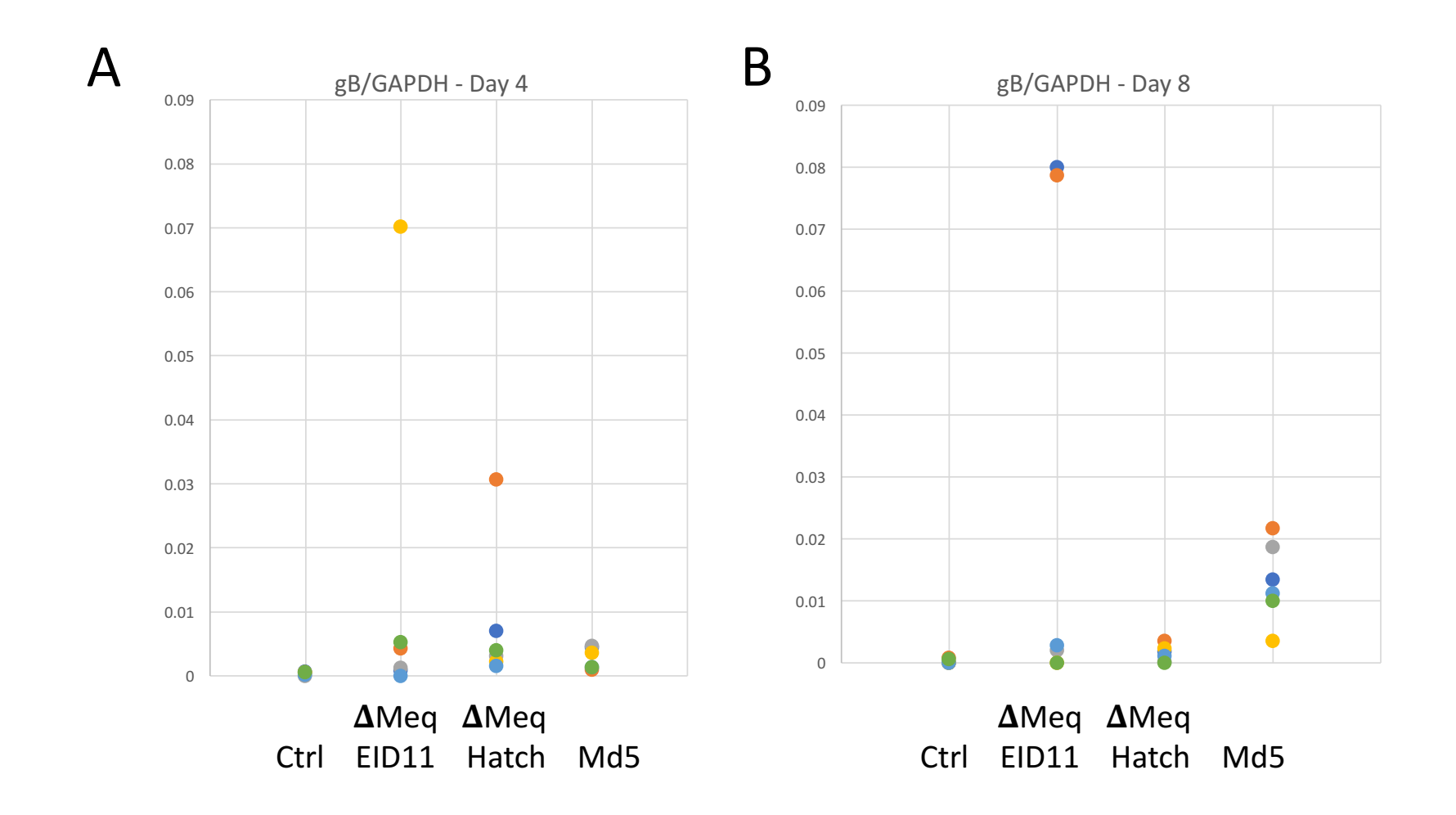


Md5-ΔMeq injected at EID 14 – Normal bird and stunted cagemate necropsied at 57 days post-hatch

Pancreatic atrophy associated with severe stunting



<u>Figure 3.S1. Variable necropsy results from *in ovo* injection at EID 14.</u> Necropsy results of birds shown in Figure 3.2, showing pancreatic atrophy associated with severe stunting in one chick.



<u>Figure 3.S2. Viremia in individual birds, Experiment 2.</u> Copies of gB per genomic copy of GAPDH are shown for days 4 (A) and 8 (B) post-hatch. N=6 birds per group per timepoint.

REFERENCES

REFERENCES

Bader, S. R. et al. Acute paretic syndrome in juvenile White Leghorn chickens resembles late stages of acute inflammatory demyelinating polyneuropathies in humans. J. Neuroinflammation 7, 7-26 (2010).

Biggs, P. M. Marek's disease – the disease and its prevention and its prevention by vaccination. Br. J. Cancer 31, 152–155 (1975).

Churchill, A. E. & Biggs, P. M. Agent of Marek's disease in tissue culture. Nature 215, 528–530 (1967).

Fulton, J. E. et al. A high-density SNP panel reveals extensive diversity, frequent recombination and multiple recombination hotspots within the chicken major histocompatibility complex B region between BG2 and CD1A1. Genet. Sel. Evol. 48, 1-15 (2016).

Kenzy, S. G., Cho, B. R. & Kim, Y. Oncogenic Marek's disease herpesvirus in avian encephalitis (temporary paralysis). J. Natl. Cancer Inst. 51, 977–982 (1973).

Lampert, P., Garrett, R. & Powell, H. Demyelination in allergic and Marek's disease virus induced neuritis comparative electron microscopic studies. Acta Neuropathol. 40, 103–110 (1977).

Lampert, P. W. Autoimmune and virus-induced demyelinating diseases. Am. J. Pathol. 91, 175-208 (1978).

Lawn, A. M. & Payne, L. N. Chronological study of ultrastructural changes in the peripheral nerves in Marek's disease. Neuropathol. Appl. Neurobiol. 5, 485–497 (1979).

Le Douarin, N. et al. Evidence for a thymus-dependent form of tolerance that is not based on elimination or anergy of reactive T cells. Immunol. Rev. 149, 35–53 (1996).

Lee, L. F. et al. Properties of a meq-deleted rMd5 Marek's disease vaccine: protection against virulent MDV challenge and induction of lymphoid organ atrophy are simultaneously attenuated by serial passage in vitro. Avian Dis. 57, 491–497 (2013).

Lee, L. F., Lupiani, B., Silva, R. F., Kung, H.-J. & Reddy, S. M. Recombinant Marek's disease virus (MDV) lacking the Meq oncogene confers protection against challenge with a very virulent plus strain of MDV. Vaccine 26, 1887–1892 (2008).

Lupiani, B. et al. Marek's disease virus-encoded Meq gene is involved in transformation of lymphocytes but is dispensable for replication. Proc. Natl. Acad. Sci. USA 101, 11815–11820 (2004).

Marek, J. Multiple Nervenentzündung (Polyneuritis) bei Hühnern. DTW. Dtsch. Tierarztl. Wochenschr. 15, 417–421 (1907).

Niikura, M., Kim, T., Silva, R. F., Dodgson, J. & Cheng, H. H. Virulent Marek's disease virus generated from infectious bacterial artificial chromosome clones with complete DNA sequence and the implication of viral genetic homogeneity in pathogenesis. J. Gen. Virol. 92, 598–607 (2011).

Okazaki, W., Purchase, H. G. & Burmester, B. R. Protection against Marek's Disease by vaccination with a herpesvirus of turkeys. Avian Dis. 14, 413-429 (1970).

Osterrieder, N., Kamil, J. P., Schumacher, D., Tischer, B. K. & Trapp, S. Marek's disease virus: from miasma to model. Nat. Rev. Microbiol. 4, 283–294 (2006).

Parker, M. A. & Schierman, L. W. Suppression of humoral immunity in chickens prevents transient paralysis caused by a herpesvirus. J. Immunol. 130, 2000–2001 (1983).

Payne, L. N. & Biggs, P. M. Studies on Marek's disease. II. Pathogenesis. J. Natl. Cancer Inst. 39, 281–302 (1967).

Payne, L. N. Marek's disease in comparative medicine. J. R. Soc. Med. 72, 635–638 (1979).

Payne, L. N. Developments in avian leukosis research. Leukemia 6, 150S-152S (1992).

Pepose, J. S., Stevens, J. G., Cook, M. L. & Lampert, P. W. Marek's disease as a model for the Landry-Guillain-Barré syndrome: latent viral infection in nonneuronal cells accompanied by specific immune responses to peripheral nerve and myelin. Am. J. Pathol. 103, 309–320 (1981).

Purchase, H. G. & Sharma, J. M. Amelioration of Marek's disease and absence of vaccine protection in immunologically deficient chickens. Nature 248, 419–421 (1974).

Sharma, J. M. & Burmester, B. R. Resistance of Marek's disease at hatching in chickens vaccinated as embryos with the turkey herpesvirus. Avian Dis. 26, 134-149 (1982).

Swayne, D. E., Fletcher, O. J. & Schierman, L. W. Marek's disease virus-induced transient paralysis in chickens: demonstration of vasogenic brain oedema by an immunohistochemical method. J. Comp. Pathol. 101, 451–462 (1989).

Tahiri-Alaoui, A., Smith, L. P., Kgosana, L., Petherbridge, L. J. & Nair, V. Identification of a neurovirulence factor from Marek's disease virus. Avian Dis. 57, 387–394 (2013).

Tran, T. T. Immune tolerant hepatitis B: a clinical dilemma. Gastroenterol. Hepatol. 7, 511–516 (2011).

Witter, R. L. The changing landscape of Marek's disease. Avian Pathol. 27, S46–S53 (1998).

Witter, R. L., Sharma, J. M. & Offenbecker, L. Turkey herpesvirus infection in chickens: induction of lymphoproliferative lesions and characterization of vaccinal immunity against Marek's disease. Avian Dis. 20, 676 (1976).

Xu, M., Fitzgerald, S. D., Zhang, H., Karcher, D. M. & Heidari, M. Very virulent plus strains of MDV induce an acute form of transient paralysis in both susceptible and resistant chicken lines. Viral Immunol. 25, 306–323 (2012).

Zhang, Y. Immunological tolerance in chickens hatching from eggs injected with cell-associated herpesvirus of turkey (HVT). Dev. Comp. Immunol. 27, 431–438 (2003).

CHAPTER 4

Conclusions and Further Work

In the previous chapters, I have described two lines of research which have shed light on the role of adaptive immunity in contributing to both resistance to, and pathogenicity of, Marek's disease (MD). First, I have demonstrated that differences in the in vivo proliferative responses of cells bearing two TCR families between resistant and susceptible birds can be localized to the CTL compartment, and I have described the divergent selection of the T cell receptor (TCR) repertoire in MHC-matched genetically MD-resistant and susceptible chickens, indicating that TCR repertoire has likely been shaped to maximize or minimize a successful cell-mediated response to MD in these lines. Secondly, I have identified a syndrome of lymphocytic neuropathy in chicks infected with non-oncogenic MDV in ovo, prior to thymic maturation; this model disentangles the oncogenic lymphoproliferative aspect of MD from its inflammatory neuropathic component, and points the way forward to understanding the immune cellmediated aspects of acute MD. Reconciling the contributions of adaptive immunity to both disease resistance and pathology will help guide research strategies toward the development of more disease-resistant animals and more effective vaccines. As I am in the position of being able to continue this research in the immediate future, the remainder of this brief chapter will outline my research plans to expand these lines of inquiry, as well as point out areas that can be studied by others in the future.

A more thorough investigation of the chicken anti-MDV and anti-tumor TCR repertoire is warranted. Next-generation sequencing methods to perform deep profiling of the TCR

repertoires of human and mouse species have recently been developed (Freeman et al. 2009; Warren et al. 2011; Linnemann et al 2013), and these kinds of methods can be extended to the chicken in both MDV-naïve and infected states, although complete annotation of the TCR genes will first be required in order to modify existing software pipelines which can analyze these types of data. Recently we have begun annotating the TCRbeta locus in the chicken reference sequence, though BAC sequencing, and will need to extend this to the TCRalpha locus as well in order to allow full TCRalpha/beta repertoire profiling. Our PacBio genome analysis of resistant and susceptible chicken lines has indicted that at least the TCRbeta locus is subject to divergent selection, and therefore it may be necessary to profile TCR variants from multiple inbred and commercial lines to capture the full diversity present at the sequence level. Additionally, it would be of interest to compare the TCR diversity in domestic and semi-domestic chickens with that of the parental jungle fowl species, in order to examine the effects of selection pressures in intensively-managed poultry on TCR repertoires, in comparison to natural host-viral interactions in wild populations.

Secondly, it will be important to functionally characterize TCR variants that have been found to be divergent between MD-resistant and susceptible chickens. Previous research has indicated that the TCR Vbeta-1 and Vbeta-2 families differ in their ability to recognize and lyse MDV serotype-2 infected target cells (Omar and Schat, 1997), and our research suggests that TCR Vbeta-1-bearing CTLs play a more important role in vivo during MDV infection. Since we have also identified differences between the Vbeta-1 repertoires of resistant and susceptible lines at the sequence level, elucidating the relative importance of the CDR1 region to binding B2 haplotype MHC molecules presenting MDV antigens in vitro will be important to disentangle

stochastic effects of TCR usage differences from the effects of identified sequence variants. Additionally, the presence of early visible shifts in TCR clonality suggests that immunodominant responses may be present and represent functionally important clones that can control either infection or transformation. Structural differences in the TCR loci in MD-resistant and susceptible birds may bias the expression of resistance-linked CDR3 clonotypes through recombination of particular V, D and J elements. Functionally important T cell clones should be identified at the clonotype level and tested in vitro for lysis against MHC-matched target cells loaded with candidate MD antigens or tumor neoantigens. Eventually, it may also become possible to test resistance-linked TCR clonotypes in vivo through single-TCR-expressing chickens, once genome modification of chickens by CRISPR/Cas9 becomes routine (Morin et al. 2017; Han and Lee 2017). Because the chicken TCR and MHC systems are reduced relative to mammals (reviewed in Smith 2014; c.f. Glusman et al., 2001), it is more likely that the T cell response to a virus such as MDV can be optimized in this species by selection or genetic engineering for TCR variants with the ability to recognize important antigenic epitopes, although this optimization will require a thorough understanding of interactions between TCR and MHC loci variants.

Thirdly, I intend to further elucidate the role of adaptive immunity in MDV neuropathy.

As described in chapter 3, chicks infected with non-oncogenic MDV during early of embryogenesis fail to control the infection and develop a fatal neuropathic syndrome, and although a rapid drop in infection in both blood and nerve tissues occurs, likely due to high lytic T cell infection combined with extreme bursal and thymic atrophy, neuropathy still develops, and lymphocytic nerve lesions are seen in some birds. This suggests a potential autoimmune

component (such as molecular mimicry of a self-antigen present in peripheral nerves), and lends such an interpretation to a previous discovery that a single MDV gene (pp14) is necessary for MD neuropathy (Tahiri-Alaoui et al, 2014). I would suggest that the pp14 protein, and its sub-epitopes, should be tested for the ability to induce immune-mediated neuropathy independently of MDV infection, and additionally, have plans to study its role in the neuropathogenicity of early *in ovo* infection with non-oncogenic MDV. I also plan to extend my early *in ovo* infection studies to commercial vaccine strains, in order to determine whether these commonly-used vaccines present a risk of neuropathic disease to immunocompromised hosts, potentially explaining the idiopathic layer paralysis syndrome which occurs in some commercial flocks (Bacon et al. 2001; Gall et al. 2018); and I will also test pp14-deleted vaccine strains in vivo to establish their safety and efficacy.

Integrating an understanding of both TCR-mediated cellular immunity to MD, and the potential for an autoimmune component of the disease, may allow the development of chickens with a TCR repertoire that is optimized for recognition of important MDV or tumor epitopes, and against recognition of a potential autoimmune antigen contributing to neuropathic disease; as well as the development of vaccine strains which present optimal epitopes for the development of anti-MD memory but lack those epitopes that could lead to autoimmunity in immunocompromised birds. Lessons learned from studying the chicken TCR repertoire may additionally lead to a better understanding of TCR-mediated immune and autoimmune mechanisms in other important species.

REFERENCES

REFERENCES

Bacon, L. D., Witter, R. L. & Silva, R. F. Characterization and experimental reproduction of peripheral neuropathy in White Leghorn chickens. Avian Pathol. 30, 487–499 (2001).

Freeman, J. D., Warren, R. L., Webb, J. R., Nelson, B. H. & Holt, R. A. Profiling the T-cell receptor beta-chain repertoire by massively parallel sequencing. Genome Res. 19, 1817–1824 (2009).

Gall, S. et al. Use of real-time PCR to rule out Marek's disease in the diagnosis of peripheral neuropathy. Avian Pathol. 47, 427–433 (2018).

Han, J. Y. & Lee, B. R. Isolation and characterization of chicken primordial germ cells and their application in transgenesis. in Avian and Reptilian Developmental Biology (ed. Sheng, G.) 1650, 229–242 (Springer New York, 2017).

Linnemann, C. et al. High-throughput identification of antigen-specific TCRs by TCR gene capture. Nat. Med. 19, 1534–1541 (2013).

Morin, V., Véron, N. & Marcelle, C. CRISPR/Cas9 in the chicken embryo. in Avian and Reptilian Developmental Biology (ed. Sheng, G.) 1650, 113–123 (Springer New York, 2017).

Omar, A. R. & Schat, K. A. Characterization of Marek's disease herpesvirus-specific cytotoxic T lymphocytes in chickens inoculated with a non-oncogenic vaccine strain of MDV. Immunology 90, 579–585 (1997).

Tahiri-Alaoui, A., Smith, L. P., Kgosana, L., Petherbridge, L. J. & Nair, V. Identification of a neurovirulence factor from Marek's disease virus. Avian Dis. 57, 387–394 (2013).

Warren, R. L. et al. Exhaustive T-cell repertoire sequencing of human peripheral blood samples reveals signatures of antigen selection and a directly measured repertoire size of at least 1 million clonotypes. Genome Res. 21, 790–797 (2011).